AD-783 578

HARMONIC GEAR DRIVES

E. G. Ginsburg

Foreign Technology Division
Wright-Patterson Air Force Base, Ohio

28 June 1974

AD 783 578

Security Classification

DOCUMENT CONTROL DATA - R & D

(Security classification of title, body of abstract and indexing annotation must be entered when the overall report is classified)

1. ORIGINATING ACTIVITY (Corporate author)
Foreign Technology Division
Air Force Systems Command
U. S. Air Force

2a. REPORT SECURITY CLASSIFICATION
UNCLASSIFIED

2b. GROUP

3. REPORT TITLE
HARMONIC GEAR DRIVES

4. DESCRIPTIVE NOTES (Type of report and inclusive dates)
Translation

5. AUTHOR(S) (First name, middle initial, last name)
Ye. G. Ginsburg

6. REPORT DATE	7a. TOTAL NO. OF PAGES	7b. NO. OF REFS
1969	~~201~~ 214	37

8a. CONTRACT OR GRANT NO.	9a. ORIGINATOR'S REPORT NUMBER(S)
AFFDL Contract 69C1720	FTD-MT-24-690-74
b. PROJECT NO.	
c.	9b. OTHER REPORT NO(S) (Any other numbers that may be assigned this report)
d.	

10. DISTRIBUTION STATEMENT
Approved for public release; distribution unlimited.

11. SUPPLEMENTARY NOTES	12. SPONSORING MILITARY ACTIVITY
	Foreign Technology Division Wright-Patterson AFB, Ohio

13. ABSTRACT

09, 20

214

DD FORM 1 NOV 65 1473

UNCLASSIFIED
Security Classification

EDITED MACHINE TRANSLATION

FTD-MT-24-690-74 28 June 1974

HARMONIC GEAR DRIVES

By: Ye. G. Ginsburg

English pages: 201

Source: Volnovyye Zubchatyye Peredachi, 1969, pp. 1-159

Country of Origin: USSR
Requester: AFFDL/PTC
This document is a SYSTRAN machine aided translation, post-edited for technical accuracy by: Bernard L. Tauber
Approved for public release; distribution unlimited.

PREPARED BY:

TRANSLATION DIVISION
FOREIGN TECHNOLOGY DIVISION
WP-AFB, OHIO.

TABLE OF CONTENTS

U. S. BOARD ON GEOGRAPHIC NAMES TRANSLITERATION SYSTEM

Block	Italic	Transliteration	Block	Italic	Transliteration
А а	*А а*	A, a	Р р	*Р р*	R, r
Б б	*Б б*	B, b	С с	*С с*	S, s
В в	*В в*	V, v	Т т	*Т т*	T, t
Г г	*Г г*	G, g	У у	*У у*	U, u
Д д	*Д д*	D, d	Ф ф	*Ф ф*	F, f
Е е	*Е е*	Ye, ye; E, e*	Х х	*Х х*	Kh, kh
Ж ж	*Ж ж*	Zh, zh	Ц ц	*Ц ц*	Ts, ts
З з	*З з*	Z, z	Ч ч	*Ч ч*	Ch, ch
И и	*И и*	I, i	Ш ш	*Ш ш*	Sh, sh
Й й	*Й й*	Y, y	Щ щ	*Щ щ*	Shch, shch
К к	*К к*	K, k	Ъ ъ	*Ъ ъ*	"
Л л	*Л л*	L, l	Ы ы	*Ы ы*	Y, y
М м	*М м*	M, m	Ь ь	*Ь ь*	'
Н н	*Н н*	N, n	Э э	*Э э*	E, e
О о	*О о*	O, o	Ю ю	*Ю ю*	Yu, yu
П п	*П п*	P, p	Я я	*Я я*	Ya, ya

*ye initially, after vowels, and after ъ, ь; e elsewhere. When written as ё in Russian, transliterate as yё or ё. The use of diacritical marks is preferred, but such marks may be omitted when expediency dictates.

* * * * * * * * * * *

GRAPHICS DISCLAIMER

All figures, graphics, tables, equations, etc. merged into this translation were extracted from the best quality copy available.

RUSSIAN AND ENGLISH TRIGONOMETRIC FUNCTIONS

Russian	English
sin	sin
cos	cos
tg	tan
ctg	cot
sec	sec
cosec	csc
sh	sinh
ch	cosh
th	tanh
cth	coth
sch	sech
csch	csch
arc sin	$\sin^{-1}$
arc cos	$\cos^{-1}$
arc tg	$\tan^{-1}$
arc ctg	$\cot^{-1}$
arc sec	$\sec^{-1}$
arc cosec	$\csc^{-1}$
arc sh	$\sinh^{-1}$
arc ch	$\cosh^{-1}$
arc th	$\tanh^{-1}$
arc cth	$\coth^{-1}$
arc sch	sech^{-1}
arc csch	csch^{-1}
rot	curl
lg	log

Harmonic gear drives. Ginsburg, Ye. G., "Machine-building" Publishing House, 1969, 160 pages, 12 Tables. Seventy-eight illustrations. References 37 titles.

This book presents questions of the theory, design, and constructions of a new type of gear drive - harmonic. In these drives, in the process of their operation the displacement of the waves of deformation of one of the parts occurs, because of which a large kinematic and power effect is realized, and also the large multiple pairing of engagement and, as a result, high precision of the transmission of rotation is achieved.

The book examines some questions of the technology of the manufacture of the basic parts of harmonic drives.

The book is intended for technical-engineering personnel and scientists who are engaged in the creation of new mechanical drives, and can also be used by students of higher technical educational institutions who are studying this speciality.

The reviewer is Distinguished Figure of Science and Engineering of the RSFSR, Doctor of Technical Sciences Prof. V. N. Kudryavtsev.

PREFACE

One of the most important tasks in the field of domestic machine-building is the reduction in the overall dimensions, weight, and cost of the mechanical drive. In the solution of this problem, a specific role should be played by the use of a new type of gear drive which has received the name "harmonic." A distinctive feature of the latter is the use of flexible gear wheels through which the drives acquire new properties and possibilities. At the same time, the practical introduction of harmonic drives into different fields of machine-building is connected with the solution of a whole series of technical problems not previously arisen and the creation of a method for the calculation of these transmissions.

The purpose of this book is to acquaint the readers with the operating principle and examples of the rational use of harmonic drives, and also to present one of the first methods for their geometric and strength calculation. The book also examines questions of the study of kinematics and the efficiency of harmonic drives and recommendations are given regarding the design and technology of the manufacture of the basic parts and units.

The author recognizes that not all of the recommendations given in the book are optimum and that all the questions interesting to the readers cannot be examined for the present. The harmonic

drives are very new and their investigation is continuing. At the same time, the use of the material in the book will aid the specialists who work in the field of reduction-gear building to create efficient and completely effective drives at the present stage of knowledge. Taking into account that this book is the first which illuminates the theory and the scientific bases of the calculation of harmonic drives, and intending to work further on the development of the optimum method for their calculation, the author will gratefully accept all observations and desires about this book.

THE BASIC DESIGNATIONS

The letter designations of the parameters and values common for the flexible and rigid gears of a harmonic drive are marked respectively by the subscript $_g$ and $_Ж$ or a numerical subscript according to the kinematic scheme. The subscript of value can consist of several letters and numbers.

Designations which pertain to kinematic and geometric calculations of harmonic drives.

B - width of toothed ring;

c_0 - the coefficient of radial clearance;

$d=2r$ - the diameter of equivelocity circle;

$d_д$ - pitch circle diameter;

d_{gH} - the diameter of the central (neutral) circle of the flexible component in a nondeformed state;

$d_{r.H}$ - the diameter of the rolling contact;

$d_{вн}$ - the diameter of the internal circumference of the ring along which the rolling contacts roll;

$D_e=2R_e$ - the diameter of the projection of the teeth;

D_1 - the diameter of dedendum circle;

E - the elastic modulus of the material;

f_0 - the coefficient of the addendum;

$h_з$ - the working depth of the teeth;

i - gear ratio ($i>1$);

k_Δ - the deformation coefficient of the flexible component;

m - the modulus of engagement;

m_y - the conditional modulus of engagement of the equivelocity curve;

n - the rotational speed of the component;

L - the length of the flexible component;

q - the coefficient of the width of the toothed ring;

R_0 - the radius of the base circle of a rigid component with the involute profile of teeth;

r_{min} - the minimum radius of curvature of the equivelocity curve of the flexible component;

t - tooth pitch;

z - the number of teeth;

α_∂ - the shaped angle of the initial outline of the rack;

α_{cp} - shaped angle in the middle point of the tooth for height;

δ - the wall thickness of the flexible component;

η - efficiency;

ϑ - the coefficient of the wall thickness of the flexible component;

0 - the polar angle of involute profile;*

ξ - the extension factor of the initial outline;

ψ - loss factor;

ω - the angular velocity of the component.

Designations which relate to stress calculations.

M - the torsional moment;

P_n - the force of normal pressure;

p - specific pressure in the contact of teeth;

$\theta_{нр}$ - the theoretical factor of variation of pressure distribution along the length of teeth;

$\sigma_в$ - the ultimate strength of the material;

$\sigma_т$ - the yield point of the material;

---

*Translator's Note: May be θ. Illegible in original.

σ_{-1} - endurance limit of material to bending with a symmetrical cycle of change in the stresses;

σ_k - contact stress;

$\theta_{из}$ - the bending stress of the teeth;

τ_{-1} - the endurance limits of material to torsion with a symmetrical cycle of change in the stresses;

C_k - the coefficient of contact stresses;

N - power

n_σ - safety factor for normal stresses;

n_τ - a safety factor for tangential stresses;

$k_{нр}$ - the effective variation factor of pressure distribution along the length of teeth and between the teeth;

k_z - the coefficient which considers the number of teeth which simultaneously participate in the work;

$k_{нр.н}$ - the variation factor of load distribution along the length of the teeth.

CHAPTER I

HARMONIC GEAR DRIVES AND THEIR USE

1. GENERAL INFORMATION ABOUT HARMONIC DRIVES

The harmonic drive is one of the varieties of mechanical transmissions. The name "harmonic" is connected with the fact that the conversion of motion in the mechanism of this drive is realized because of the displacement of the wave of deformation of one of the components which is made flexible, and the corresponding synchronous displacement of the zone of engagement or frictional contact of the components. Displacement of the wave of deformation of the flexible component is caused by a movable rod or by a nonmechanical device called a wave generator.

Harmonic drives sometimes include drives in which instead of the flexible component a chain or rigid components connected in a specific manner are utilized for the same purpose.

In spite of the fact that simple and differential mechanisms with flexible components for the conversion of rotary motion are long known [1, 18], the use of such mechanisms in the form of coaxial gear reducers or multipliers was initiated comparatively recently. For the first time, single-stage harmonic reducers began to be made in the USA according to the patent issued to the inventor, V. Masser, in 1959.

The possibility of obtaining a large kinematic effect, low overall dimensions, rational layout, the realization of translation of motion through impenetrable walls, and a number of other properties of harmonic drives attracted the attention of a large number of engineers and scientists. At present, harmonic drives received considerable propagation in the form of special-purpose and also several-purpose reducers.

The general-purpose reducers produced in the USA went on the world market and are proving to be considerably more effective in many instances than worm and planetary gears with the same operational parameters.

The schematic diagram of a single-stage harmonic gear drive in accordance with V. Masser's patent is presented in figure 1. The kinematic drive chain consists of three components: the wave generator 1 (subsequently designated as H) made in the form of an oval cam with a flexible bearing, flexible component 2 which is an elastic thin-walled container with external teeth connected with a shaft, and a rigid component 3 with internal teeth and made together with the housing. The flexible and rigid components have respectively the number of teeth $z_г$ and $z_ж$.

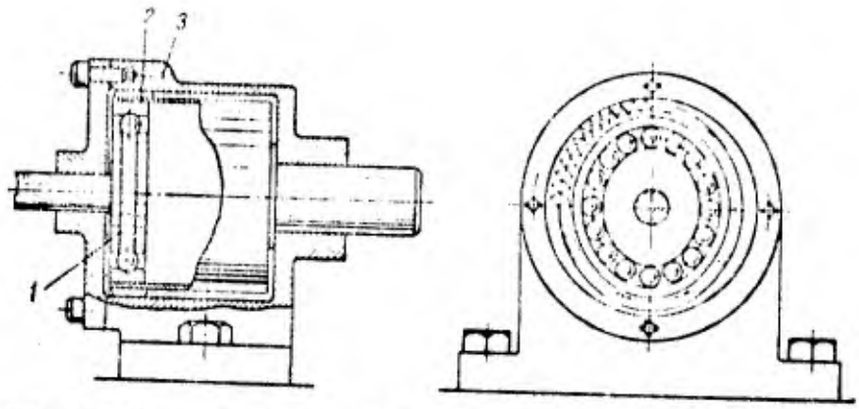

Figure 1. Diagram of a harmonic gear drive.

The flexible component in the state of elastic deformation (from the direction of the free end) is mounted on the wave generator, and the shape of the latter assures the engagement of the teeth of the components at their full working height in the zone of the greatest deformation and the full disengagement of the teeth in the zone of smallest deformation.

Rotation of the wave generator causes motion along the circumference of the wave of deformation of the flexible component. If with equal pitches $z_{ж}>z_{г}$ and the difference in the numbers of teeth is a multiple of the number of waves of deformation, then with a fixed rigid component during one revolution of the wave generator the shaft of the flexible component will turn through the angle which corresponds to $z_{ж}-z_{г}$ angular pitches of the flexible component in the direction opposite to the rotation of generator.

The drive can be made so that the flexible component will not rotate, then with the rotation of the generator the rigid component will accomplish rotation through an angle equal to $z_{ж}-z_{г}$ angular pitches in the direction of rotation of generator.

It is obvious that the absolute value of the gear ratio in these cases will be determined from the relations:

with a standing rigid component with a driving generator

$$i_{нг}^{ж}=-\frac{z_г}{z_ж-z_г},$$

with a standing shaft of the flexible component with a driving generator

$$i_{н.ж}^{г}=\frac{z_ж}{z_ж-z_г}.$$

To assure the minimum level of stresses which appear with the deformation of the flexible component it is advantageous

to accept the difference in the number of teeth of the components as equal to the number of waves of deformation n, i.e.,

$$z_w - z_g = n.$$

Then simple expressions are obtained for determining the transmission ratio

$$i^{w}_{wg} = -\frac{z_g}{n} \text{ and } i^{g}_{gw} = \frac{z_w}{n}.$$

The subscript of the transmission ratio serves to indicate which component of the drive stopped. It is natural that by stopping the wave generator the mechanism for the transmission of rotation between the rigid and flexible component can be obtained with the transmission ratio

$$i^{H}_{gw} = \frac{z_w}{z_g}.$$

The number of waves of deformation of the flexible component can be any number, beginning with n=1; however, it is advantageous to accept n=2, 3.

Figure 2 shows diagrams of single-wave and three-wave drives. With n≥2 and symmetrical cams, the reactions on the part of the flexible component are closed in the body of the cam and are not transferred to the supports. Even from the examination of this simplified diagram of a harmonic drive its interesting possibilities are visible.

Attention is drawn to the feasibility of the multiple pairing of engagement, which makes it possible to lower considerably the loading of the teeth in comparison with other forms of gear drives and, consequently, also to decrease the dimensions of the teeth. The great multiple pairing of engagement in several zones indisputably makes it possible to raise the kinematic precision of transmission and the evenness of the transmission of rotation.

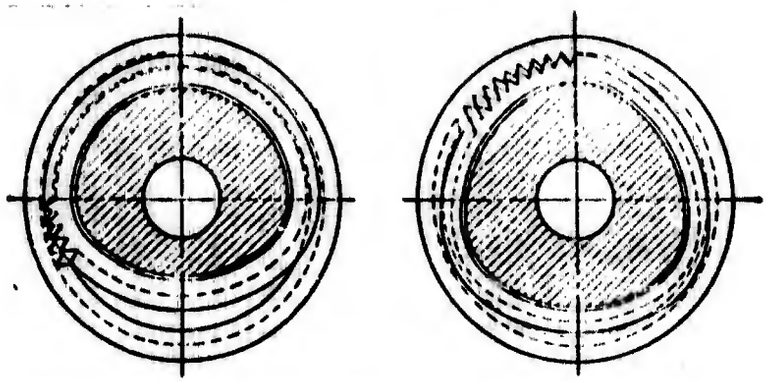

Figure 2. Diagrams of single-wave and three-wave drives.

In the harmonic drives with a fixed wave generator the sliding speed of the teeth is very low, which shows up positively in their efficiency.

Very tempting is the possibility of using the space within the flexible component for the placement of a motor or additional devices in it. At the same time, in spite of the external simplicity of harmonic drives, the creation of their rational and effective design required the solution of a number of problems. For several years in our country and abroad investigations were conducted whose results make it possible to give concrete recommendations regarding the calculation and design of harmonic drives at present.

2. EXAMPLES OF APPLICATION

This chapter examines the most typical of the entire variety of the harmonic drives of designs whose description is presented systematically in periodical and scientific literature.

Single-stage drives find application in power and kinematic autonomous or built-in reducers and accelerators with a range of transmission ratios of $60<i<300$. Up to now this range was not encompassed by single-stage drives of other types.

Figure 3 depicts the construction of the single-stage two-wave reducer of the "United Shoe Machinery" firm [29] produced in the USA from 1960 restored by us from drawings and photographs which are encounted in the literature.

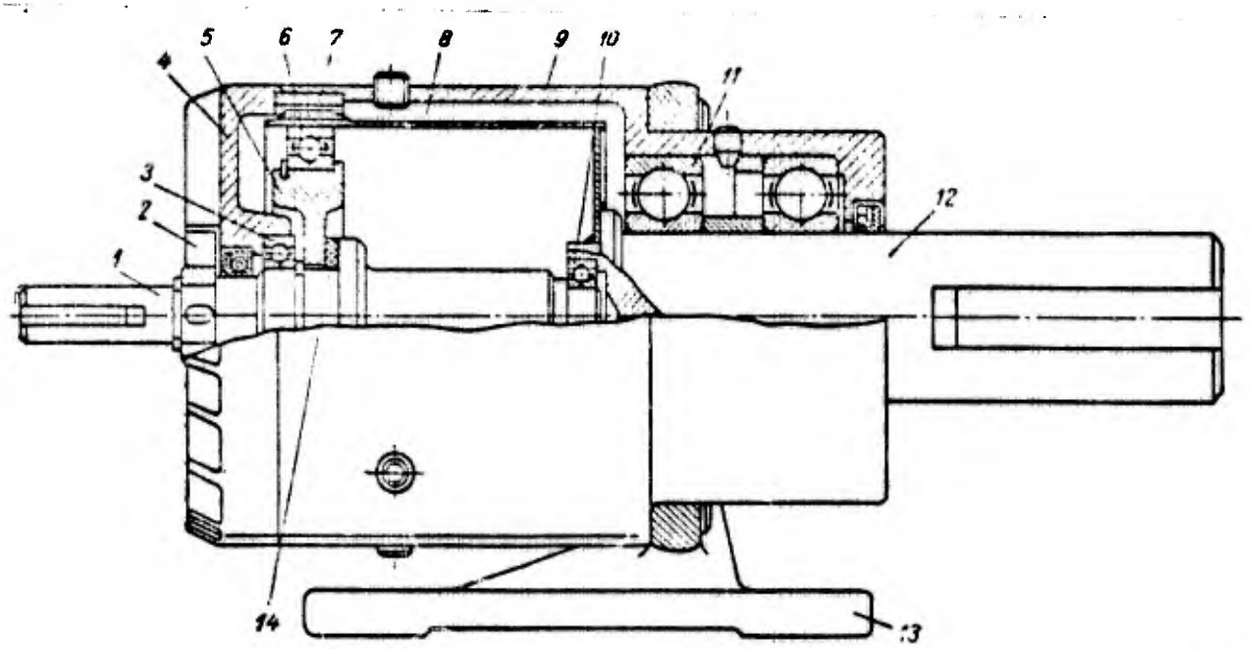

Figure 3. Reducer with single-stage harmonic drive.

The design of the reducer is original. The wave generator 5 is a rigid cam connected with a shaft 1 with the aid of an elastic rubber clutch 14 intended to contribute to uniform load distribution over two zones of engagement. Between the cam and the deformed flexible component is a ball bearing 6 with flexible deformable races. The flexible component 8 is made in the form of a thin-walled solid housing or tube with a welded-on bottom and it is connected with a shaft 12. The rigid component 7 is a rim with internal teeth connected with the left cover of the reducer 4 in which one support 3 of a high-speed shaft is also located. The second support 10 of the high-speed shaft is arranged within a low-speed one.

In the right part of the housing 9 two bearings 11 of low-speed shafts are located. A bracket 13 is screwed to the housing which has grips for the emplacement of the reducer. On the housing lid from the direction of the wave generator there are radial fins to increase the cooling area and an impeller 2 is put on the high-speed shaft. According to the indicated design concept a number of reducers are produced with transmission ratios from 78 to 260 and transmitted powers from 0.083 to 3.2 hp. The drive of the reducer is realized from motors with a rate of rotation of 1725 rpm. With the greatest power, the diameter of the flexible component which determines the transverse dimensions of the reducer in the last analysis is 164 mm. The length of the flexible component is approximately equal to the diameter. The efficiency of the reducer varies within the limits of η=0.80-0.90.

The overall dimensions and weight of the reducers of the examined series are considerably less than the serially produced reducers of other types with the same kinematic and power characteristics.

Figure 4 shows a series single-stage three-wave motor-reducer produced by the "Dyura" company [as transliterated] (USA) [29] in which a plastic flexible component and so-called planetary wave generator are used. The motor-reducer consists of a motor 1 whose shaft 2 is in frictional contact with three double roller-planet pinions 4 which directly deform the flexible component 3 and create three symmetrical zones of deformation of the latter, and during rotation - three waves of deformation. The symmetry of the arrangement of the rollers is assured by a separator. The flexible component is a cast plastic housing connected with a driven shaft 7 with the aid of a spline joint. Located within the flexible component is a spacing shell 5. The rigid component is made together with the housing of the reducer 6. The planetary generator is seemingly a high-speed stage to which a harmonic slow-speed stage is connected in series.

GRAPHIC NOT REPRODUCIBLE

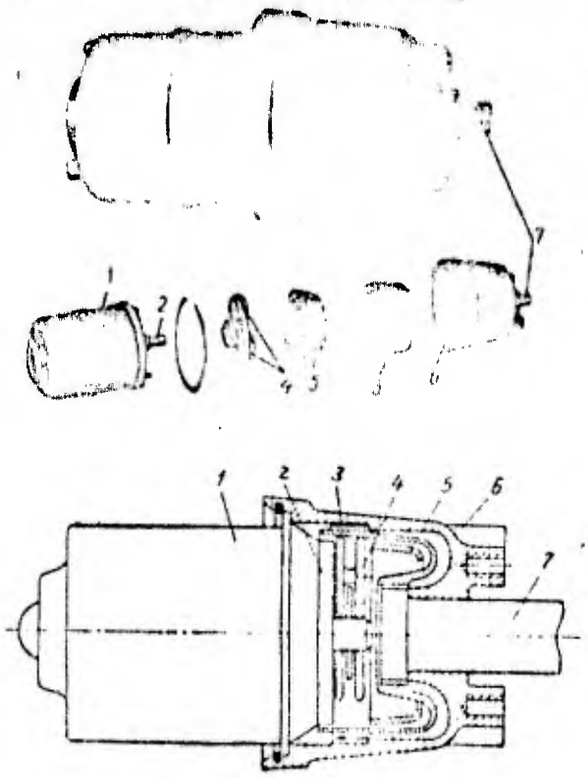

Figure 4. Motor-reducer with three-wave drive and planetary wave generator.

The principle of operation of the planetary generator is that the rollers which create the deformation of the flexible component are planet pinions of the frictional planetary mechanism. The gear ratio of the planetary generator is determined from the formula: $i_{сеч} = 1 + \frac{d_{ролика}}{d_{вала}}$. In the reducer being considered it is $i_{сеч}$ =7, and the harmonic drive $i_{волн}$ =64. The total transmission ratio i=448.

The reducer is used with small loads. The greatest torsional moment on the output shaft is 184 kgf·cm, engine power 12 W. It is natural that with a planetary wave generator and frictional contact of the rollers with the shaft their slipping is possible, which does not assure rigid kinematics of the mechansim.

The single-stage harmonic drives can be connected successively or be made in the form of closed drives, which achieves the obtaining of very large transmission ratios.

Figure 5 depicts a motor-reducer with a two-stage closed harmonic drive [29]. The flanged electric motor 6, through shaft 7, rotates the wave generator of the first stage, which produces the deformation of the flexible component 8 through the ball bearing with flexible races. The rigid component of the first stage 2 is fastened on a low-speed shaft 1 of the second stage and slowly rotates with the shaft. The bottom of the flexible component of the first stage is connected with the wave generator of the second stage 5, and the flexible component of the second stage 3 is fastened to the low-speed shaft 1. The rigid component of the second stage 4 is motionlessly fastened in the housing of the reducer.

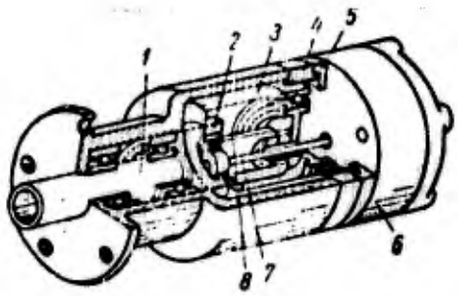

Figure 5. Motor-reducer with a two-stage closed harmonic drive.

A ball bearing with flexible races is also placed between the wave generator 5 and the flexible component 3. The transmission ratio of the reducer with two-wave drives is determined by the expression

$$i = \frac{2z_{ж1} + z_{z1}z_{z2}}{4}, \qquad (1)$$

where $z_{ж1}$ - the number of teeth of the rigid component of the first stage; z_{z1} - the number of teeth of the flexible component of the first stage; z_{z2} - the number of teeth of the flexible component of the second stage [sic].

There are descriptions of two-stage drives called double [29]. A typical design of a reducer with a double drive is presented in figure 6.

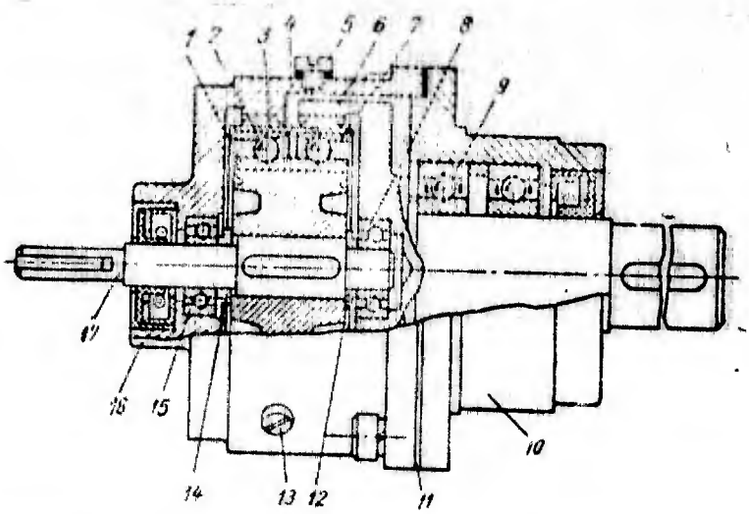

Figure 6. Reducer with a double harmonic drive (type Г-2М-Н).

The wave generator with intermediate rolling contacts 2 (balls) deforms the short flexible component 3 which has two toothed rings. One of the rings enters into a wave engagement with the rigid rim which is made together with the housing 4, and the second rim is coupled in wave engagement with a wheel 6 connected with the output shaft.

Chapter II will examine in detail the kinematics of this drive. It should be noted that in the indicated design the flexible component is not connected with the rotation of the shaft, by virture of which its length is determined only by the width of two toothed rings. This makes possible the use of the drive for mechanisms with limited overall axial dimensions with $2500<i<100,000$.

Of interest is the use of harmonic drives for the transmission of rotation through an impenetrable wall. In this case, the task of the separation of hermetically sealed regions with the translation of motion is solved without the use of seals or special diaphragms. Figure 7 shows the design of this drive [29]. Fastened on the shaft of the electric motor 1 is a two-wave generator 2 with intermediate rolling contacts (balls). A flexible component 3 to decrease the stresses in the zone of the greatest deformation with two attached faces is made with a complex form.

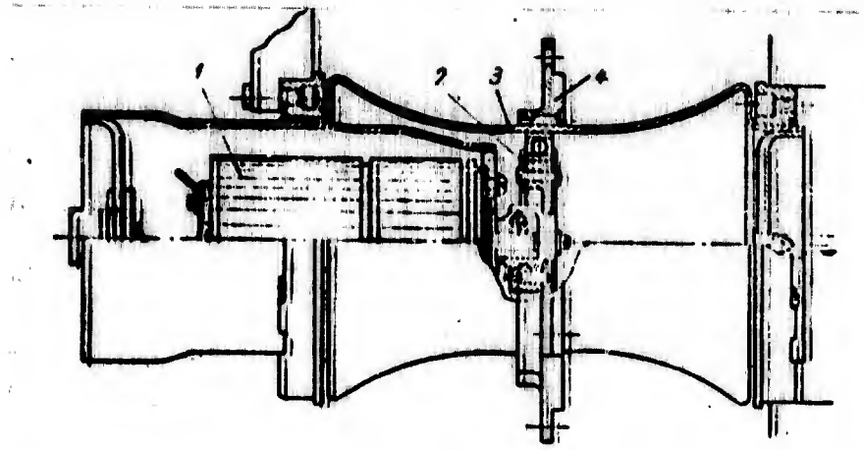

Figure 7. Diagram of the use of a wave mechanism for the transmission of rotation through an impenetrable wall.

In the middle portion the flexible component has external teeth meshed with the teeth of the rigid component 4. The latter is made in the form of two screwed semirings. The region within the flexible component is hermetically sealed and turns out to be isolated from the surrounding space. Such a type of harmonic drive finds use in the drives of space craft [29].

The possibility of the realization of large gear ratios and assurance of high kinematic accuracy makes it advisable to use harmonic drives as kinematic. Figure 8 depicts a rotary dividing table, the precise rotation of whose face chuck is accomplished with the aid of a harmonic drive. The design feature of the table is the use of an encompassing wave generator 1 and the arrangement, within the flexible component 2, of a rigid component 3 connected with the face chuck of the table.

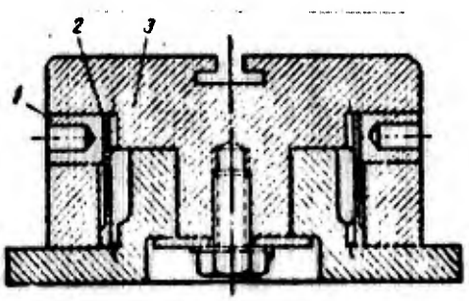

Figure 8. Dividing table with harmonic drive.

The wave generator 1 is a ring with an internal oval surface, by rotation of which a wave of deformation of the flexible component 2 is created. The flexible component has the toothed ring which engages the rigid component, and a second ring for connection with the fixed housing of the table.

The harmonic drives found application in the kinematic mechanisms of precision machine tools, as precision tape-drawing mechanisms, and in a number of other devices.

As noted above, the creation of the waves of deformation of the flexible component can be realized not only mechanically. Electrical, hydromechanical and pneumatic devices can be utilized as a generator. Figure 9 shows a schematic diagram of an electromagnetic wave generator [29]. The rotating magnetic field forces the waves of deformation of the flexible component manufactured from magnetic material to displace. To increase the force of the magnetic field, different schemes of unipolar superposed magnetization are used.

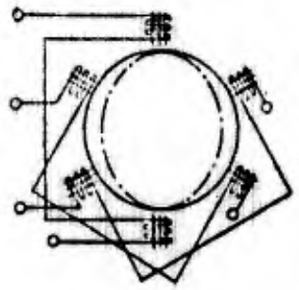

Figure 9. Diagram of an electromagnetic wave generator.

The electromagnetic generator makes it possible to build a wave reducer directly in the motor. As a result of the absence of fast-rotating parts, the drive possesses extremely rapid response and comparatively high efficiency; however, the load ability of such drives is low and it is advantageous to utilize them mainly in instruments. A motor of such a type was invented by A. I. Moskvitin in 1944 (author's certificate No. 68211).

Figure 10 gives the design concept of a hydromechanical two-wave generator. Deformation of the flexible component and the

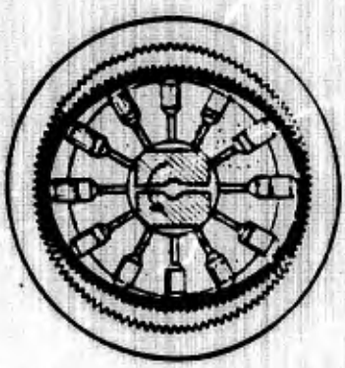

Figure 10. Diagram of harmonic drive with hydromechanical wave generator.

displacement of the wave of deformation is realized by a piston stroke under the effect of the pressure of a liquid. Distribution of the fluid is accomplished through the rotation of a distributive roller; in this case, part of the diametrically opposite cylinders is connected in turn with a high-pressure cavity, and part - with a low pressure cavity which also creates the motion of the wave of deformation of the flexible component.

The use of a hydromechanical drive can insure a considerable gain in strength and substantially lower the sluggishness of the drive when using flexible components of large diameters. Expenditures of power on distribution of the fluid are insignificant, by virtue of which the distributive motor can have very small dimensions and the moment of inertia of the rotor is many times less than the moment of inertia of a mechanical generator. At the same time, transmissions with a hydraulic generator have low efficiency, and their cost and weight are more than when using mechanical wave generators.

The principle of design of a pneumomechanical generator consists of the fact that the deformation of the flexible component 1 (figure 11) and the creation of several driving waves of its deformation are realized by gases emerging under pressure from openings 2 in the body of a rotating cylinder 3. The diameter of the cylinder is equal to the smallest internal diameter of the deformed flexible component. Rotation of the cylinder is realized through the reactive moment created by the gases emerging from nozzle 4 or 5.

In harmonic drives flexible components not only of cylindrical form can be utilized. In the reducer shown in figure 7, the

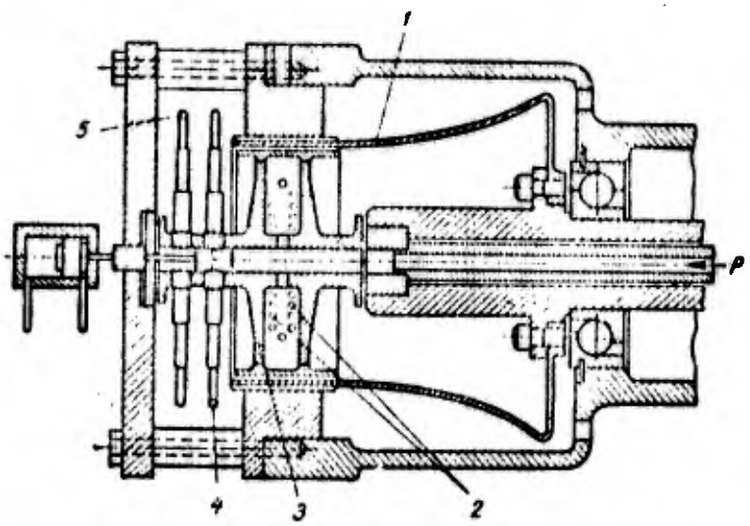

Figure 11. Harmonic drive with pneumo-mechanical generator.

flexible component has a so-called double bell shaped form [29]. Suggestions on the choice of this form of the component are given in the U.S. patent description [36].

In axial cross section, the line passing through the middle of the wall thickness, according to the patent, is a curve formed by the generatrix of a cylinder and two circular arcs conjugate with it. The purpose of the assignment of this form entails the elimination of misalignments in the contact of teeth which appear with the deformation of the cylindrical component from the direction of one face.

Figure 12 shows an end harmonic drive in which the flexible component 2 is flat and is made in the form of a disc which converts into a shaft and which has end teeth [10]. The rigid component 1 in this drive is made conical because of which the difference in the number of teeth of the rigid and flexible components is obtained. The presented drive has a two-wave planetary generator which consists of a disc 3, two balls 4 and a separator 5. The disc is the driving component of the drive. Teeth of the components are made with flat lateral faces and apex angle of 60-40°.

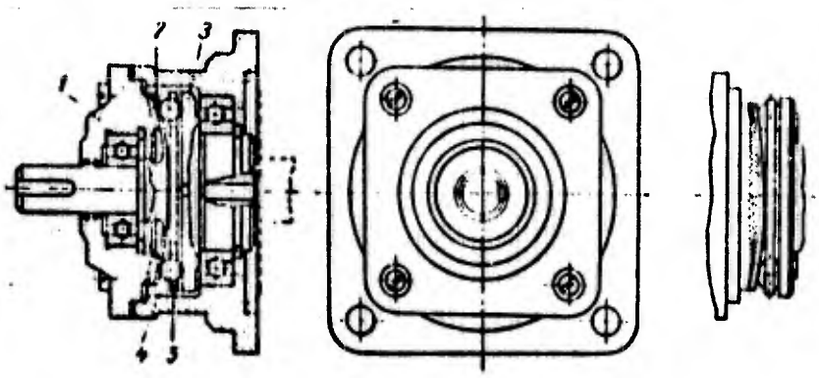

Figure 12. Harmonic gear drive with flat flexible component.

The end wave drive possesses small overall axial dimensions and can be both power and kinematic.

The given examples are sufficient to demonstrate the properties and the very wide possibilities of harmonic drives. Unquestionably the rational introduction of harmonic drives in the practice of machine and instrument manufacture should provide a large design and economic effect.

CHAPTER II

STRUCTURE AND KINEMATICS

3. FLEXIBLE COMPONENTS AND THEIR PROPERTIES

In connection with the fact that the distinctive feature of harmonic drives is the presence of flexible components in them, it is necessary to examine some questions of their theory.

We will call *flexible* the component of the mechanism which undergoes elastic deformation in the process of motion. Subsequently, we will be interested in a special class of flexible components - closed. We call *closed* the flexible components which are thin-walled plates or shells whose initial central surface before deformation is a surface of revolution. We will call the *central* surface the surface passing through the middle of the wall thickness of the component. The motion of these components in the mechanism relative to a support or some other rigid component will occur around the axis of the initial surface. The deformation of flexible components causes a change in the form of the central surface. We will call the deformed central surface the *surface of deformation*.

The initial surface of the flexible component can consist of one or several sections described by different equations. Figure 13 shows some possible forms of the initial surfaces of the

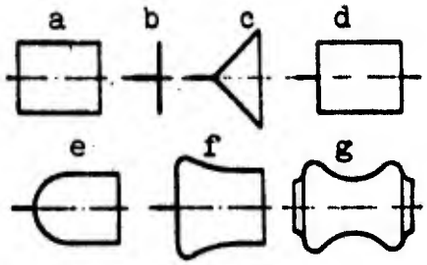

Figure 13. Possible forms of the initial surfaces of flexible components.

flexible components: cylindrical (a), flat (b) conical (c); they are developable and are *called simple initial surfaces*. The surfaces presented in figure 13d-g, are complex and respectively consist of: a cylinder and plane, cylinder and hemisphere, cylinder, two conjugate sections of tori and a plane, and five conjugate sections of tori.

Since simple initial surfaces are developable, their bending along the linear generatrix does not cause a change in the lengths of any curves lying on this surface. The bending deformation of complex initial surfaces in any directions is linked with elongation or compression of the material of the component in these surfaces.

The deformation of the flexible component with a given shape of surface of deformation can be realized geometrically with the aid of the corresponding arrangement or form of the conjugate components, and also the application of constants in accordance with the value of one or several concentrated forces.

Motion can be imparted to the flexible component with which all points of its central surface will lie in the surface of deformation. For example, for the belt drive shown in figure 14a the surface of deformation will consist of two semicylinders and two planes; the rotation of the sheaves will cause the motion of all points of the flexible component in the surface of deformation. Figure 14b shows a surface of deformation in which the flexible component which has an initial conical surface can move. In the examined cases, the vectors of the velocity of motion of any point of a flexible component lie in planes tangent to the surface of deformation at right angles to the generatrices of the initial surface.

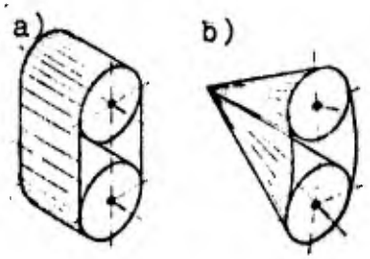

Figure 14. Surfaces of deformation of flexible components.

Lines on the surface of deformation which are trajectories of the points of the central surface of the moving flexible component are called *constant-velocity curves*. For the closed components constant-velocity curves are also closed. If a point of a flexible component, moving along a closed constant-velocity curve, arrives at the initial position, the component completes a full revolution. It is possible to show [7] that the mean-integral angular velocity of point P of a flexible component that travels at constant speed v along a constant-velocity curve over the surface of deformation relative to the axis of the initial surface of the flexible component is equal to the angular velocity of point P_1 which also moves with speed v over the circumference $R_э$, whose length L is equal to the length of constant-velocity curve (figure 15). This proposition ensues from the fact that

$$\int_0^{\frac{L}{v}} \omega_p \, dt = 2\pi,$$

where $\int_0^{\frac{L}{v}} \omega_p \, dt$ - the angular path covered by the point during one revolution of the flexible component.

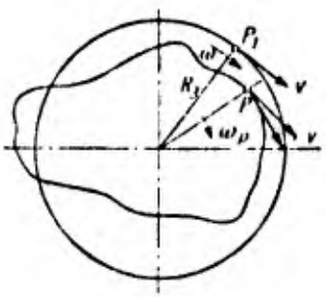

Figure 15. For the determination of the mean-integral angular velocity of rotation of a flexible component.

to draw the conclusions:

1) that the value of the mean-integral angular velocity of all points of a flexible component at a constant velocity of motion of one point is a constant which does not depend on the form of the constant-velocity curves;

2) if during the motion of a deformed flexible component the constant-velocity curve of even one point of the component is a circle, the angular velocity of the motion of this point is equal to the mean-integral velocity of the motion of all other points.

Hence ensues a very important conclusion about the nature of the work of the flexible components (simple and complex) which change to a rigid shaft (see figure 1). The motion of the flexible component relative to the fixed surface of deformation, in which all points of the central surface of the component move along the constant-velocity curves (on the surface of deformation) at constant velocities, will cause the rotation of the shaft connected with the component at a constant angular velocity. The motion of the flexible component relative to the surface of deformation can be called simple since it is determined by one independent parameter - the mean-integral angular velocity.

In mechanisms, the case occurs where the very surface of deformation also accomplishes motion with respect to the support. In this case, the motion of the flexible component becomes complex and the velocity of each point of the component is made up of velocity in relative motion (relative to the surface of deformation). Figure 16 shows a flexible component 1, the shape of the surface of deformation of which is provided by two sheaves 2 connected with a carrier 3. The carrier is connected with a support with the aid of a simple joint and rotates with velocity ω_N. The flexible component itself moves with velocity v_r relative to the surface of deformation. In this case the instantaneous absolute velocity of point A of the component equals

$$\vec{v} = \vec{v}_e + \vec{v}_r,$$

where $v_e = \omega_N \cdot AO$ is the velocity in translational motion.

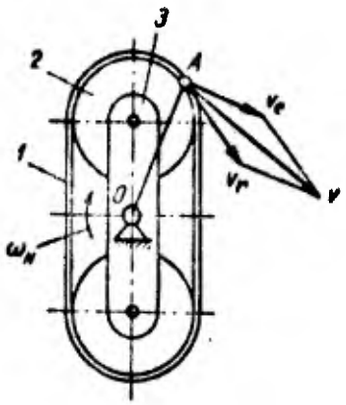

Figure 16. Determining the absolute velocity of motion of a point of a flexible component.

4. KINEMATICS OF HARMONIC DRIVES

Let us examine the mechanism of a very simple frictional two-wave drive (figure 17) which consists of four components: the wave generator 1, flexible component 2, rigid component 3 and of support 4. Let us distinguish the following kinematic pairs: the wave generator and support which comprise a class V rotary pair; flexible component and wave generator - class V rotary pair; flexible component and rigid component - highest frictional class IV kinematic pair with the linear or point contact of the components; and rigid component and support - class V rotary pair. The class V rotary kinematic pair which consists of a flexible component and support is passive in this mechanism and does not affect the kinematics of the mechanism since the flexible component is reliably centered on the wave generator.

It is possible to determine the number of degrees of mobility W of the mechanism with the aid Chebyshev's formula

$$W = 3(n-1) - 2p_5 - p_4, \qquad (2)$$

where n - the number of all components of the mechanism; p_5 - the number of class V kinematic pairs (not allowing for passive pairs); p_4 - the number of class IV kinematic pairs.

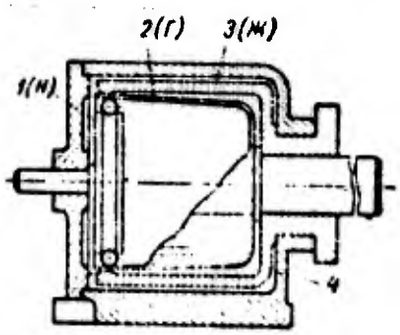

Figure 17. Differential harmonic drive.

In view of the fact that the axes of rotation of all components are parallel, the mechanism is considered plane. By accepting $n=4$; $p_5=3$ and $p_4=1$ according to the scheme we obtain

$$W = 3(4-1) - 2 \cdot 3 - 1 = 2.$$

The examined mechanism is differential and the motion of all its components is determined by two independent parameters (the angular rates of rotation of any two components). In order to leave the mechanism with one degree of mobility, it is necessary to stop the motion of one of the components after connecting it motionlessly with the support.

If we stop the motion of the wave generator H, then we will obtain a simple frictional mechanism with a flexible component and the transmission of rotation between the shafts connected with the flexible component and the rigid one. In this mechanism, the flexible component will accomplish simple motion. After stopping the rigid component 3, we obtain a planetary wave frictional mechanism whose flexible component accomplishes a complex motion. In this mechanism, the transmission of rotation will occur between components H and 2. After stopping the shaft of the flexible component 2, we obtain a planetary wave frictional mechanism in which the flexible component accomplishes motion relative to the wave generator and the transmission of rotation occurs between components H and 3.

Before beginning the determination of the transmission ratio of the mechanism of harmonic drive in the differential version, one ought to examine the kinematics of a simple frictional mechanism with flexible and rigid components.

In order that the rotation of the rigid component would cause the motion of the flexible component relative to the fixed wave generator, it is necessary to create in the zone of direct contact of the geometric elements of components a force of friction whose moment would be more than the moment applied to the rigid component. Creation of the necessary forces of friction requires the application of the corresponding normal forces on the part of the wave generator. There are designs in practice in which it is possible to create sufficiently large forces of friction. However, in frictional transmission because of unavoidable slipping of surfaces it is impossible to insure the constancy of the transmission ratio. If we disregard slipping and consider the flexible component infinitely thin, then during the rotation of the rigid component at angular velocity $\omega_{ж}$ and accordingly the circular velocity v on the cylindrical surface of a contact with radius $R_{ж.сн}$, the points of the flexible component which is in contact with the rigid component will move at the same velocity. These points can belong to one constant-velocity curve of the flexible component or, with the appropriate shape of the surface of deformation and the initial surface - to the family of identical constant-velocity curves. In this case, the shaft which is flexibly connected with the flexible component will rotate with an angular velocity $\omega_в$ determined according to the formula (see figure 15)

$$\omega_в = \frac{v}{R_в} = \frac{v2\pi}{L}. \qquad (3)$$

If the initial surface of the flexible component on the section of the frictional contact is made cylindrical and the surface of deformation assures obtaining linear contact with low thickness and deformations of the flexible component, it is possible to

consider with accuracy sufficient for practical purposes that the radius of the external cylindrical surface of the nondeformed flexible component $R_{г.н\,нар} = R_г$. Then the transmission ratio of the mechanism being examined will be

$$i^{н}_{г.ж} = \frac{\omega_г}{\omega_ж} = \frac{R_{г.н\,нар}}{R_{ж\,внутр}}. \qquad (4)$$

The organic shortcomings inherent to frictional kinematic pairs, from the very beginning of the development of harmonic drives, forced turning primary attention to the use of gearing.

Let us examine the same version of a harmonic drive with a standing wave generator with the use of toothed flexible and rigid components.

Let us assume that assured in the process of the engagement of each pair of teeth is motion at identical velocities v of the points lying on some closed curves invariable along the length which belong respectively to the flexible and rigid component and called equivelocity curves (figure 18). We consider also that the pitches of the teeth t measured along these equivelocity curves are constant (see Chapter III).

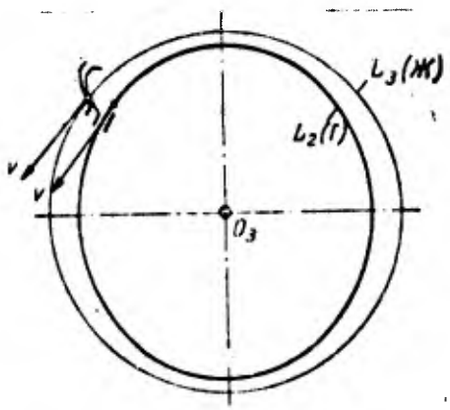

Figure 18. Equivelocity curves of flexible and rigid components.

Then the transmission ratio of the mechanism will equal

$$i^{н}_{г.ж} = \frac{L_{ж}}{L_г},$$

where L_g - the length of the equivelocity curve of the flexible component; $L_ж$ - the length of the equivelocity curve of the rigid component.

It is obvious that $L_g = tz_g$ and $L_ж = tz_ж$ and the transmission ratio of the mechanism is determined from the expression

$$i^н_{gж} = \frac{tz_ж}{tz_g} = \frac{z_ж}{z_g}. \qquad (5)$$

For the transfer to the differential version of the drive, let us impart to the entire mechanism rotation with velocity $\omega_н$; then it is possible to consider that flexible 2 and rigid 3 (figure 17) components accomplish complex motion together with the generator and relative to it. In this case, the absolute angular velocities of the shafts connected with these components will be equal to:

$$\omega_g = \omega_{eg} + \omega_{rg}; \quad \omega_ж = \omega_{eж} + \omega_{rж},$$

where ω_{eg} and $\omega_{eж}$ are translational rotational velocities.

Taking into account the fact that $\omega_{eg} = \omega_{eж} = \omega_н$, the equations take the form

$$\omega_{rg} = \omega_g - \omega_н; \quad \omega_{rж} = \omega_ж - \omega_н.$$

Since ω_{rg} and $\omega_{rж}$ are rotational velocities of the components relative to the wave generator, on the basis of expression (5) obtained with a stationary generator it is possible to record

$$i^н_{gж} = \frac{\omega_{rg}}{\omega_{rж}}$$

or

$$i^н_{gж} = \frac{\omega_g - \omega_н}{\omega_ж - \omega_н} = \frac{n_g - n_н}{n_ж - n_н};$$

taking into account (5) we obtain

$$i^н_{gж} = \frac{n_g - n_н}{n_ж - n_н} = \frac{z_ж}{z_g}. \qquad (6)$$

The obtained expression is the known Willis formula.

With the stopped rigid component ($n_{ж}=0$) from (6) we will have

$$i^{вс}_{вг} = \frac{1}{1 - i^{в}_{гвс}} = -\frac{z_г}{z_{вс} - z_г}. \qquad (7)$$

The minus sign before the expression of the transmission ratio means that the wave generator and the shaft of the flexible component have different directions of rotation.

With the standing shaft of the flexible component ($n_г=0$) from (6) we obtain

$$i^{г}_{ввс} = \frac{1}{1 - i^{в}_{ввс}} = \frac{z_{вс}}{z_{вс} - z_г}. \qquad (8)$$

From the formula it follows that the wave generator and rigid component have the identical direction of rotation.

Thus, we obtained the expressions which establish the dependence of the transmission ratio of the planetary harmonic mechanism on the transmission ratio of the same mechanism in relative motion. This procedure finds application during the determining of the transmission ratio of standard planetary mechanisms.

5. DRIVE SCHEMES

For the designation of the components of an harmonic mechanism on kinematic schemes it is necessary to introduce arbitrary representations. Table 1 gives the recommended representations of the components of the mechanism and kinematic pairs.

Figure 19a depicts the kinematic scheme of a very simple harmonic drive in the differential version. (Designations and the numbering of the components are taken as the same as in figure 17.) Figure 19b gives the scheme of a simple differential gear mechanism of the K-H-V type with a flexible shaft similar in kinematics for the transmission of the rotation of the planet pinion to a shaft coaxial with the carrier. Figure 19c and d gives the

Table 1. Arbitrary representations of components and kinematic pairs of harmonic drive mechanisms using kinematic schemes.

Name	Designation
Mechanical wave generator	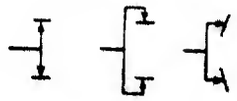
Rigid components	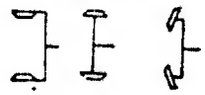
Kinematic pair: flexible component - mechanical wave generator	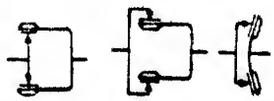
Flexible component with nonmechanical wave generator*	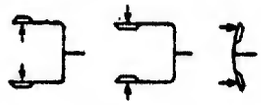

*The sign for search on the digrams of the flexible component is the presence of arrows which show in which direction the wave generator acts on it.

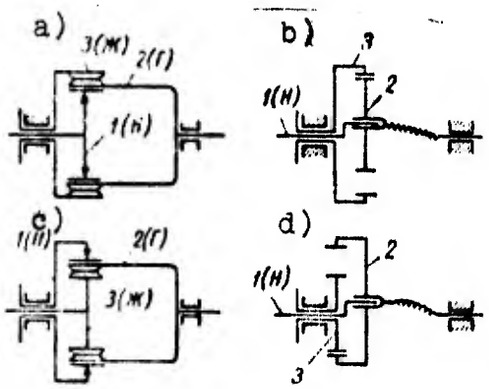

Figure 19. Kinematic drive schemes of the Г-Ж-Н type.

kinematic schemes of a harmonic gear mechanism with a wave generator which encompasses a flexible component with internal teeth similar to a mechanism of the K-H-V type whose planet pinion also has internal teeth. For such mechanisms the transmission ratio taking into account the direction of rotation of the components, is also calculated from formulas (6), (7) and (8).

It should be noted that it is advantageous to utilize mechanisms with generators which encompass the flexible component in special cases where it is not possible to obtain the layout of the drive with an internal generator. In this case one ought to consider that the use of the encompassing generators causes an increase in the overall dimensions of the mechanisms and the complication of their construction.

Thus, a standard differential or planetary mechanism corresponds to each wave mechanism. This circumstance makes it possible to utilize a diversity of schemes of standard planetary mechanisms and also known kinematic relations for wave drives. At the same time, taking into account the specific character of harmonic transmissions connected with the presence of flexible components it is expedient to introduce arbitrary designations of mechanisms distinct from those used for standard planetary drives.

The designation of a mechanism should characterize in short form the presence of different components. Let us designate the flexible components by the letter Г, rigid - Ж, and the wave generator by the letter Н. Then the above-examined harmonic mechanisms with one flexible and one rigid components and one wave generator will have the designation - Г-Ж-Н.

Great interest is presented by the harmonic drives, at the basis of which lies the mechanism Г-2Ж-Н (with one flexible component, one wave generator and two rigid components). This mechanism is similar to the planetary mechanism 2КН with two internal engagements.

The kinematic schemes of the different versions of the harmonic mechanisms Г-2Ж-Н are given in figure 20. The drive with the Г-2Ж-Н mechanism with high transmission ratios possesses very small overall axial dimensions, since the length of the flexible component

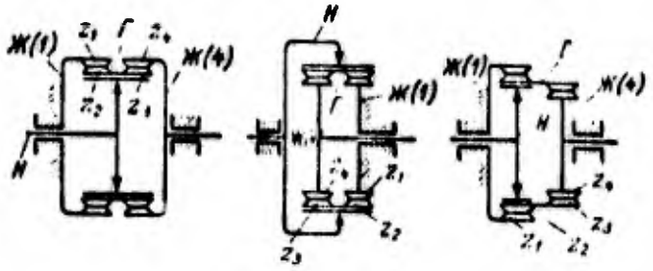

Figure 20. Kinematic scheme of drives of the Г-2Ж-Н type.

here is determined in essence by the width of two toothed rings while in harmonic mechanisms of other types, in connection with the requirement for a decrease in the misalignments of teeth in engagement and for a decrease in the stresses in the walls of the component with its deformation, it is necessary to make the components with a length equal approximately to their diameter. The surface of deformation of the flexible components in the Г-2Ж-Н mechanisms is made in the form of a cylinder, in consequence of which the misalignments of teeth in engagement are eliminated. The first two schemes, given in figure 20, are extremely constructional.

For the mechanisms considered, the transmission ratio in relative motion is determined by the expression

$$i^{H}_{14} = \frac{z_4 z_3}{z_2 z_1}. \qquad (9)$$

According to (6) we also have

$$i^{H}_{14} = \frac{n_1 - n_H}{n_4 - n_H}. \qquad (10)$$

The joint solution of (9) and (10) with $n_1=0$ gives

$$i^{1}_{H4} = \frac{n_H}{n_4} = \frac{1}{1 - \frac{1}{i^{H}_{14}}} = \frac{1}{1 - \frac{z_1 z_3}{z_2 z_4}}. \qquad (11)$$

Small overall axial dimensions with the nominal transmission ratios close to one and given with a large degree of accuracy,

can be obtained by the use of the Г-3Ж mechanism, two kinematic diagrams of which are presented in figure 21. The analog of this mechanism is 3К planetary gear.

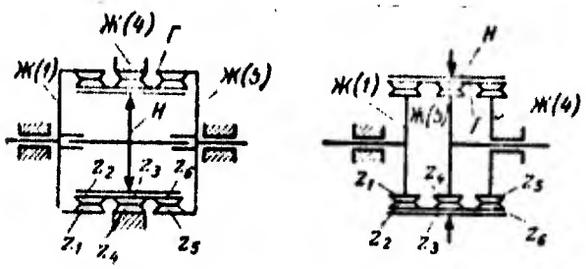

Figure 21. Г-3Ж kinematic drive scheme.

A feature of the Г-3Ж scheme is the presence of a passive wave generator, in consequence of which it does not figure in the designation of the mechanism. For the Г-3Ж mechanism it is possible to find the transmission ratio in relative motion:

$$i_{14}^{H} = \frac{z_4 z_2}{z_3 z_1} \text{ and } i_{54}^{H} = \frac{z_4 z_6}{z_3 z_5}.$$

According to (6) we also have

$$i_{14}^{H} = \frac{n_1 - n_H}{n_4 - n_H} \text{ and } i_{54}^{H} = \frac{n_5 - n_H}{n_4 - n_H}.$$

From the latter expressions with $n_4=0$, after conversion we obtain

$$i_{15}^{4} = \frac{n_1}{n_5} = \frac{1 - i_{14}^{H}}{1 - i_{54}^{H}} = \frac{1 - \frac{z_4 z_2}{z_3 z_1}}{1 - \frac{z_4 z_6}{z_3 z_5}}. \qquad (12)$$

Table 2 presents the recommended regions of transmission ratios of the harmonic mechanisms examined above. The range between the fields of use of the Г-Ж-Н and Г-2Ж-Н mechanisms can be filled because of the use of combined drives which consist of a non-harmonic gear drive and a harmonic gear drive with a Г-Ж-Н mechanism.

By the sequential connection of harmonic mechanisms unlimitedly large transmission ratios can be realized virtually. In individual cases the use of drives with closed harmonic mechanisms can be effective.

Table 2. Recommended region of the transmission ratios of harmonic mechanisms.

Designation of mechanism	Transmission ratio
Г-Ж-Н	50—300
Г-2Ж-Н	$25 \cdot 10^2$—10^5
Г-3Ж	1.02—1.05

Figure 22 depicts schemes of combined drives which consist of sequentially connected gear and harmonic mechanisms. The transmission (figure 22a) includes a simple gear mechanism with a driving wheel 1 and idlers 2, the transmission ratio of which is equal to

$$i_{1H} = -\frac{z_2}{z_1}. \qquad (13)$$

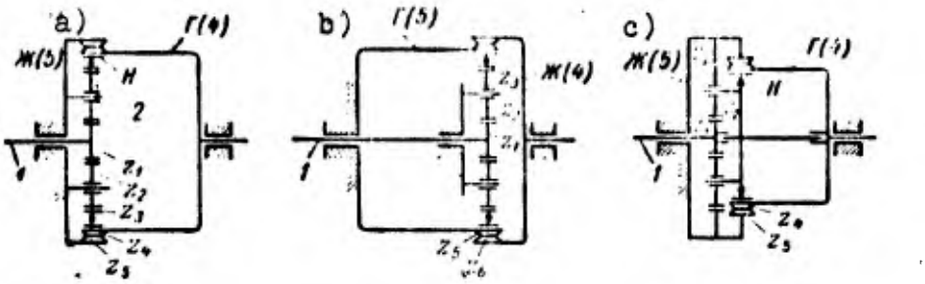

Figure 22. Kinematic schemes of combined drives.

The transmission ratio of a harmonic mechanism according to (7)

$$i^5_{H4} = -\frac{z_4}{z_5 - z_4}.$$

Then the total transmission ratio will equal

$$i^5_{14} = \frac{z_2 z_4}{z_1 (z_5 - z_4)}. \qquad (14)$$

For the scheme presented in figure 22b, the transmission ratio of the harmonic mechanism is also determined from formula (14). By accepting $i_{1H} \leq 6$, with the aid of drives (according to

figure 22a, b) it is possible to obtain the transmission ratios in the range i_{14}^{5}=300-1800.

Drive (figure 22c) includes a planetary gear mechanism with a standing central wheel which has internal teeth. The wave generator is connected with the carrier of the planetary mechanism. The transmission ratio in this case equals

$$i_{14}^{5} = -\left(1 + \frac{z_3}{z_1}\right)\frac{z_1}{z_3 - z_1} \quad (15)$$

With $\frac{z_3}{z_1} \leq 6$ it is possible to achieve transmission ratios i_{14}^{5}=350-2100.

Similar drives, if necessary, can be obtained by employing encompassing generators* in harmonic mechanisms.

The combined drives have high efficiency and also make it possible to utilize extremely effectively the space within the flexible component for the location of a high-speed motor and a decrease, in this case, in the rotational speed of the wave generator (see Chapter VI). The selection of one or another combined drive with their approximately equal kinematic characteristics is determined in essence by the possibilities of structural layout.

Figure 23 depicts the kinematic schemes of two drives which consist of successively-connected harmonic mechanisms.

In the drive given in figure 23a, the rigid components of both stages do not rotate.

---

*Translator's Note: This appears to be the best translation of the Russian word охватывающих генераторов волн. Other possible translations are: "enveloping wave generator," "encircling wave generator," and "embracing wave generator."

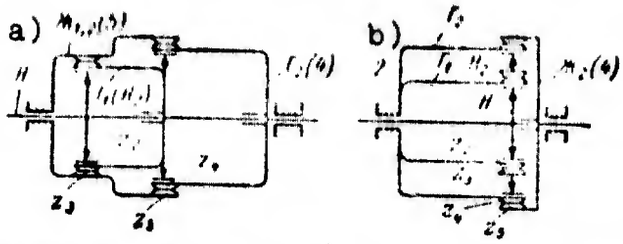

Figure 23. The successive connection of Г-Ж-Н transmissions.

On the basis of (6) let us find the total transmission ratio from the formula

$$i^{(2)}_{H1} = -\frac{z_2 z_4}{(z_3 - z_2)(z_5 - z_4)}. \qquad (16)$$

In the drive depicted on figure 23b, the flexible components do not rotate; the total transmission ratio in this case equals

$$i^{(2)}_{H1} = -\frac{z_2 z_5}{(z_3 - z_2)(z_5 - z_4)}. \qquad (17)$$

Two-stage and multistage drives with a different connection of the components of the mechanisms and also with the use of encompassing wave generators can also be created; however, their kinematic possibilities will be identical since the greatest total transmission ratios are equal to the product of the greatest transmission ratios of the base harmonic mechanisms which are part of the drive.

Closed drives are obtained with use as a basic differential wave mechanism in which the excess degree of mobility is eliminated through the establishment of a connection between the motions of any two components, i.e., the closing of the mechanism is realized. Simple geared planetary and harmonic mechanisms can be utilized as closing mechanisms. The number of different combinations of these mechanisms is rather great and in each specific case the scheme of transmission which corresponds to the kinematic, energy and structural requirements can be selected.

Let us examine the schemes of several closed drives in order to show the kinematic possibilities of the method of closing components.

Figure 24a depicts a very simple closed harmonic drive obtained from a harmonic mechanism in which the rotation of the components H and 3 is connected with the aid of a simple gear drive.

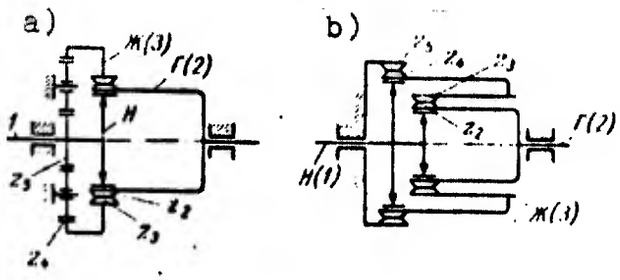

Figure 24. Kinematic schemes of closed harmonic drives.

According to (6)

$$i_{23}^{H} = \frac{n_2 - n_H}{n_3 - n_H} = \frac{z_3}{z_2}. \qquad (18)$$

At the same time

$$i_{H3} = -\frac{n_4}{n_3} = -\frac{z_4}{z_5}. \qquad (19)$$

The joint solution of equations (18) and (19) gives

$$i_{H3} = \frac{-\frac{z_3}{z_2}}{z_3 - z_3\left(\frac{z_5}{z_4} + 1\right)}. \qquad (20)$$

Investigation of this expression shows that the use of such drives makes virtually no sense, since in all cases $i_{H3} \leqslant i_{H3} \leqslant 10$.

It is also interesting to conduct an analysis of the distribution of power flows in the drive according to the scheme given in figure 24a. Let us determine the transmission ratio within the mechanism i_{21}^{H}; i_{21}^{3}. We obtain

$$i_{21}^{H} = -\frac{z_3 z_5}{z_2 z_4}; \quad i_{21}^{3} = -\frac{z_3 - z_2}{z_2}.$$

As is known [17], the ratio of the powers transferred by drives 2-H and 2-3-H which are part of the mechanism can be expressed in the following manner:

$$\frac{N_{2-H}}{N_{2-3-H}} = \frac{i_{21}^{H}}{i_{21}^{H}} = \frac{z_3 - z_2}{z_2 \frac{z_3 z_5}{z_2 z_4}}.$$

Since $\frac{z_3 - z_2}{z_2} \leq \frac{1}{50}$, it is evident that a negligible part of the power will pass through the harmonic drive. This once again confirms the inexpediency of the use of the examined scheme.

The use of planetary gears of the type 2KN with one external and one internal engagement for closing the wave mechanism is also barely effective kinematically. Such mechanisms can be obtained from the mechanisms presented in figure 22a and c if we free components 5 in them after connecting the flexible components with the support.

Broader kinematic possibilities can be obtained when using wave mechanisms as the closing mechanisms. In particular, closed drives can be formed from the mechanism presented in figure 23a by stopping component 4 and releasing component 5 and from the mechanism depicted on figure 23b by the release of component 2 and by the stopping of component 4.

The design of motor-reducer with a closed harmonic drive was given in figure 5. It should be noted that the use of closed drives to obtain large transmission ratios is not always expedient since the same effect can be obtained by simpler ways.

Let us dwell on one scheme of a closed drive with the aid of which it is possible not to increase, but to reduce the transmission ratio and thus decrease its lower limit for harmonic mechanisms. This drive (figure 24b) consists of a base harmonic mechanism with a flexible driver component and closing harmonic mechanism with a standing rigid component. The rigid component of the base mechanism is connected with the flexible closing mechanism. The transmission ratio for components 2 and 3 in relative motion will equal

$$i_{21}^{N} = \frac{n_2 - n_N}{n_1 - n_N} = \frac{z_3}{z_2}, \qquad (21)$$

at the same time the transmission ratio of the closing mechanism

$$i_{N3} = \frac{n_N}{n_3} = -\frac{z_3}{z_5 - z_4}. \qquad (22)$$

The joint solution of equations (21) and (22) it makes it possible to obtain the expression for the transmission ratio of the closed drive

$$i_{N2} = -\frac{z_2}{(z_5 - z_4)\left(1 + \frac{z_3}{z_4}\right)}. \qquad (23)$$

As an example, let us compute the value of i_{N2} for the case where z_2=90; z_3=92; z_4=100; z_5=102. According to formula (23) we will have

$$i_{N2} = -\frac{90}{(102-100)\left(1+\frac{92}{100}\right)} = -\frac{90}{3{,}84} = -23{,}4.$$

As is evident, the transmission ratio is half the minimum for the Г-2Ж-Н mechanism.

We accomplish the investigation of the power passing through the basic and closing mechanism. The transmission ratios within the drive will have the following values:

$$i_{21}^{N} = -\frac{z_3}{z_2}\left(\frac{z_5 - z_4}{z_4}\right)$$

and $$i_{21}^{3} = -\frac{z_3 - z_2}{z_2}.$$

The ratio of the powers transferred by the corresponding drives will equal

$$\frac{N_{2-N}}{N_{2-3-N}} = \frac{i_{21}^{N}}{i_{21}^{3}} \approx 1.$$

The result shows that the basic and closing wave drives transfer approximately identical powers, and the positive sign of the ratio testifies to the absence of closed power in the

mechanism. Despite the fact that according to this index the examined scheme is completely satisfactory, its use for power drives is inexpedient since the same effect can be obtained by simpler ways. At the same time, in the mechanisms of instruments with high requirements for kinematic accuracy the use of the scheme given in figure 24b can be completely justified.

Generally, the decision to use closed wave drives should be preceded by their thorough kinematic and energy analysis which can be performed by the same methods which are utilized for planetary gears [17].

Figure 25 gives the kinematic scheme of a two-wave Г-Ж-Н drive with a flat flexible component. Structurally, the flexible component takes the form of a mushroom with end teeth; its surface of deformation is a lined surface formed by three conjugate planes.

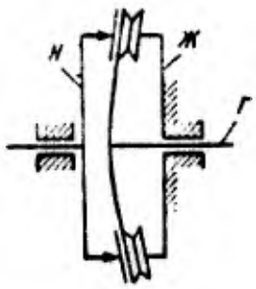

Figure 25. Kinematic scheme of a drive with a flat flexible component.

The locus of the equivelocity circles of the rigid component is a conical surface. The difference in the number of teeth of the flexible and rigid components is equal to or a multiple of the number of waves of deformation of the teeth. The transmission ratio of the examined drive is determined from formulas (7) or (8).

The presented schemes of wave drives are sufficient to show the broad kinematic possibilities of the latter. The revealed range of the rational transmission ratios of harmonic drives makes it possible to determine their place in a series of different transmission mechanisms. In the majority of cases mechanisms of Г-Ж-Н and Г-2Ж-Н should be preferable for application.

As noted above, the presence of several zones of engagement in the harmonic drives and the multiple pairing of engagement in each zone make it possible to obtain high kinematic precision of drives. According to our investigation and according to published data, the kinematic precision of a harmonic drive can be one-two degrees greater than the kinematic precision of the toothed rings of the parts of the drive. Therefore, in a number of cases it turns out to be expedient to use for precise transmissions schemes which have even unsatisfactory energy indices.

CHAPTER III

ENGAGEMENT IN HARMONIC DRIVES

6. DEFORMATION OF FLEXIBLE COMPONENTS AND ITS EFFECT ON ENGAGEMENT

The presence in the mechanism of a harmonic gear drive of a flexible component deformed during operation requires a special approach to the examination of the laws of engagement in this drive. First of all, it is necessary to determine the deformation effect of the flexible component on the form of the teeth arranged on it. With the possible values of deformation of the flexible component and also with the real relationships between the diameter of the component and the wall thickness one can hardly expect substantial change in the form of the profile and position of the teeth relative to a neutral surface. To test this proposition an experiment was conducted with a toothed ring having a wall thickness equal to 5 moduli with the number of teeth z=50. The diametric deformation of the ring was equal to two moduli. The teeth were cut by a tool with shaped angle $\alpha_0=30°$.

Figure 26 shows the form of teeth on the section of the greatest and smallest diameters of a deformed ring [5]. As is evident, even with so adverse a case, the zone of perceptible distortion of the shape does not exceed 1/3 the height of the tooth. When using thinner rings and a number of teeth $z\geq 90$ the height of the zone of distortion does not exceed 1/5 the height of the tooth and lies basically on the section of radial clearance.

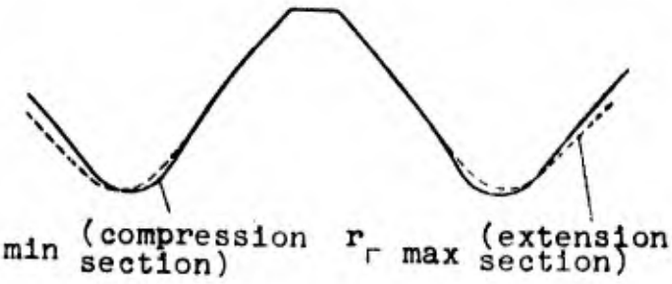

Figure 26. Deformation effect of a flexible component on the form of teeth.

Thus, the deformation of a thin flexible toothed ring by an amount up to two moduli does not cause a change in the initial form of the profiles of the teeth on the working section. This conclusion is very important for subsequent conclusions. The invariability of the profiles of the teeth in the process of the motion of the flexible component along the surface of deformation makes it possible, in the explanation of the laws of engagement, to examine the work of only one pair of teeth. Chapter II introduced the concept of equivelocity curved flexible and rigid components as the curves along which the speeds of the points of the components in motion relative to a fixed wave generator were equal.

In connection with the fact that for each mechanism the number of pairs of equivelocity curves is infinitely great, is expedient to select those curves which are disposed in the middle of the length of teeth and along which the speed of motion of the points will be constant with the constant value of angular velocity connected with the flexible component of the shaft. It is natural that this curve of the flexible component should be located in its neutral surface, since only at this surface can the segments lie whose length does not change with the deformation of the component.

If in the points which belong to the selected equivelocity curves of flexible and rigid components we arrange the apexes of some three-dimensional coordinate systems oriented in a determined manner relative to the generatrix of the flexible component and to

the equivelocity curves themselves, then it is possible to establish the connection between the coordinates of any points in these systems and, consequently, to explain the relative position of the lateral surfaces of the teeth of the flexible and rigid components in the process of their motion relative to the wave generator.

Basically, the task of the synthesis of engagement can have three solutions.

1. For the given surface of deformation, and consequently, the given form of the equivelocity curve of the flexible component, to find the form of the profiles of the teeth with which the required multiple pairing of engagement and the geometry of contact will be assured.

2. For the given technologically effective profiles of teeth of both components, to find the form of the equivelocity curve of the flexible component at which the required multiple pairing of engagement and the specific level of bending stresses in the flexible component will also be assured.

3. For the given forms of equivelocity curve and technologically effective profile of the teeth of one of the components, to find the profile of the teeth of the other component.

The concept of the "technologically effective shape of teeth" envisions the possibility of precise cutting of the teeth by highly productive methods with the use of a rather simple tool on widespread equipment. It is natural that pertaining first of all to the technologically effective shape are the involute and also circular shapes which can be cut by the rounding method on gear-milling and gear-slotting machines by hob cutters and rams. One ought to consider rectilinear shapes less technologically effective although their cutting can be performed with a sufficiently simple tool.

Special consideration is required by the question concerning the shape of the surface of deformation and, consequently, also concerning the shape of the equivelocity curve of the flexible component. It is possible to speak about the free deformation of the flexible component when it is realized by two or more equal oppositely directed forces which act in a radial direction and about the forced deformation in which the surface of deformation is determined by the form of the profile of a cam type generator, subsequently called a generator of forced deformation.

With the free deformation of the flexible component the form of the equivelocity curve is determined by the equation of the elastic line in the calculated cross section. It should be noted that as a result of the application of a working load to the teeth, the form of the curve can change. The generator of forced deformation has substantial advantages in this respect since it assures obtaining the given form of deformation and virtually its preservation in the process of the operation of the mechanism.

Any required shape of surface of deformation can be obtained by the forced method including one corresponding to free deformation. For real harmonic drives with a cylindrical flexible component, the freedom of choice of the form of equivelocity curve is limited by the greatest possible radial deformation of the flexible component, by the condition of preservation of the length of the equivelocity curve, and by the inadmissibility of a change in the sign of the curvature of equivelocity curve.

Since the value of the indicated radial deformation Δ is a function of the transmission ratio of the mechanism and lies approximately within the limits of $0<\Delta<1.5$ m, for a two-wave drive with a difference in the numbers of teeth of the components equal to two and $i_{min}=50$

$$\Delta \leqslant 0{,}01 d_{gn},$$

where d_{gn} is the diameter of the equivelocity curve of the nondeformed flexible component.

The current value of radius-vector r_g of the equivelocity curve for a cylindrical component with its free deformation by two forces is determined from Résal's formula

$$r_g = r_{cH} \mp \frac{\Delta}{0{,}297556}\left[\frac{4}{\pi} - \left(\frac{\pi}{2} - \varphi\right)\cos\varphi - \sin\varphi\right], \qquad (24)$$

where ϕ is the polar angle of the radius-vector read from the diameter of the component (figure 27a) along which the deforming forces act.

The upper sign in formula (24) pertains to the internal arrangement of the wave generator, and the lower sign pertains to the external arrangement (encompassing generator).

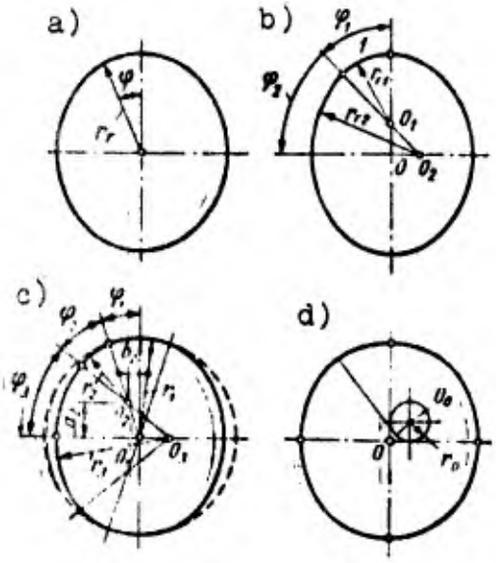

Figure 27. Different forms of equivelocity curves of flexible components.

The greatest $r_{g\ max}$ and smallest $r_{g\ min}$ radii of the curvature of the equivelocity curve determined by formula (24) can be found. For the internal arrangement of the wave generator

$$r_{g\,max} = \frac{(r_{cH} - 0{,}91828\,\Delta)^2}{r_{cH} - 4{,}27899\,\Delta}, \qquad (25)$$

$$r_{g\,min} = \frac{(r_{cH} + \Delta)^2}{r_{cH} + 5{,}27899\,\Delta}. \qquad (26)$$

The relative change in the radius of curvature of the equivelocity curve with the deformation of the flexible component characterizes the level of the stresses arising in it. It is natural that the radius of the deforming rollers of the wave generator of free deformation should be less than the minimum radius of curvature $r_{g\ min}$ after the deduction of the distance between the equivelocity curve and the surface along which the rollers roll.

Chapter VII examines the methods of shaping the wave generator of forced deformation with which the equivelocity curve can be determined by formula (24). At the same time the forced deformation of the equivelocity curve can be given not a less technologically effective, but a simpler form.

Let us examine as an example several possible versions of the deformation of a flexible component.

Figure 27b shows the equivelocity curve described by two conjugate arcs of different radii. The equivelocity curve given in figure 27c consists of three sections of constant curvature outlined by circular arcs [37], in this case, section 1 has a radius equal to $r_1=r_{sN}+\Delta$.

Figure 27d depicts the curve of variable curvature which has the form of an involute of a circle at angle $\phi=90°$.

The radii r_{s1} and r_{s2} of the sections of the curve given in figure 27b are connected by the following relationships:

$$\left.\begin{aligned} r_{sN}+\Delta &= r_{c1}+(r_{c2}-r_{c1})\sin\varphi_2,\\ \varphi_1 r_{c1}+r_{c2}\left(\frac{\pi}{2}-\varphi_1\right) &= r_{sN}\frac{\pi}{2}. \end{aligned}\right\} \qquad (27)$$

For $\phi_1=\phi_2=45°$ of (27) it follows that

$$r_{s\min}=r_{c1}=\frac{r_{sN}+\Delta-2r_{sN}\sin 45°}{1-2\cdot\sin 45°}, \qquad (28)$$

$$r_{s\max}=r_{c2}=2r_{sN}-r_{c1}. \qquad (29)$$

The radii of curvature of the equivelocity curve with three sections of constant curvature and the central angles of these sections (figure 27c) are connected by the equations

$$\left.\begin{aligned} r_2\varphi_2+r_3\varphi_3 &= \frac{\pi}{2}r_{sN}-(r_{sN}+\Delta)\varphi_1,\\ r_2\cos\varphi_1+(r_3-r_2)\sin\varphi_3 &= (r_{sN}+\Delta)\cos\varphi_1,\\ \varphi_1+\varphi_2+\varphi_3 &= \frac{\pi}{2}. \end{aligned}\right\} \qquad (30)$$

The equivelocity curve, according to figure 27d, consists of four arcs of involutes. A radius of evolutes of involutes is determined on the basis of the following considerations.

The arc length of the involute is equal to

$$L_{\psi}=0.5r_0\psi^2,$$

where r_0 is the radius of the evolute; ψ - the auxiliary angle. Then the arc length of the involute included between two mutually perpendicular normals is equal to

$$L=L_{(\psi+90^\circ)}-L_{\psi}=\frac{1}{2}r_0\left(\psi_0+\frac{\pi}{2}\right)^2-\frac{1}{2}r_0\psi_0^2=\frac{r_0\pi}{2}\left(\psi_0+\frac{\pi}{4}\right).$$

Assuming that from the condition of the retention of length of the equivelocity curve $L=\frac{\pi}{2}r_{\text{ем}}$, we will have $\frac{\pi}{2}r_{\text{ем}}=\frac{\pi}{2}r_0(\psi_0+\frac{\pi}{4})$

$$\text{and } r_0=\frac{r_{\text{ем}}}{\psi_0+\frac{\pi}{4}}. \qquad (31)$$

The value of the angle ψ_0 is found on the basis of figure 28.

On the strength of the known property of the involute which consists of the equality of the length of arc of the evolute and segment of the normal to involute MA, we have

whence $$\psi_0 r_0+r_0=r_{\text{ем}}+\Delta,$$

$$\psi_0=\frac{r_{\text{ем}}+\Delta}{r_0}-1. \qquad (32)$$

From the joint solution of relations (31) and (32) after exclusion of ψ_0 we obtain the expression for determining the radius of the evolute

$$r_0=\frac{\Delta}{0{,}214602}\approx 4{,}66\Delta. \qquad (33)$$

The initial value of the auxiliary angle in this case equals

$$\psi_0=0{,}214602\frac{r_{\text{ем}}}{\Delta}-\frac{\pi}{4}. \qquad (34)$$

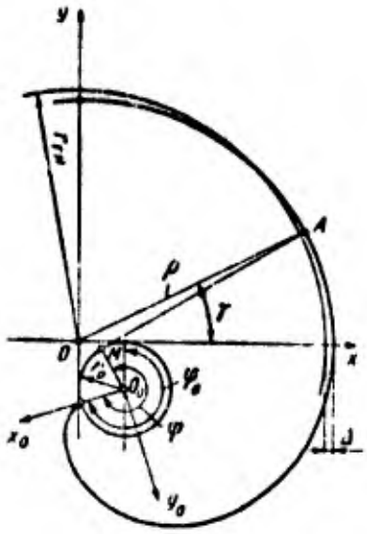

Figure 28. For the derivation of the equation of the involute of the equivelocity curve.

Then the parametric equation of the involute in coordinate system $x_0O_0y_0$ (figure 28) will be

$$\left.\begin{aligned} x_0 &= r_0 \cos\psi + r_0\psi \sin\psi, \\ y_0 &= r_0 \sin\psi - r_0\psi \cos\psi, \end{aligned}\right\} \qquad (35)$$

where ψ is the current value of the auxiliary angle.

Equation (35) can be rewritten in coordinate system xOy, whereupon it takes the form:

$$\left.\begin{aligned} x &= r_0 [\psi \cos(\psi - \psi_0) - \sin(\psi - \psi_0) + 1], \\ y &= r_0 [\psi \sin(\psi - \psi_0) + \cos(\psi - \psi_0) - 1] \end{aligned}\right\} \qquad (36)$$

or in polar coordinates

$$\left.\begin{aligned} \rho &= \sqrt{x^2 + y^2}, \\ \gamma &= \operatorname{arc\,tg} \frac{y}{x}. \end{aligned}\right\} \qquad (37)$$

Unlike Résal's curve in which the greatest positive and negative deformations are not equal, the use of an involute curve assures the equality of these deformations.

The smallest and greatest radii of curvature of the involute of the equivelocity curve on the section being examined are determined respectively from the expressions

$$r_{e\max} = r_{eH} - \Delta + r_0, \qquad (38)$$

$$r_{e\min} = r_{eH} + \Delta - r_0. \qquad (39)$$

To compare the properties of the equivelocity curves of different form, table 3 gives the maximum values of radii of curvature calculated according to formulas (25, 26), (28, 29), and (38, 39) using the following parameters of the nondeformed component and its deformation: r_{eH} =50 mm, Δ=1 mm.

For the curve, two versions are examined according to figure 27c where $\phi_1=\phi_2=\phi_3=30°$ and $\phi_1=10°$, but $\phi_2=\phi_3=40°$.

As is evident from table 3, the smallest change in the radii of 2.4 mm is provided by the use of an equivelocity curve formed by two circular arcs at angles of $\phi_1=\phi_2=45°$. The involute curve has an amount of increase in the zone of positive deformation equal to 3.65 m [sic]. In the same zone, Résal's curve has an increase in radius of 3.8 mm. The smallest decrease in the radius of curvature of the flexible component with the deformation of the latter along a curve with three sections of constant curvature and $\phi_1=30°$ will be 10.2 mm, and with $\phi_1=10°$ - 3.81 mm, i.e., the same as that of Résal's curve. At the same time, in the stressed zone the radius of curvature of the curve will be only 1 mm more than the initial one. A maximum increase in the radius with $\phi_1=10°$ and $\phi_2=\phi_3=40°$ will be 4.56 mm, i.e., more than of all other curves. Since the bending stresses with the deformation of the flexible component are proportional to an increase in the radii of curvature, most favorable for obtaining the minimum stresses is obviously the form of the curve outlined along two conjugate circular arcs.

Table 3. Comparison of the value of the radii of curvature of the equivelocity curve with different forms of deformation of the flexible component.

Equivelocity curve	r_{max}	r_{min}
According to Résal's equation	52.7	46.2
Described by two conjugate circular arcs	52.4	47.6
Involute	53.65	46.35
Described by three conjugate circular arcs with $\phi_1=30°$	59.2	39.8
Described by three conjugate circular arcs with $\phi_1=10°$	53.56	46.19

Table 4. Comparison of the form of different equivelocity curves.

Form of curve	Polar angles					
	0°	10°	20°	30°	40°	45°
Involute	51.0000	50.9386	50.7687	50.5149	50.2032	50.0347
Résal's curve	51.0000	50.9372	50.7625	50.5078	50.1993	50.0362
Two conjugate circular arcs	51.0000	50.9549	50.8090	50.5780	50.2359	50.0327
Three conjugate circular arcs	51.0000	51.0000	50.9326	50.7396	50.3894	50.1606

Let us also explain how the above examined curves on a section limited by a polar angle of 45° differ.

The results of the computation of radii of the vectors of the curves for $r_{\delta N}$=50 mm and radial deformation Δ=1 mm are reduced to table 4.

As is evident, the equivelocity curve determined by Résal's equation and the involute with $\phi \leq 45°$ virtually coincide (when $(\Delta/r_{\delta N}) \leq 1/50$ this difference in the curves is still decreased). This agreement has great significance since it makes it possible to have the identical characteristics of engagement with different nominal laws of formation of equivelocity curves and makes it possible to approximate Résal's curve with the aid of an involute.

One ought to focus attention on the comparison of different curves according to one more index which plays an important role in the process of analysis and synthesis of engagement. This index with the computation of the arc length of the curve is the possibility of operating with formulas which include integrals expressed by elementary functions. In this respect the assignment of the equivelocity curve in the form of an involute or conjugate circular arcs turns out to be very expedient.

The formulas for determining the arc length of a Résal curve includes an integral not expressed by elementary functions. A similar shortcoming is had by a number of other curves from which, in principle, it would be possible where necessary to assign the form of the equivelocity curve.

Possible versions of the solution of the problem of the synthesis of the engagement of a harmonic drive were examined above, and the properties of equivelocity curves and shapes of teeth different in form are also explained. We will now turn to an investigation of the laws of engagement. The basic law of engagement, which is most conveniently formulated in the following form, can be applied to harmonic drives in quite general form: projections of the vectors of the absolute velocities of the contact points of the profiles of the teeth of flexible and rigid components (relative to the wave generator) to a common normal to the profiles at the point of their contact should be equal.

Let us examine the engagement of two teeth, one of which belongs to a flexible, and the other to a rigid component. On the basis of the Bernoulli hypothesis and the above-expressed propositions about the deformation of teeth, we will assume that the axis of symmetry of the tooth of a flexible component regardless of the deformation of the latter is always normal to the neutral line of the walls of the flexible component with which the equivelocity curve coincides. On this normal lies the instantaneous center of curvature of the equivelocity curve at the corresponding point. Therefore, it can be considered that the tooth of the flexible component of interest to us at each point in time seemingly belongs to some cylindrical wheel, the radius of whose initial circumference is equal to the instantaneous value of the radius of curvature of the equivelocity curve of the flexible component (figure 29).

The instantaneous pitch point P_1 will be located at the point of intersection of the straight line passing through the center of the rigid wheel and the instantaneous center of curvature of the

flexible wheel with the common normal to the profiles of the teeth. The geometric point of the instantaneous pitch points can also be found.

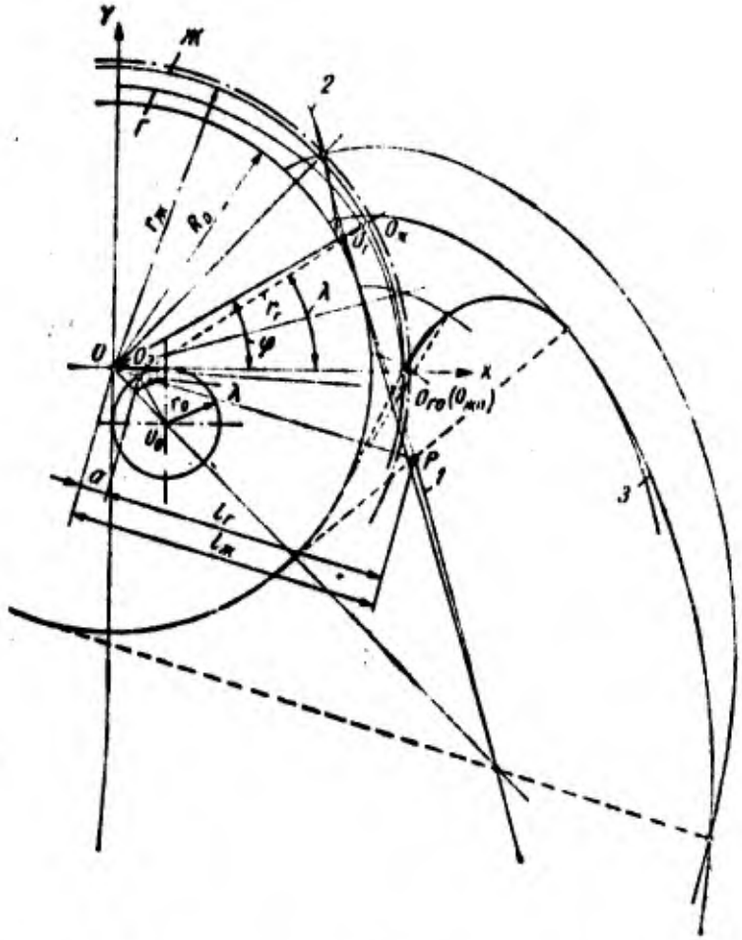

Figure 29. Study of involute engagement of harmonic drives.

At the same time the distance from instantaneous pitch point on the straight line which connects centers O and O_2 (figure 29) to these centers should be inversely proportional to the angular velocities of the wheels (rigid and flexible).

Instantaneous angular velocity of the replacing wheel is determined from the expression

$$\omega_{si} = \frac{V}{r_{si}},$$

where v is the rate of movement of the point of the component over the equivelocity curve; r_{ei} - the radius of curvature of the equivelocity curve at the point of its intersection with the axis of symmetry of the tooth.

Knowing the form of the equivelocity curve, we actually have the capability to find the position of the pitch point at each point in time through which the common normal to the teeth should pass.

If we now assign the profile of one of the teeth and find that normal which at a given moment can traverse the instantaneous pitch point, then the point from which the normal is drawn will be the point of engagement. The locus at the points of engagement will be the line of action.

Let us investigate the case of the synthesis of engagement with an involute equivelocity curve and the involute shapes of the internal teeth of a rigid component. This selection is interesting in that the equivelocity curve will have variable curvature and approximate Résal's curve, and the profiles of the teeth of the rigid component will be most technologically effective since practically the only possibility of their cutting under production conditions is connected with the use of gear-slotting equipment and involute rams.

Figure 29 depicts the equivelocity curves of a rigid component (Ж) and flexible (Г). We will assume that at the moment of the greatest deformation of the flexible component the axes of symmetry of the teeth of both components coincide with each other and with coordinate axis Ox. If we now give motion to the components with regard to a fixed wave generator with which their points $O_{ж0}$ and $O_{г0}$ will displace along the equivelocity curves at equal velocities v, then after a certain time interval these points will cover identical paths of $O_{ж0}O_{ж}$ and $O_{г0}O_{г}$, and the normal to the equivelocity curves which coincide with the axes of symmetry of the teeth will turn toward the x-coordinate axis respectively by angles ϕ and λ.

The connection between these angles is established on the basis of the equality of the path covered by points $O_{эк0}$ and $O_{в0}$.

Let us designate the arc lengths: $O_{эк0}O_{эк}=L_{эк}$ and $O_{в0}O_{в}=L_{в}$.

From the properties of the involute we have

$$L_{в} = \frac{1}{2} r_0\psi^2 - \frac{1}{2} r_0\psi_0^2,$$

but $\psi=\psi_0+\lambda$ and then

$$L_{в} = \frac{1}{2} r_0 (2\lambda\psi_0 + \lambda^2).$$

At the same time, according to figure 29 $L_{эк}=r_{эк}\phi$. By equating $L_{эк}$ and $L_{в}$, we obtain

$$\varphi = \frac{r_0}{2r_{эк}} (2\lambda\psi_0 + \lambda^2), \qquad (40)$$

where ψ_0 is determined from relation (32).

The center of curvature of any point of an involute curve Γ lies on an involute of radius r_0 at the point of tangency with it of the normal to the involute. These points at each point in time are the instantaneous centers of the corresponding replacing rigid wheels, to which the displacing tooth of flexible component belongs seemingly.

If we draw a straight line through the center of the rigid component and the instantaneous center of the replacing wheel, then it is possible to determine the position of the instantaneous pitch point on it (figure 29).

The distance from pole P to centers O and $O_{в}$ should be inversely proportional to the instantaneous angular velocities of rotation of the axes of symmetry of the teeth $\omega_{в1}$ and $\omega_{эк}$

$$\frac{l_{эк}}{l_{в}} = \frac{\omega_{в1}}{\omega_{эк}}. \qquad (41)$$

With equality of velocities $v_{в}$ and $v_{эк}$ expression (41) takes the form

$$\frac{l_{\infty}}{l_{\varepsilon}} = \frac{r_{\infty}}{r_{\varepsilon}},$$

where r_{ε} is the current value of the radius of curvature of the equivelocity curve of the flexible component.

Let us designate $l_{\infty} - l_{\varepsilon} = a$ (where a is the instantaneous interaxial distance), then

$$l_{\infty} = \frac{a r_{\infty}}{r_{\infty} - r_{\varepsilon}}. \tag{42}$$

Figure 29 shows that

$$a = \sqrt{r_0^2 (1 - \cos\lambda)^2 + r_0^2 (1 - \sin\lambda)^2} = \\ = r_0 \sqrt{3 - 2(\cos\lambda + \sin\lambda)}. \tag{43}$$

After the substitution of (43) in (42) we obtain

$$l_{\infty} = \frac{r_0 r_{\infty} \sqrt{3 - 2(\cos\lambda + \sin\lambda)}}{r_{\infty} - r_{\varepsilon}}.$$

If we accept the instantaneous value of r_{ε} according to the relation

$$r_{\varepsilon} = r_{\infty} - q - r_0 + r_0\lambda,$$

in which $q = r_{\infty} - r_{\varepsilon H} - \Delta$, then we obtain

$$l_{\infty} = \frac{r_{\infty} \sqrt{3 - 2(\cos\lambda + \sin\lambda)}}{\frac{q}{r_0} + 1 - \lambda}. \tag{44}$$

This is the polar equation of the locus of the pitch points.

Figure 29 depicts the plotting of curve 1, determined by equation (44) with q=0. It is interesting to note that in this case the form of the curve depends only on the parameters of the rigid wheel and remains constant in any transmission respects.

According to the statement of the problem, the teeth of rigid wheel have involute shapes and all normals to them are tangent to the basic circumference R_o. In order to find the instantaneous point of engagement on the working tooth profile, it is necessary to draw a normal to the tooth profile from the instantaneous pitch

point which corresponds to angle λ. This normal should be tangent to the basic circumference R_o and therefore is the only one for this position of the tooth determined by angle $\phi=f(\lambda)$.

By changing the parameter λ, the locus of the instantaneous contact points - line of action - can be found on the stationary plane. The intersection of the line of action with the addendum circle of the rigid wheel and curve of projections of the flexible wheel determines the working sections of the line of action.

As is evident from figure 29, in which the possible working sections of lines of action 2 and 3 are separated by heavy line, the total length of these sections is very small and does not satisfy the requirements for the assurance of large multiple pairing of engagement. It must be noted that a change in the possible limits of parameter q ($0<q<0.5\Delta$) does not give any perceptible effect.

A similar picture in the overlapping part will occur when using other possible equivelocity curves of variable curvature.

It is natural that in the examined case the shapes of teeth of the flexible component will be not the involute, but an envelope of the family of the involute profiles of the rigid component. The equation of these profiles can be obtained by rewriting the equation of the line of action in a mobile coordinate system with the vertex lying on the equivelocity curve and axes which coincide with the directions of the normal and the tangent to the curve. However, the very fact of the impossibility of obtaining the desired multiple pairing of engagement makes superfluous the finishing of the solution of problem to the end with the mathematical determination of the form of the profiles of teeth of the flexible component.

Let us examine the possibilities of the synthesis of engagement with an equivelocity curve given on the working section in the form of a circle (figure 27b) and the involute profile of the teeth of the rigid component. Correct engagement in this case is possible

if the profiles of the teeth of the flexible component are also involute, since we are dealing with common involute internal gearing. As is known, the engagement factor in internal gearing with a standard initial outline cannot be more than 3, which immediately determines the low theoretical multiple pairing of engagement in such a drive (actually multiple pairing will be somewhat higher).

Thus, it is impossible to obtain correct engagement with the assurance of simultaneous participation, in the work, of at least 20% of the teeth with the technologically effective involute shapes of the teeth of the rigid component. As investigations showed [6], the same conclusion can also be drawn with the use of involute teeth of the flexible component. An exception is the case where the equivelocity curve is given in the form of three conjugate circular arcs (see figure 27c) so that the radius of curvature on section 1 would be equal to the radius of the equivelocity curve of the rigid component. In this case the simultaneous engagement of the teeth along the length of section 1 occurs.

It should be noted that in certain cases engagement in accordance with this scheme can be extremely rational since almost complete gear contact on section 1, even with its limited length, and also the absence of slipping the teeth completely compensate for the shortcoming of the scheme which consists of the higher level of bending stresses on the adjacent sections of the component.

It is interesting to focus attention on the fact that with the transmission of the torsional moment in one direction not only the teeth lying along one side from the axis of symmetry of the wave of deformations participate in the work, but also the teeth lying along the other side of the axis symmetrically arranged in zone 1. Furthermore, the total area of the lateral surfaces of the teeth which are in contact and which transmit circular force will be approximately twice as large as in the case of using other forms of equivelocity curves with identical polar angles of the sections of

engagement. That is, according to the nominal value of specific pressure in the contact of teeth the drive with the form of the deformation of the flexible component according to figure 27c and $\phi_1=10°$ will be equivalent to the drive with the equivelocity curve, for example, in the form of an involute (figure 27d) with the polar angle of each of the two sections of engagement equal to 40°.

It is extremely expedient to employ engagement according to the examined scheme in drives of the Г-2Ж-Н type in the assurance of the permissible stress level, and also in drives of the Г-Ж-Н type with a gear ratio more than 150; in this case, the use of flexible components of tubular construction is preferable.

Above we noted that circular profiles can pertain to the technologically effective profiles of teeth. The fact is, that with the cutting of such shapes by the rolling method and the arrangement of the center of the arc on the initial curves of machine engagement, the circular profiles of the tool are completely duplicated on the workpiece [20]. The design and methods of manufacture of rams with circular shapes have been developed and are illuminated in [28].

Figure 30 depicts a scheme for the synthesis of engagement with circular profiles of teeth of the rigid component. The equivelocity curve of the flexible component has an involute form and, for the sake of simplicity of the solution of the problem, is tangent to the equivelocity curve of the rigid component at the point on the axis Ox (q=0). On figure 30 the construction of the line of instantaneous pitch points determined by equation (44) is also carried out.

The circular profiles of the teeth are drawn for each value of angle λ and of the corresponding value ϕ computed according to formula (40). In this regard, the centers of the circle of the profile have coordinates $a+r_{ж}$ and b in the coordinate system connected with the axis of symmetry of the tooth of the rigid component.

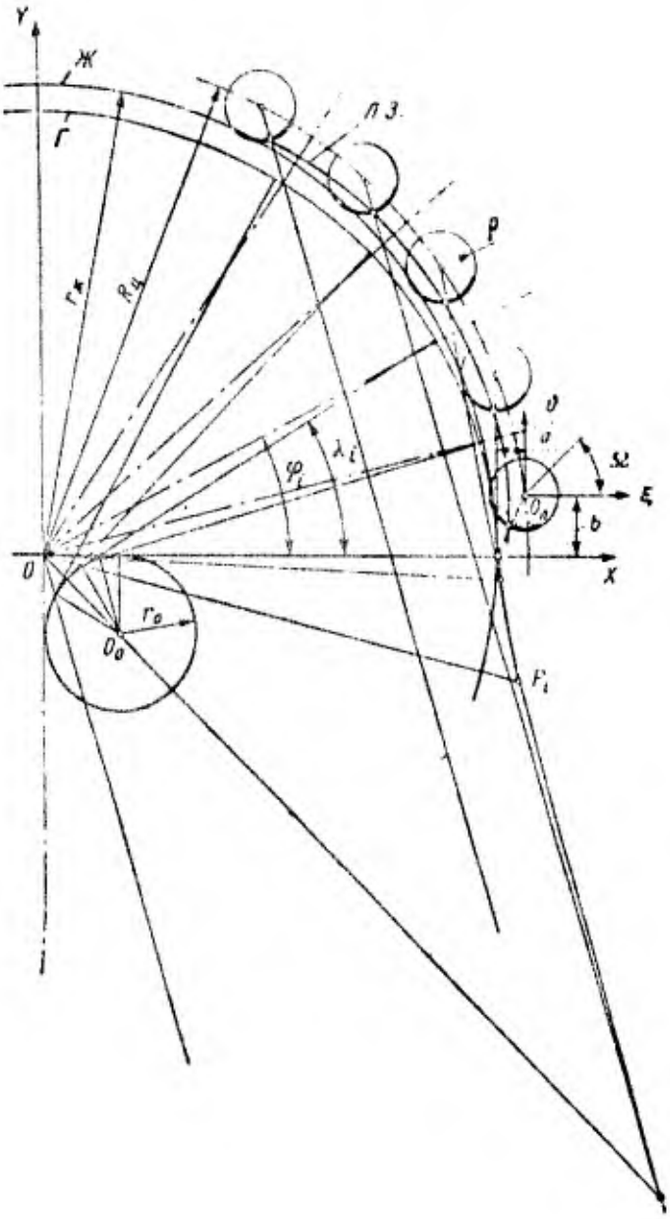

Figure 30. Synthesis of the engagement of a harmonic drive with circular profiles of teeth of the rigid component.

From the points of line of instantaneous pitch points normals are drawn to the corresponding circular profiles. The intersection of the normals to the profiles and of the profiles themselves determines the contact points, and the locus of the contact points is the line of action in a fixed plane.

As is evident from the construction, the line of action can be disposed within the limits of the height of the teeth of the rigid component on a considerable arc which assures the large multiple pairing of engagement. The profiles of the teeth of the flexible component will envelop the family of circular profiles of teeth of the rigid component in relative motion.

Examined below in general form is the analytical solution of the problem of determining the equation of the line of action and profile of the teeth of the flexible component.

The equation of the circular profiles of the teeth of the rigid component in a mobile coordinate system $\xi O_n \eta$ (figure 30)

$$\left.\begin{aligned} \xi &= \rho \cos \Omega, \\ \eta &= \rho \sin \Omega, \end{aligned}\right\} \tag{45}$$

where ρ is a radius of the arc of the profile; Ω - the polar angle read from axis $O_n\xi$. This equation, rewritten in coordinate system xOy, is an equation of the family of circles and takes the form

$$\left.\begin{aligned} x &= \rho \cos(\Omega + \varphi) + (a + r_{\infty}) \cos \varphi - b \sin \varphi, \\ y &= \rho \sin(\Omega + \varphi) + (a + r_{\infty}) \sin \varphi + b \cos \varphi, \end{aligned}\right\} \tag{46}$$

where $a+r_{\infty}$ and b are the coordinates of the center of the circle O_n.

The equation of the normal to the circles of family (46) is written in the following manner:

$$x'(X - x) + y'(Y - y) = 0, \tag{47}$$

where X and Y are the current coordinates of the normal; x and y are coordinates of the point of the circle through which the normal passes.

After the computation of derivatives the equation takes the form:

$$\frac{X - x}{\cos(\Omega + \varphi)} = \frac{Y - y}{\sin(\Omega + \varphi)}. \tag{48}$$

If we separate from the congruence of the normals those normals which for a given position of the axis of symmetry of the tooth determined by the angle ϕ pass through the corresponding instantaneous pitch point, we will obtain the coordinates of a specific pitch point.

The coordinates of the position of the instantaneous pitch point are found from the construction given in figure 30, taking into account (44)

$$\left.\begin{aligned} x_p &= \frac{r_{\infty}(1-\sin\lambda)}{\frac{q}{r_0}+1-\lambda}, \\ y_p &= \frac{r_{\infty}(1-\cos\lambda)}{\frac{q}{r_0}+1-\lambda}. \end{aligned}\right\} \qquad (49)$$

Equating in (48) $X=x_p$ and $Y=y_p$, after conversions we obtain the equation of the engagement

$$\frac{y-y_p}{x-x_p} = \operatorname{tg}(\Omega+\varphi). \qquad (50)$$

The connection between angles ϕ and λ is established on the basis of (40). Angle ϕ_0 is determined from formula (34), and r_0 from (33).

Utilizing expressions (46), (49), (50), (40), and (32), we obtain a system of equations which determine the coordinates of the points of the line of action (in figure 30, Л. 3.) for each value of angle ϕ:

$$\left.\begin{aligned} x &= \rho\cos(\Omega+\varphi)+(a+r_{\infty})\cos\varphi - b\sin\varphi, \\ y &= \rho\sin(\Omega+\varphi)+(a+r_{\infty})\sin\varphi + b\cos\varphi, \\ &\frac{y\left(\frac{q}{r_0}+1-\lambda\right)-r_{\infty}(1-\cos\lambda)}{x\left(\frac{q}{r_0}+1-\lambda\right)-r_{\infty}(1-\sin\lambda)} = \operatorname{tg}(\Omega+\varphi), \\ &\varphi = \frac{r_0}{r_{\infty}}\left(\frac{\lambda^2}{2}-\lambda\right)+\frac{1}{r_{\infty}}(r_{cs}+\Delta)\lambda. \end{aligned}\right\} \qquad (51)$$

With the aid of the formulas of conversion, equation (51) can be rewritten in a mobile coordinate system connected with the axis of symmetry of the flexible component. In this form it will represent the equation of the profile of the flexible component. The profile of the teeth of the flexible component is a curve of the equidistant trajectory of the center of the circular profile of the rigid component in relative motion. In connection with this, by knowing the equation of this trajectory it is possible to find the tooth profile of the flexible component. By rewriting the coordinates of the center of the circular profile from the coordinate system of the rigid component in the system connected with the axis of symmetry of the tooth of the flexible component taking into account the designations given in figure 30, we obtain equations (with $q \neq 0$):

$$x = (a + r_{ж}) \cos(\varphi - \lambda) - b \sin(\varphi - \lambda) + r_0 (\sin\lambda - \cos\lambda + 1 - \lambda) \quad (r_{ж} = q),$$

$$y = (a + r_{ж}) \sin(\varphi - \lambda) + b \cos(\varphi - \lambda) + r_0 (\sin\lambda + \cos\lambda - 1),$$

in which, on the basis of (40) and (51) with $r_{вн} + \Delta = r_{ж} - q$

$$\varphi - \lambda = \frac{1}{r_{ж}} \left[r_0 \left(\frac{\lambda^2}{2} - \lambda \right) - q\lambda \right].$$

Figure 31 shows the tooth profile of a flexible component obtained by bending the teeth of the rigid component with a circular profile with $z_{ж} = 100$ and $\rho = 1.55 m_y$ (see section 8). Chapter VII examines a method of cutting the teeth of the flexible component in which the process of the bending of these teeth by the teeth of the rigid component is automatically reproduced.

It is also necessary to explain the possibility of using circular profiles of teeth in the case of using an equivelocity curve outlined by two conjugate circular arcs.

With convex circular shapes of the teeth of the rigid component and the constant curvature of the equivelocity curve of the flexible

component, on the working section an extra-centroid epicycloidal cogging with large multiple pairing will occur [17]. A diagram of this engagement is shown in figure 32.

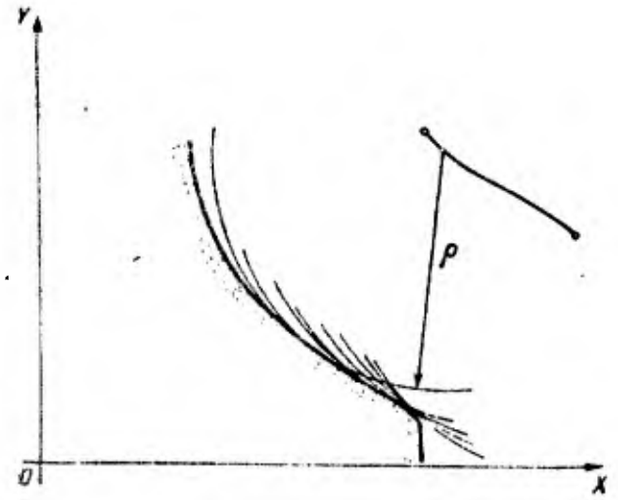

Figure 31. Determining the form of the profile of the teeth of a flexible component with circular profiles of a rigid component.

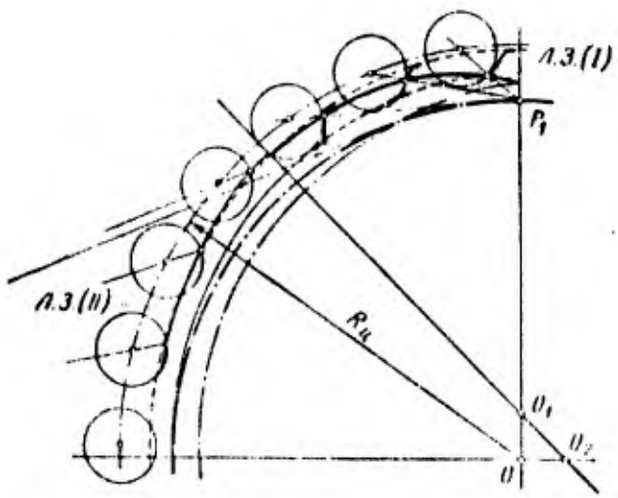

Figure 32. Diagram of extra-centroid epicycloidal cogging of a harmonic drive.

Thus, the construction of theoretically precise technologically effective gearing with the assurance of large multiple pairing is possible on the basis of the use of circular profiles of the internal teeth of the rigid component. At the same time, an essential shortcoming of such gearing is the impossibility of giving the value of radii of circular profiles ρ greater than the pitch of the teeth, in connection with which the extremely low cited* radii of curvature are obtained which causes the appearance of high contact stresses in the places of gear contact. This circumstance should be considered when selecting the scheme of engagement, especially for power drives. Furthermore, the use of small moduli in harmonic drives can cause great difficulties during the manufacture of special tools for cutting teeth with circular profiles.

Above it was shown that the use of technologically effective involute profiles of teeth does not assure obtaining the correct engagement with large multiple pairing in harmonic drives. At the same time, in the practice of reduction-gear construction approximate engagements with the theoretically nonconjugate lateral surfaces of teeth are widely applied. At the basis of the construction of the approximate engagements lies the requirement for the assurance of minimum nonconjunction commensurable with the errors in the manufacture of the elements of the gearing. By nonconjugation in this case we mean the disruption of the constancy of the velocity of motion of the vertex of the coordinate system connected with a tooth of the flexible component along the equivelocity curve of this component with a constant velocity of motion of the vertex of the coordinates of a tooth of the rigid component along the corresponding equivelocity curve.

In connection with harmonic drives the task of the synthesis of the approximate engagement should be reduced to determining the form and parameters of the deformation of the flexible component in which the technologically effective shapes of the teeth will

---

*Translator's Note: May also be "reduced radii."

assure their minimum nonconjunction in the process of joint operation.

Investigations on the selection of the most advantageous form of deformation of the flexible component with the technologically effective involute profiles of the teeth show that a decrease in the nonconjunction of the teeth is achieved by means of an increase in the radius of curvature of the equivelocity curve of the flexible component at points lying on the greatest diameter, and by the approach of the value of this radius to the radius of the equivelocity curve of the rigid component. With the identical value of diametric deformation, an increase in the indicated radii of curvature leads to an increase in the stresses which appear in the wall of the flexible component.

How should the problem of the selection of the form and parameters of deformation of the flexible component be solved?

The goal is reached most effectively by the assignment of an equivelocity curve with three conjugate circular arcs according to figure 27c with $\phi_1=10°$. In this case, the selection of the value of the shaped angle of the teeth plays virtually no role although at the moment of the emergence of the teeth from contact, to avoid their interference it is desirable to have the largest possible value of the angle. There is considerable interest (at least at the present stage of development of the designs of harmonic drives and their placement into production) in the use of widespread tools with $\alpha_0=20°$.

The required increase in the shaped angle of the teeth of the flexible and rigid components in this case can be accomplished through the selection of the corresponding extensions of the initial outline.

In connection with the fact that the full investigation of the work of flexible components with an equivelocity curve according

to figure 27c still is not finished, we cannot recommend this form of deformation for drives of the Г-Ж-Н type with i<150, or with the flexible components which have the form of a cup with a stop-end or circular bottom. In these cases, one ought to recommend a simpler and more sufficiently investigated form of deformation of the flexible component in accordance with figure 27a, b, d. As will be shown below, because of the selection of the shifts of the initial outline and value of deformation, it is also possible with the indicated equivelocity curves to insure the sufficiently good coupling of the teeth and the multiple pairing of the contact. At the same time, the calculation of the geometry of the drives and the technology of the manufacture of the parts of the wave generators for the achievement of deformation in accordance with figure 27a, b, d are sufficiently developed and simple.

The recommended three forms of deformation with equivelocity curves according to figure 27a, b, d are approximately equivalent in their qualitative indices; therefore, we believe that the use of one form or the other of the curve should be determined by the technological possibilities of the production in which the manufacture of the drives is assumed.

7. THE GEOMETRY OF APPROXIMATE ENGAGEMENT

Basically the task of the synthesis of the approximate engagement can be solved in the following manner. The equation of the family of profiles of teeth of the rigid component is written in a mobile coordinate system connected with the axis of symmetry of the tooth of the flexible component and the parameters with which the minimum width of the region occupied by the family on a specific section and also the required position of the region of the family concerning the assigned tooth profile of the flexible component will be obtained are determined.

Let us examine the synthesis of the approximate engagement of a two-wave drive with an involute equivelocity curve of the flexible component and involute profiles of teeth of both components.

The pitch of the teeth t on the equivelocity curve of the flexible component is determined by the ratio of the length of the curve L to the number of teeth z_g.

Since $L=2\pi r_{gH}$,

$$t = \frac{L}{z_g} = \frac{2\pi r_{gH}}{z_g}.$$

We introduce the concept of the *conditional modulus* m_y in accordance with the equivelocity curve. Then the expression will occur

$$m_y = \frac{t}{\pi} = \frac{2r_{gH}}{z_g}.$$

It is possible to establish the relation between the conditional modulus and the modulus of the tool by which the flexible component is cut

$$m_y = \frac{m}{z_c}\left|z_c - 2(f_0 + c_0) + 2\xi_g - \vartheta\right|, \qquad (52)$$

where f_0 and c_0 are the parameters of the initial outline; ξ_g - the extension factor of the initial outline in cutting of the flexible component; $\vartheta = \frac{\delta}{m_y} = \frac{\delta}{m}$ - the coefficient of the wall thickness of the flexible component on the section of the arrangement of the teeth (δ - wall thickness).

The value of the radial deformation of the flexible component Δ is expressed as a conditional modulus in the following manner:

$$\Delta = k_\Delta m_y. \qquad (53)$$

Let us find the equation of the family of involute profiles of the rigid component in the coordinate system of a tooth of the flexible component.

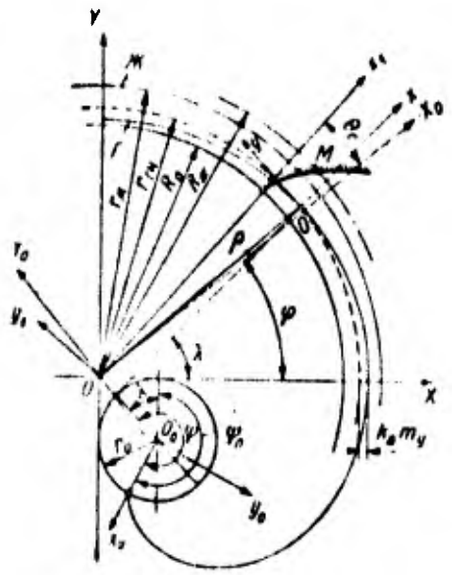

Figure 33. Diagram for the synthesis of approximate engagement with an involute equivelocity curve.

According to fig. 33, the equation of the involute tooth profile of the rigid component in coordinate system x_1Oy_1 will be

$$\left.\begin{aligned} x_1 &= R_0(\cos\varepsilon + \varepsilon\sin\varepsilon),\\ y_1 &= R_0(\sin\varepsilon - \varepsilon\cos\varepsilon), \end{aligned}\right\} \qquad (54)$$

where ε is an auxiliary angle.

Rewriting equation (54) in the coordinate system xOy whose axes are tangent and normal to the involute equivelocity curve which has the radius of the involute r_0 determined from formula (33), we obtain:

$$\left.\begin{aligned} x &= R_0\{(\cos\varepsilon + \varepsilon\sin\varepsilon)\cos(\lambda - \varphi - \theta_e) + \\ &+ (\sin\varepsilon - \varepsilon\cos\varepsilon)\sin(\lambda - \varphi - \theta_e)\} + r_0(\sin\lambda - \\ &- \cos\lambda + 1 - \lambda) - r_{\text{ж}} + (1 - k_\Delta)m_y;\\ y &= R_0\{(\sin\varepsilon - \varepsilon\cos\varepsilon)\cos(\lambda - \varphi - \theta_e) - \\ &- (\cos\varepsilon + \varepsilon\sin\varepsilon)\sin(\lambda - \varphi - \theta_e)\} + r_0(\sin\lambda + \\ &+ \cos\lambda - 1), \end{aligned}\right\} \qquad (55)$$

where λ is an auxiliary polar angle of the mobile coordinate system xOy in system XOY; $\phi=f(\lambda)$ - the polar angle of the mobile coordinate system of the rigid component X_0OY_0 in system XOY; θ_e - a polar angle of the point of an involute profile lying on axis OX_0. The dependence of the angle ϕ on angle λ is established by formula (40).

If we assume that the cutting of internal involute teeth of the rigid component is performed by the rolling method by gear cutters and at some radius $R_{\text{ж}}$ the indentations will have angular thickness 2γ, then it is possible to write the expression for determining the angular difference ($\lambda - \phi - \theta_e$) which enters equation (55)

$$\lambda - \varphi - \theta_e = \frac{2\lambda + k_\Delta\left(\frac{2\lambda - \lambda^2}{0{,}2146\,02} - 2\lambda\right)}{z_{\text{ж}}} - \gamma - \operatorname{inv}\alpha_{\text{ж}}, \qquad (56)$$

where $\alpha_{\text{ж}}$ is an angle of the profile of the involute on radius $R_{\text{ж}}$.

From an examination of equations (55) and (56) it follows that with given $z_{эс}$ and $\alpha_{эс}$ the only independent parameter which affects the properties of the family is k_{Δ}. A change in value of k_{Δ} leads to a change in the form and slope of trajectory of the points of the involute profile of the teeth of the rigid component in the coordinate system of the flexible component with the relative motion of the teeth and to a change in the thickness of the layer of the family of these profiles.

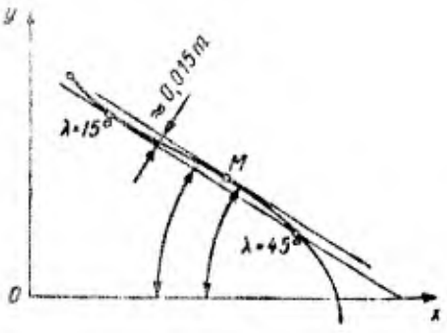

Figure 34. Trajectory of point M of the tooth profile of a rigid component in the coordinate system of a tooth of the flexible component.

For $z_{эс} \geq 100$, the trajectory curvature of the points of the involute tooth profile of the rigid component in the coordinate system of a tooth of the flexible component on a section characterized by $10° < \lambda < 45°$ is very small and approximately equal to the curvature of the involute shape itself, i.e., fig. 34 (for $z_{эс}=100$ the height of the arrow of the arc of the profile does not exceed 0.015m and with an increase in the number of teeth it increases somewhat).

Equating the tangent of the angle between the tangent to the tooth profile of the rigid component at point M (lying on circumference $R_{эс}$) and the axis of symmetry of the indentation of the tooth to the tangent of the slope angle of the secant of the trajectory of point M (in coordinate system xOy) which intersects the trajectory at the points determined by angles $\lambda=45°$ and $\lambda=15°$ will give us the equation for determining the value of the coefficient of k_{Δ} with which the greatest thickness of the region of the family on the section characterized by values $5<\lambda<45$, for $z_{эс} \geq 100$ will have the minimum value. The conjunction of the teeth beyond the section limited by $\lambda=45°$ is impossible since the profiles of the teeth interfere. The working depth of the teeth in this case should be such as to eliminate contact of the teeth beyond the limits of the section taken.

Extension of the working section of engagement by an angle larger than 45° with the corresponding increase in the working depth leads to an increase in the thickness of the region of the family and nonconjunction of the teeth. A decrease in the maximum angle λ and in the nonconjunction of the teeth is connected with a decrease in the working depth and an increase in the working specific pressure on the lateral surfaces of the teeth, which is irrational. When $\lambda=45°$ the thickness of the region of the family on the average corresponds to the tolerance level for the profile for the involute wheels manufactured according to the 7th degree of accuracy (GOST (All-Union state standard) 9178-59).

In general form, the equation for the determination of the value of k_Δ with an involute equivelocity curve is written in the following form:

$$\frac{\begin{array}{l}R_0\,|B(\cos\beta_1-\cos\beta_2)-A(\sin\beta_1-\sin\beta_2)|+\\ +r_0(\sin\lambda_1-\sin\lambda_2+\cos\lambda_1-\cos\lambda_2)\end{array}}{\begin{array}{l}R_0\,|B(\sin\beta_2-\sin\beta_1)+A(\cos\beta_2-\cos\beta_1)|+\\ +r_0(\cos\lambda_2-\cos\lambda_1-\sin\lambda_2+\sin\lambda_1+\lambda_2-\lambda_1)\end{array}}=\operatorname{tg}\left[\alpha_{x}-\gamma+\frac{2\lambda_{cp}+k_\Delta\left(7{,}32\lambda_{cp}-4{,}66\lambda_{cp}^2\right)}{z_x}\right], \tag{57}$$

where

$$R_0=\frac{1}{2}\,mz_x\cos\alpha_0;$$

$$r_0=4{,}66m_y k_\lambda;$$

$$m_y=m\left[z_x-2(f_0+c_0)+2\xi_x-\theta\right];$$

$$\beta_1=\lambda_1-\varphi_1-\theta_1;$$

$$\beta_2=\lambda_2-\varphi_2-\theta_2;$$

$$\text{for } \lambda_2=45°\quad \beta_2=\frac{0{,}5\pi+k_\Delta 2{,}87439}{z_x}-\gamma-\operatorname{inv}\alpha_x;$$

$$\text{for } \lambda_1=15°\quad \beta_1=\frac{0{,}523598+k_\Delta 1{,}59688}{z_x}-\gamma-\operatorname{inv}\alpha_x;$$

$$\cos\alpha_x=\frac{R_0}{R_x},\quad R_x=\frac{1}{2}(z_x+2\xi_x)m,$$

$$\xi_{ж} = \xi_{\varepsilon} - \left(1 - k_{\Delta}\frac{m_{\mu}}{m}\right),$$

$$\gamma = \frac{0{,}5\pi + 2\xi_{ж}\operatorname{tg}\alpha_{\partial}}{z_{ж}} + \operatorname{inv}\alpha_{\partial} - \operatorname{inv}\alpha_{ж};$$

$$B = \sin e - e\cos e;$$

$$A = \cos e + e\sin e;$$

$$e = -(\alpha_{ж} + \operatorname{inv}\alpha_{ж}) = -\operatorname{tg}\alpha_{ж};$$

$$\lambda_{ср} = \frac{\lambda_1 + \lambda_2}{2}.$$

Depending on availability a tool with the initial outlines according to the GOSTs 3058-64 and 9587-61 or with the initial outline used for involute spline joints can be utilized. The initial outline for spline joints has $\alpha_{\partial}=30°$; in this case it is advantageous to accept $\xi_{\varepsilon}=0$. For the initial outlines with $\alpha_{\partial}=20°$, for purposes of the rectification of the trajectory of point M (fig. 34) one ought to use the angles of the profile on the circumference $R_{ж}\alpha_{ср} \geq 25°$ which is obtained due to the extension of the initial outline.

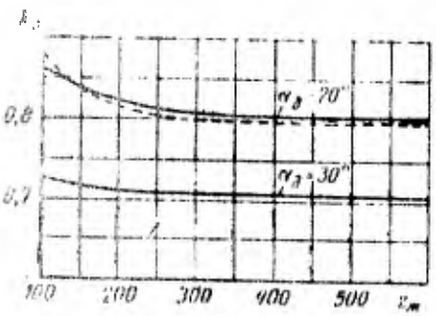

Figure 35. Graph for determining the profile coefficients of a flexible component.

It is recommended that the extension factor be selected according to formula $\xi=0.022\ z_{\varepsilon}$. Figure 35 depicts the graphs $k_{\Delta}=f(z_{ж})$ obtained as a result of the calculations for the cases $\alpha_{\partial}=30°$, $\xi_{\varepsilon}=0$ and $\alpha_{\partial}=20°$ and $\xi_{\varepsilon}=0.022\ z_{\varepsilon}$. Values of k_{Δ} taken from the graphs are utilized for the geometric calculation of the drive. For the heavily loaded drives and drives with nonmetallic flexible components, for purposes of the compensation of the deformations of teeth one ought take k_{Δ} 0.1 more than on the graph (fig. 35).

The formulas and an example of the geometric calculation of a drive with approximate engagement for $\alpha_{\partial}=20°$ are given in table 5, for $\alpha_{\partial}=30°$ - in table 6. As is evident from the tables and the graph given in fig. 35, the use of the angle $\alpha_{\partial}=30°$ makes it possible to use the lesser value of deformation, and also a lesser

Table 5. Formulas and an example of the geometric calculation of a two-wave drive for $\alpha_0 = 20°$ with i=115; $z_g = 228$; $z_ж = 230$; m=1 mm; $f_0 = 1$; $c_0 = 0.25$.

Parameter	Designation	Calculation formula	Example of the calculation
Deformation coefficient of the flexible component	k_Δ	Selected according to graph fig. 38	$k_\Delta = 0{,}81$
Coefficient of the wall thickness of the flexible component	θ	Selected according to graph fig. 51	$\theta = 2$ Beneath the teeth we take $\theta = 2.5$
Extension factor of the initial outline of the teeth of the flexible component	ξ_c	$\xi_c = 0{,}022 z_c$	$\xi_c = 0{,}022 \cdot 228 = 5$
Conditional modulus	m_y	$m_y = m\left[\frac{z_c - 2(f_0 + c_0) + 2\xi_c - \theta}{z_c}\right]$	$m_y = 1\left[\frac{228 - 2(1 + 0{,}25) + 2 \cdot 5 - 2{,}5}{228}\right] = 1{,}022$
Radius of the neutral circumference of the non-deformed flexible component	r_{cn}	$r_{cn} = 0{,}5 z_c m_y$	$r_{cn} = 0{,}5 \cdot 228 \cdot 1{,}022 = 116{,}3$ мм
Pitch circle diameter of the flexible component	d_{dc}	$d_{dc} = z_c m$	$d_{dc} = 228 \cdot 1 = 228$ мм

Parameter	Designation	Calculation formula	Example of the calculation
Pitch circle diameter of the rigid component	$d_{\partial ж}$	$d_{\partial ж} = z_ж m$	$d_{\partial ж} = 230 \cdot 1 = 230$ мм
Diameter of the circumference of the projections of the flexible component	$D_{ек}$	$D_{ек} = d_{\partial к} + 2\xi_ж m$	$D_{ек} = 228 + 2 \cdot 5 \cdot 1 = 238$ мм
Expansion factor of the initial outline for the rigid component	$\xi_{ж}$	$\xi_{ж} = \xi_к - \left(1 - k_\Delta \frac{m_y}{m}\right)$	$\xi_{ж} = 5 - \left(1 - 0{,}81 \frac{1{,}022}{1}\right) = 4{,}829$
Radius of the equivelocity circumference of rigid component	$r_ж$	$r_ж = 0{,}5 z_ж m_y$	$r_ж = 0{,}5 \cdot 230 \cdot 1{,}022 = 117{,}6$ мм
Diameter of the circumference of the projections of the rigid component	$D_{еж}$	$D_{еж} = d_{\partial ж} - 2(f_0 - \xi_ж) m$	$D_{еж} = 230 - 2(1 - 4{,}829) \cdot 1 = 237{,}66$ мм
Radius of the evolute of the equivelocity curve of the flexible component	r_0	$r_0 = \frac{k_\Delta m_y}{0{,}214602}$	$r_0 = \frac{0{,}81 \cdot 1{,}022}{0{,}214602} = 3{,}40$ мм

working depth of the teeth, than with $\alpha_\partial = 20°$; in this case, naturally, the use of special rams is required.

Figure 36 gives the structure of the family profiles of the tooth of the rigid component in the coordinate system of a tooth of the flexible component for a drive with $z_{жс} = 180$, $z_г = 178$, $\alpha_\partial = 30°$, and $k_\Delta = 0.72$. The dashed line shows the position of the tooth profile of the flexible component. From the figure it follows that on the section $10° < \lambda < 45°$ the almost full coincidence of the profiles occurs. Figure 36 also shows that the trajectory of the edge of the internal tooth of the rigid component after the point characterized by angle $\lambda = 45°$ intersects the tooth profile of the flexible component and if with $\alpha_\partial = 30°$ we accept $h_г = m$, then in the first operating period of the drive the teeth of both components will make contact actually with the upper edges in the zone $45° < \lambda < 55°$. Therefore the working depth of approach is taken as $h_г = m$ with $\alpha_\partial = 20°$ and $h_г = 0.8m$ with $\alpha_\partial = 30°$; in this case, nevertheless, in the first moment of work the teeth make contact with the upper edges.

The gradual increase in the load in process of the breaking-in of the drive and the deformation of the teeth occurring in this case cause the rapid wear of the edges of the teeth, which will continue to the start of the work of the teeth on the entire arc of engagement and the equalizing of the level of specific pressures in their contact. As the experimental study showed, this process of breaking-in the teeth with the rounding of the edges occurs extremely rapidly.

Realization of contact in the period of break-in wear by precisely the upper edges of the teeth is intentionally envisioned during the development of the system of engagement since this contact occurs at the moment when the teeth of the flexible component are located on the section of the equivelocity curve, the radius of curvature of which is equal to the radius of the central line of the nondeformed part. Local bending stresses in the root of the teeth in the wall of the flexible component as a result of its

Table 6. Formulas and an example of the geometric calculation of a two-wave drive for $\alpha_\beta = 30^\circ$ with i=115, $z_g = 228$; $z_{ж} = 230$; m=1; $f_0 = 0.5$; $c_0 = 0.385$.

Parameter	Designation	Calculation formula	Example of the calculation
Deformation coefficient of the flexible component	k_Δ	Selected according to graph fig. 38	$k_\Delta = 0{,}71$
Coefficient of the wall thickness of the flexible component	ϑ	$\vartheta = \frac{[\sigma]}{E}\left(\frac{z_r}{7{,}32 k_\Delta} - 1\right) z$	$\vartheta = \frac{500}{2{,}1 \cdot 10^5}\left(\frac{228}{7{,}32 \cdot 0{,}71} - 1\right) 228 = 2{,}32$
Extension factor of the initial outline for a flexible component	ξ_z	$\xi_z = 0$	$\xi_z = 0$
Conditional modulus	m_y	$m_y = m\left[\frac{z_r - 2(f_0 + c_0) + 2\xi_z - \vartheta}{z_r}\right]$	$m_y = 1\left[\frac{228 - 2(0{,}5 + 0{,}385) - 2{,}32}{228}\right] = 0{,}982$ мм
Radius of the neutral circumference of the nondeformed flexible component (equivelocity circumference)	r_{zN}	$r_{zN} = 0{,}5 z_r m_y$	$r_{zN} = 0{,}5 \cdot 228 \cdot 0{,}982 = 112$ мм
Pitch circle diameter of the flexible component	d_{dz}	$d_{dz} = z_g m$	$d_{dz} = 228 \cdot 1 = 228$ мм

Parameter	Designation	Calculation formula	Example of the calculation
Pitch circle diameter of the rigid component	$d_{\partial ж}$	$d_{\partial ж} = z_{ж} m$	$d_{\partial ж} = 230 \cdot 1 = 230$ мм
Diameter of the circumference of the projections of the flexible component	$D_{ег}$	$D_{ег} = d_{\partial г} + 0{,}6m$	$D_{ег} = 228 + 0{,}6 \cdot 1 = 228{,}6$ мм
Extension factor of the initial outline for a rigid component	$\xi_{ж}$	$\xi_{ж} = \xi_{г} - \left(1 - k_{\Delta} \frac{m_y}{m}\right)$	$\xi_{ж} = 0 - \left(1 - 0{,}71 \frac{0{,}982}{1}\right) = -0{,}304$
Radius of the equivelocity circumference of the rigid component	$r_{ж}$	$r_{ж} = 0{,}5 z_{ж} m_y$	$r_{ж} = 0{,}5 \cdot 230 \cdot 0{,}982 = 112{,}9$ мм
Diameter of the circumference of the projections of the rigid component	$D_{ежс}$	$D_{ежс} = d_{\partial г} - 2(f_0 - \xi_{ж}) m$	$D_{ежс} = 230 - 2(0{,}5 + 0{,}304) \cdot 1 = 228{,}39$ мм
Radius of the evolute of the equivelocity curve of the flexible component	r_0	$r_0 = \frac{k_{\Delta} m_y}{0{,}214602}$	$r_0 = \frac{0{,}71 \cdot 0{,}982}{0{,}214602} = 2{,}83$ мм

deformation are absent on this section, and the higher level of bending stresses of the teeth is not dangerous.

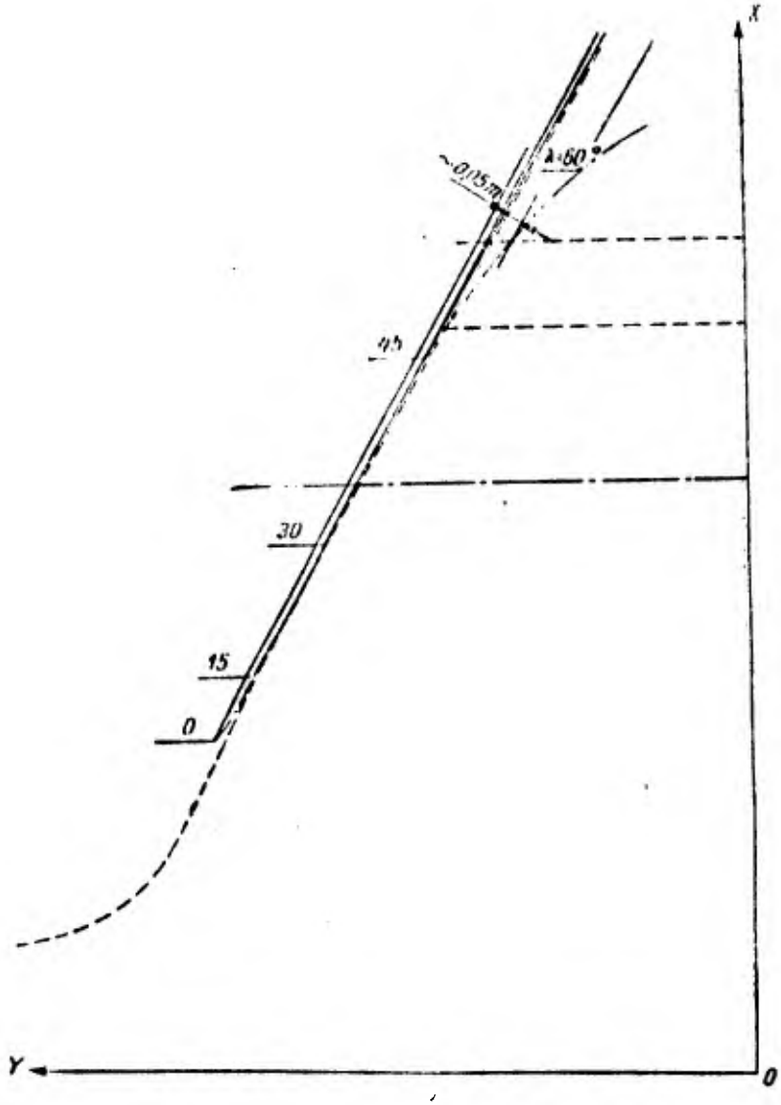

Figure 36. Family of the profiles of teeth of the rigid component in the coordinate system connected a tooth of a flexible system.

Analogously, the synthesis of the approximate engagement is accomplished with the circular form of the equivelocity curve of the flexible component on the working section and the involute shapes of the teeth. Above it was noted that the use of this form of equivelocity curve makes it possible to accomplish precise involute gearing; however, in this case one of the important

properties of harmonic drives cannot be realized - the large multiple pairing of engagement.

The equation of the involute profiles of teeth of the rigid component assigned in coordinate system x_0Oy_0 (fig. 37) and rewritten in the coordinate system xOy, the horizontal axis of which coincides with the radius of the circular equivelocity curve and the vertical axis tangent to this curve, takes the form

$$\left.\begin{aligned} x &= R_e[\cos(\varepsilon + 0_e + \varphi - \lambda) + \varepsilon \sin(\varepsilon + \\ &\quad + 0_e + \varphi - \lambda)] - a\cos\lambda; \\ y &= R_e[\sin(\varepsilon + 0_e + \varphi - \lambda) - \varepsilon\cos(\varepsilon + \\ &\quad + 0_e + \varphi - \lambda)] + a\sin\lambda, \end{aligned}\right\} \qquad (58)$$

where ϕ and λ are the polar angles of x_0Oy_0 and xOy coordinate system in the fixed coordinate system; a is the distance between centers of curvature of equivelocity curves of the rigid and flexible components. There is the following connection between angles ϕ and λ:

$$\lambda = \varphi \frac{r_{\infty}}{r_{e1}}, \qquad (59)$$

where r_{∞} and r_{e1} are radii of curvature on the working section of the equivelocity circumference of the rigid and the equivelocity curve of the flexible components.

Radius r_{e1} is found from equations (27).

Taking into account the effect of the deformation coefficient of the flexible component, the value r_{e1} is determined from the formula

$$r_{e1} = \frac{\left(1 - \frac{\pi\cos\Omega}{\pi - 2\Omega}\right) r_{\infty} + k_{\Delta} m_y}{1 - \cos\Omega - \frac{2\Omega\cos\Omega}{\pi - 2\Omega}},$$

where Ω is the angle at which the equivelocity curve is described by the radius r_{e1}. When $\Omega = \pi/4$

$$r_{e1} = \frac{0{,}41422 r_{\infty} - k_{\Delta} m_y}{0{,}41422} = m_y \frac{0{,}5 \cdot 0{,}41422 z_c - k_{\Delta}}{0{,}41422} = \\ = m_y (0{,}5 z_c - 2{,}41422 k_{\Delta}). \qquad (60)$$

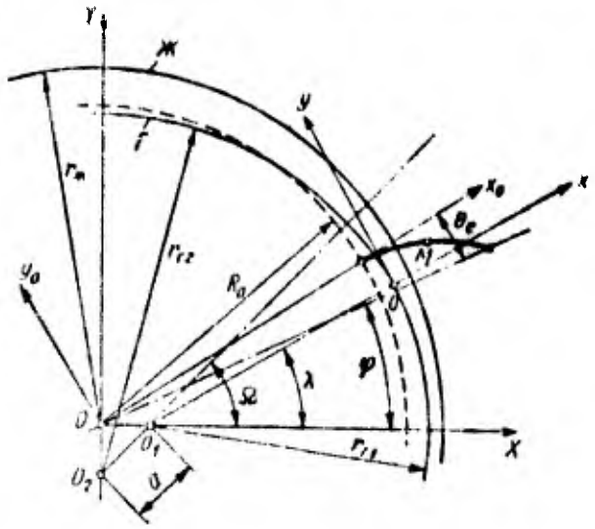

Figure 37. For the synthesis of the approximate engagement of a harmonic drive with the equivelocity curve which consists of two conjugate circular arcs.

After substitution of the value λ from (59) in equations (58) we obtain

$$\left.\begin{aligned} x &= R_0[\cos(\varepsilon + \theta_e + \varphi q_\varphi) + \varepsilon\sin(\varepsilon + \theta_e + \varphi q_\varphi)] - \\ &\quad - a\cos(1 - q_\varphi)\varphi, \\ y &= R_0[\sin(\varepsilon + \theta_e + \varphi q_\varphi) - \varepsilon\cos(\varepsilon + \theta_e + \varphi q_\varphi)] + \\ &\quad + a\sin(1 - q_\varphi)\varphi, \end{aligned}\right\} \qquad (61)$$

where $q_\varphi = \left(1 - \frac{r_{2c}}{r_{c1}}\right)$.

Expressions (61) are the equation of the family of the involute tooth profiles of the rigid component in the coordinate system connected with the tooth of the flexible component. The parameters of this family with fixed values of m_y and Ω depend on the deformation coefficient of the flexible component k_Δ. By the selection of the corresponding value of k_Δ it is possible to attain the minimum thickness of the layer of the family of involute profiles on the possible working sections of the teeth.

The task of the determination of the optimum value of k_Δ is solved by equating the slope angles to the axis Ox of the secant trajectory of point M in the coordinate system xOy and the tangent to the involute profile at point M. The indicated secant passes through two points of the trajectory determined by the parameter of bending ϕ with values ϕ=5° and ϕ=Ω.

The equation utilized for the search for the optimum value of k_Δ takes the form:

$$\frac{R_0[\sin(\varepsilon+\theta+5'q_\psi)-\sin(\varepsilon+\theta+\Omega q_\psi)]+e[\cos(\varepsilon+\theta+\Omega q_\psi)-\cos(\varepsilon+\theta+5'q_\psi)]]+a[\sin(1-q_\psi)5'-\sin(1-q_\psi)\Omega]}{R_0[\cos(\varepsilon+\theta+\Omega q_\psi)-\cos(\varepsilon+\theta+5'q_\psi)-e[\sin(\varepsilon+\theta+5'q_\psi)-\sin(\varepsilon+\theta+\Omega q_\psi)]]-a[\cos(1-q_\psi)\Omega-\cos(1-q_\psi)5']} = \operatorname{tg}\left[\alpha_{\text{ж}}-\gamma-q_\varphi\frac{\Omega+5'}{2}\right], \quad (62)$$

where $\alpha_{\text{ж}}$; γ and ε are found through the same expressions as for formula (57).

For the computation of the value m_y and ξ_e the same formulas are utilized as in the previously examined version of engagement.

Determining the value of k_Δ for a different number of teeth of wheels is carried out in the "Minsk-2" computer. A graph of the function $k_\Delta=f(z_g)$ is presented in fig. 35 by a dashed line (for $\alpha_\partial=20°$, $\Omega=45$). The working depth of the teeth is taken as equal to m.

Figure 38 shows the families of the involute profiles of teeth of the rigid component in the coordinate system of the teeth of the flexible component with $z_{\text{ж}}=100$. As is evident, the thickness of the layer of the family is extremely low and does not exceed 0.015 m. Inscribed in the family is the involute tooth profile of the flexible component (dashed line).

Table 7 gives the formulas for the geometric calculation of a two-wave drive with the equivelocity curve of the flexible component outlined at angle $\pi/2$ by two conjugate circular arcs.

Let us examine the geometry of engagement with the assignment of an equivelocity curve of the flexible component by three conjugate circular arcs according to fig. 27c, and with assurance of full contact of the teeth on the working depth on arc ϕ_1. In order that the stresses which appear in the flexible component with this form of deformation would be approximately the same as in the case of the assignment of the equivelocity curve according to Résal's

equation, it is necessary to select the radii of the conjugate arcs and their central angles from the condition

$$r_2 \approx r_{min} \text{ (Résal)}. \tag{63}$$

The accomplished investigations show that for the satisfaction of this condition it is possible to recommend the following values of angles: $\phi_1=10°$; $\phi_2=40°$, and $\phi_3=40°$. Then the radii of the conjugate circular arcs are determined from the formulas:

$$\left.\begin{aligned} r_1 &= r_{cn} + \Delta = r_{sr}, \\ r_2 &= r_{cn} - 3{,}81\Lambda, \\ r_3 &= r_{cn} + 3{,}56\Lambda. \end{aligned}\right\} \tag{64}$$

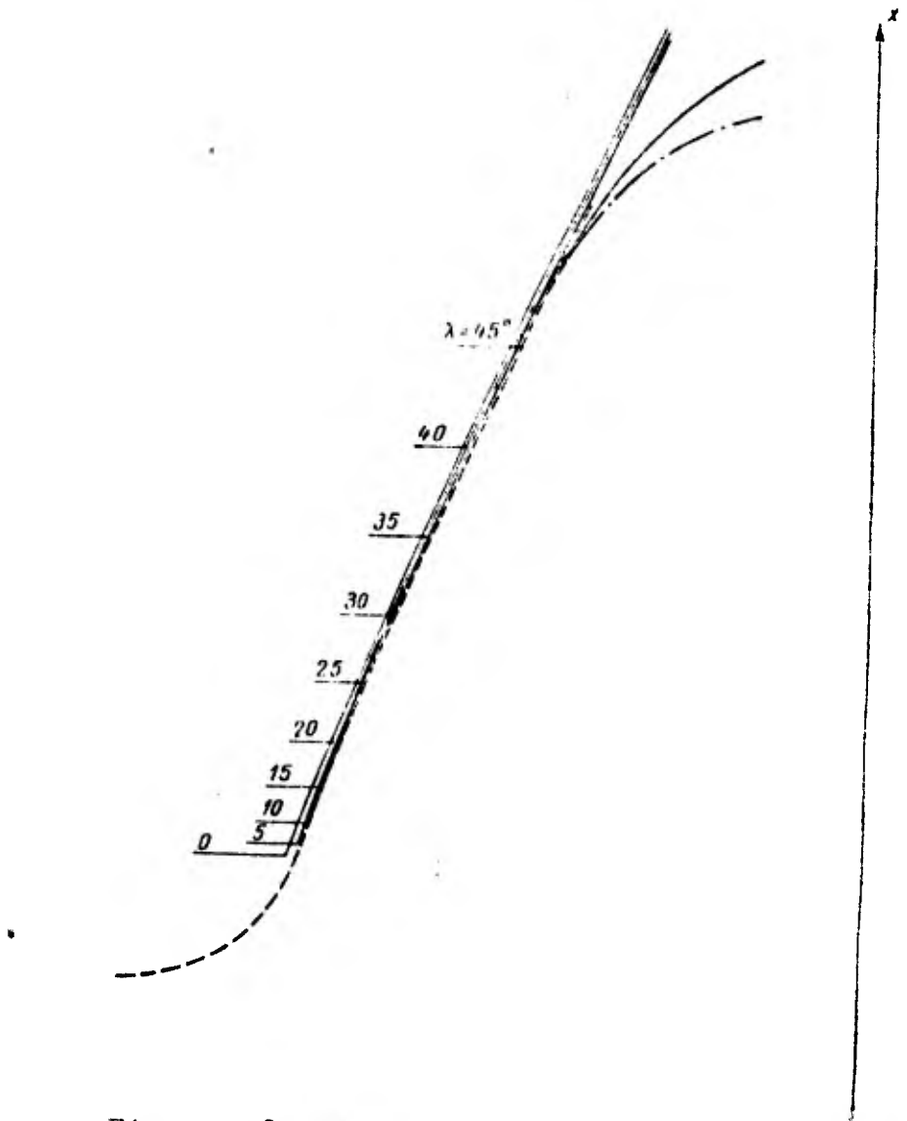

Figure 38. Family of profiles of the teeth of the rigid component in the coordinate system of the flexible component with a circular equivelocity curve.

Table 7. Formulas and an example of the geometric calculation of a two-wave drive for $\alpha_д$=20° with i=115; $z_г$=228; $z_ж$=230; m=1 mm; f_0=1; c_0=0.25; Ω=45°.

Parameter	Designation	Calculation formula	Example of the calculation
Deformation coefficient of the flexible component	$k_Δ$	Selected from the graph fig. 38 (dashed curve) taking into account recommendations on page 68.	$k_Δ = 0{,}814$
Coefficient of the wall thickness of the flexible component	$θ$	$θ = \frac{0.186\,[σ]\,z_г^2}{E k_Δ}$	$θ = \frac{0{,}186 \cdot 500 \cdot 228^2}{2{,}1 \cdot 10^5 \cdot 0{,}814} = 2{,}8$ We take $θ = 3$
Extension factor of the initial outline of the flexible component	$ξ_г$	$ξ_г = 0{,}022 z_г$	$ξ_г = 0{,}022 \cdot 228 = 5$
Conditional modulus	m_y	$m_y = m\left[\frac{z_г - 2(f_0 + c_0) + 2ξ_г - θ}{z_г}\right]$	$m_y = 1\left[\frac{228 - 2\,(1 + 0{,}25 - 0{,}5 \cdot 3{,}0 - 5)}{228}\right] = 1{,}0206$ мм
Radius of the neutral circumference of the nondeformed flexible component	$r_{гн}$	$r_{гн} = 0{,}5 z_г m_y$	$r_{гн} = 0{,}5 \cdot 228 \cdot 1{,}0206 = 116{,}348$ мм
Pitch circle diameter of the flexible component	$d_{dг}$	$d_{dг} = m z_г$	$d_{dг} = 1 \cdot 228 = 228$ мм

Parameter	Designation	Calculation formula	Example of the calculation
Pitch circle diameter of the rigid component	$d_{\partial ж}$	$d_{\partial ж} = mz_ж$	$d_{\partial ж} = 1 \cdot 230 = 230$ мм
Correction factor of the initial outline of the rigid component	$\xi_{ж}$	$\xi_{ж} = \xi_{\partial} - \left(1 - k_{\Delta}\frac{m_y}{m}\right)$	$\xi_{ж} = 5 - \left(1 - 0{,}814\frac{1{,}0206}{1}\right) = 4{,}835$
Radius of the equivelocity circumference of the rigid component	$r_{ж}$	$r_{ж} = 0{,}5m_y z_ж$	$r_{ж} = 0.5 \cdot 1{,}0206 \cdot 230 = 117{,}369$ мм
Radius of the equivelocity curve of the flexible component on the working section	r_{c1}	$r_{c1} = m_y(0{,}5z_c - 2{,}4142k_{\Delta})$	$r_{c1} = 1{,}0206(0.5 \cdot 228 - 2{,}4142 \cdot 0{,}814) = 114{,}343$ мм
Diameter of the circumference of the projections of the rigid component	$D_{fж}$	$D_{fж} = d_{\partial ж} - 2(f_0 - \xi_{ж})m$	$D_{fж} = 230 - 2(1 - 4{,}835) \cdot 1 = 237{,}62$ мм
Radius of the equivelocity curve of the flexible component on the nonoperative section	r_{c2}	$r_{c2} = 2r_{cм} - r_{c1}$	$r_{c2} = 2 \cdot 116{,}348 - 114{,}343 = 118{,}353$ мм
Diameter of the circumference of the projections of the flexible component	D_{c2}	$D_{c2} = d_{\partial c} + 2\xi_c m$	$D_{c2} = 228 + 2 \cdot 5 \cdot 1 = 238$ мм

Formulas (64) are obtained by the transformation of relations (30).

The connection between the parameters of the equivelocity curve and the dimensions of teeth with involute profiles is established in the following manner. With the assigned number of teeth and modulus of engagement the pitch circle diameter of the nondeformed flexible component is determined

$$d_{0.c} = mz_c.$$

To exclude the interference of the teeth the extension factor of the initial outline is accepted according to the formula

$$\xi_c = 0{,}022z_c.$$

With this value of ξ_c, the shaped angle at the middle point for height of the teeth will be approximately equal to 26°.

The conditional modulus of engagement according to the equivelocity curve is determined from relation (52)

$$m_y = \frac{m}{z_c}[z_c - 2(f_0 + c_0) + 2\xi_c - \vartheta],$$

in which $ is the coefficient of the wall thickness of the flexible component and can be determined from the graph fig. 51. The possibility of using this graph for the case under consideration is based on condition (63). The use of drives with the zone of full contact as kinematic [drives] with the low loading of the flexible component by the torque [torsional moment] makes it possible to increase arc ϕ_1 to $\phi_1'=30°$. Being given angle ϕ_1 and accepting $\phi_2 \approx \phi_3$, from equation (70) we find the value $r_{min}=r_2$ and from relation (138) we determine the value of coefficient $; in this case it should be ≥ 1.

It is also possible immediately to find minimally allowable value r_2 with a given number of teeth and a radius of the neutral circumference of the nondeformed flexible component. For this purpose, accepting $=1, $[\sigma]=600$ kgf/cm^2 and $E=2.0\cdot10^6$ kgf/cm^2, from

expression (138) we find

$$r_{min} = \frac{r_{zN}}{\frac{|\varphi|z_z}{2\pi}+1} = \frac{r_{zN}}{3{,}18\cdot 10^{-4}z_z+1} \leqslant r_a.$$

The radius of the neutral circumference of the nondeformed flexible component will equal

$$r_{zN} = 0.5 m_y z_z .$$

Accordingly the radius of the equivelocity curve of the rigid component is determined from the formula

$$r_{zc} = 0{,}5 m_y z_{zc}.$$

The extension factor of the initial outline for the rigid component is calculated from the relation

$$\xi_{zc} = \xi_z - \left(1 - \frac{m_y}{m}\right). \qquad (65)$$

With the selected extension factors of the initial outline ξ_z and ξ_{zc}, the interference of the teeth at angle ϕ_2 will not occur. It is expedient to take the addendum $f_0 = 0.8$.

8. GEOMETRY OF PRECISE ENGAGEMENT WITH CIRCULAR PROFILES OF TEETH

Despite the fact that the use of a theoretically precise engagement with circular profiles of teeth in harmonic drives is inexpedient in the majority of cases, we consider it necessary, nevertheless, to examine the geometry of this engagement, which can be extremely usefully for the readers who are striving for deeper research on the problems connected with the theory of harmonic drives.

Realization of precise engagement with circular profiles of the teeth of the rigid component requires the determination of the geometric parameters of the teeth and the components themselves. Calculation begins with the selection of the diameter of the center

line in the calculated cross section of the nondeformed flexible component. With the assigned kinematics of the drive and number of waves of deformation of the component, the conditional pitch or modulus m_y is found along the center line

$$m_y = \frac{d_{cp}}{z_e} = \frac{2r_{en}}{z_e}, \tag{66}$$

where d_{cp} is the diameter of the average circumference of the flexible component in the calculated cross section equal to the diameter of equivelocity circumference ($d_{cp}=d_{en}=2r_{en}$); z_e - the number of teeth of the flexible component.

The amount of deformation of flexible component is expressed as the conditional modulus in the following manner:

$$\Lambda = k_\Delta m_y,$$

where k_Δ is the deformation coefficient.

By considering that the central surface coincides with neutral [surface], it is possible to write the expression for the coefficient of the thickness of the flexible component on the strength of the permissible values of the bending stresses with its static deformation by the generator of waves of involute form (see chapter V)

$$\vartheta = \frac{\delta}{m_y} = \frac{[\sigma]}{E}\left(0{,}1366\frac{z_e}{k_\Delta} - 1\right)z_e.$$

Knowing the wall thickness δ of the flexible component on the section of the arrangement of the teeth, we can determine the diameter of the tooth spaces of the nondeformed flexible component

$$D_{i\,en} = d_{en} + \delta. \tag{67}$$

According to fig. 39, the radius of the surface of the indentations of the flexible component in the direction of the greatest deformation will equal

$$R_{in} = \frac{d_{en}+\delta}{2} + \Delta = m_y\left(\frac{z_e+\vartheta}{2} + k_\Delta\right). \tag{68}$$

Then the radius of the circumference of the projections of the teeth of the rigid component is determined from the expression

$$R_{ex} = R_{ia} + cm_{\mu}, \qquad (69)$$

where c is the coefficient of radial clearance. It is advantageous to take c=0.20.

From an examination of fig. 30 it is evident that the length of the working section of the line of action depends on radius ρ of the circular profile of the teeth of the rigid component. An increase in the radius ρ will lead to a reduction in length of the working section. A decrease in the radius ρ is inexpedient in connection with the corresponding decrease in the value of the cited* radius of curvature in the contact of the teeth.

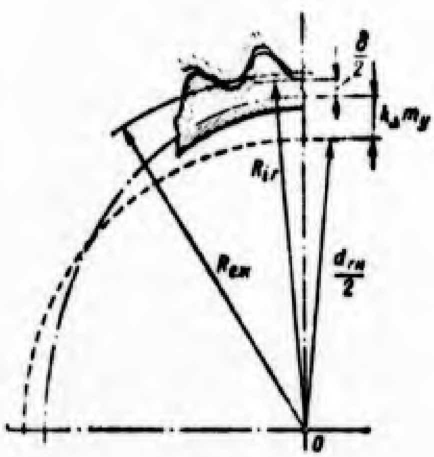

Figure 39. Diagram for determining the diameter of the projections of the rigid component.

The use of circular profiles is justified in assuring large multiple pairing of engagement; therefore, for the determination of the optimum value of a radius ρ let us assign the requirement that the line of action intersects the circumference of projections of the rigid component R_{ex} at least with a polar angle λ=60°. Determining the necessary value ρ is accomplished with the use of equations (51) for $\sqrt{x^2+y^2}=R_{ex}$ with the assigned values of parameters a, b, and λ.

For simplicity of the solution of the problem, we will consider that

$$\frac{q}{r_0} + 1 - \lambda = 0. \qquad (70)$$

*Translator's Note: May also be "reduced radius."

Since $q=(1-k_\Delta)m_y$, taking into account (33) and (53) condition (70) takes the form

$$0{,}214602\left(\frac{1}{k_\Delta}-1\right)+1-\lambda=0.$$

By taking $\lambda=60°$, we will obtain the corresponding value of $k_\Delta=0.81972$, with which condition (70) is assured. Taking into account (70), the equations which enter system (51) will be written in the following manner:

$$\left.\begin{aligned} x &= \rho\cos(\Omega+\varphi)+(a+r_{ж})\cos\varphi-b\sin\varphi,\\ y &= \rho\sin(\Omega+\varphi)+(a+r_{ж})\sin\varphi+b\cos\varphi,\\ \frac{1-\cos\lambda}{1-\sin\lambda} &= \operatorname{tg}(\Omega+\varphi),\\ \varphi &= 4{,}66\frac{k_\Delta}{z_{ж}}\lambda\left(\lambda-\frac{\pi}{2}\right)+\frac{z_c}{z_{ж}}\lambda. \end{aligned}\right\} \qquad (71)$$

There is no difficulty in determining the unknown value ρ. The value of angle ϕ is found from the fourth equation and from the third - the angle Ω. The first and second equations after squaring and summation take the form

$$R_{ж}^2=\rho^2+2\rho\left|b\sin\Omega+(a+r_{ж})\cos\Omega\right|+b^2+(a+r_{ж})^2. \qquad (72)$$

If we now assign values of parameters a and b; then the solution of equation (72) can be accomplished and the value ρ found. Selection of parameters a and b is accomplished on the basis of fig. 40.

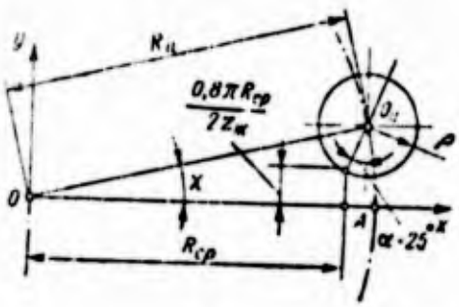

Figure 40. Determining the position of the center of the circular profile of teeth of the rigid component.

As calculations showed, it is advantageous to take the value of angle α as approximately equal to 25°. At this angle, $k_\Delta=0.81972$ and the profile of the teeth of the flexible component has the smallest curvature.

Being given the requirement that the thickness of the tooth of the deformed flexible component on radius

$R_{cp}=R_{exc}+0.81972m_y$ is equal to $0.8\,\pi R_{cp}/2z_{sc}$, we obtain formulas for determining the value of the parameters of interest to us

$$a+r_{sc}=R_{cp}+\rho\sin 25^\circ, \tag{73}$$

$$b=0{,}8\frac{\pi R_{cp}}{2z_{sc}}+\rho\cos 25^\circ. \tag{74}$$

With $z_{sc}=100$, we obtain $\rho=1.65m_y$, with $z_{sc}=720$ $\rho=1.55m_y$.

The diameter of the circumference of the projections of the flexible component is determined from the assumption that the apexes of the teeth lie on the curve which with $\lambda=60°$ intersects the last point of engagement. For this, accepting in formula (37) $\rho_s=R_{exc}$, we eliminate x and y from (36) and find the value ψ

$$\psi=0{,}36603+\sqrt{\frac{R_{exc}^2}{r_0^2}-0{,}13490}.$$

Taking into account that $\psi=\lambda+\psi_0$, with $\lambda=60°$, we will have

$$\psi_0=\psi-1.0472,$$

whence

$$R_{ai}=r_0(\psi_0+0{,}7854)$$

or

$$R_{ai}=r_0\left[\sqrt{\frac{R_{exc}^2}{r_0^2}-0{,}13490}+0{,}10423\right]. \tag{75}$$

Since the second term under the radical will always be considerably less than the first, formula (75) can be rewritten in the following form:

$$R_{ai}\approx R_{exc}+0{,}10423r_0. \tag{76}$$

The cutting of the teeth with circular profiles of the rigid component can be realized extremely simply by rolling if we take for the initial circumference of machine engagement the circumference on which the centers of the circular profiles lie. The

radius of this circumference R_y is determined on the basis of fig. 40 from the expression

$$R_y = l\sqrt{(a + r_{ж})^2 + b^2}.$$

Taking into account (56; 57) and (61; 62) with $\rho=1.65m_y$ we will have

$$R_y = m_y \sqrt{\left(\frac{z_s + 0}{2} + c + 2k_\Delta\right)^2\left(1 + \frac{0{,}64\pi^2}{4z_{ж}^2}\right) + \cdots \rightarrow}$$
$$\leftarrow \cdots + 3{,}3\left(\frac{z_s + 0}{2} + c + 2k_\Delta\right)\left(\sin 25° + \frac{0{,}8\pi \cos 25°}{2z_{ж}}\right) + 1{,}65^2. \qquad (77)$$

The modulus of the teeth on the circumference R_y is determined from the formula

$$m = \frac{2R_y}{z_{ж}}. \qquad (78)$$

By substituting the values of the R_y from (77) in (78) with $k_\Delta=0.81972$ and $c=0.2$ taken above, we obtain

$$m = \frac{2m_y}{z_{ж}} \sqrt{\left(\frac{z_s + 0}{2} + 1{,}83944\right)^2\left(1 + \frac{0{,}16\pi^2}{z_{ж}^2}\right) + \cdots \rightarrow}$$
$$\leftarrow \cdots + 3{,}3\left(\frac{z_s + 0}{2} + 1{,}83944\right)\left(\sin 25° + \frac{0{,}4\pi \cos 25°}{z_{ж}}\right) + 1{,}65^2. \qquad (79)$$

In connection with the fact that in the derived formula $z_{ж} \geq 100$ the values $0.64\pi^2/4z_{ж}^2 \leq 0.00016$ and $0.8\pi \cos 25°/2z_{ж} \leq 0.011$ they can be disregarded and for practical purposes formula (79) can be presented in the following form:

$$m_1 = \frac{2m_y}{z_{ж}} \sqrt{\left(\frac{z_s + 0}{2} + 1{,}83944\right)^2 + \cdots \rightarrow}$$
$$\leftarrow \cdots + 1{,}3946\left(\frac{z_s + 0}{2} + 1{,}83944\right) + 2{,}7225. \qquad (80)$$

For purposes of standardizing the tool for cutting teeth of the parts of harmonic drives it is expedient to take standard values of the modulus for circumference R_y, and to find the value of the conditional modulus m_y from formula (80). In this case

$$m_y = \frac{m z_ж}{2 + k_y^2 + 1{,}3916 k_y + 2{,}725}, \qquad (81)$$

where

$$k_y = \frac{z_ж + \theta}{2} + 1{,}83944.$$

For the construction of the initial outline of the rack which determines the geometry of the gear-machining tools, it is also necessary to find the mutual arrangement of the centers of the circumferences which describe the opposite sides of the teeth or troughs of the outline.

As follows from fig. 40, for determining arc $O_y A$ it is necessary to find angle χ from the expression

$$\operatorname{tg} \chi = \frac{b}{R_{cp} + \rho \sin 25^\circ}$$

or

$$\operatorname{tg} \chi = \frac{\frac{0{,}4\pi R_{cp}}{z_ж} + \rho \cos 25^\circ}{R_{cp} + \rho \sin 25^\circ}. \qquad (82)$$

With $z_ж=100$ $\tan \chi=0.04087$ and with $z_ж=720$ $\tan \chi=0.00563$.

By equating arc length $O_y A$ to the tangent of the angle, we find that $\overset{\frown}{O_y A}_{(z=100)} \approx 2{,}04m$ and $\overset{\frown}{O_y A}_{(z=720)} \approx 2{,}02m$.

Thus, the arc length $O_y A$ is a function of the number of teeth of the rigid wheel. It is natural that for standardizing the tools it is expedient to select a constant value of this arc. Let us accept $\overset{\frown}{O_y A} = 2{,}04\, m$. One ought to focus attention on the fact that according to (68) $m=f(m_y; z_ж)$ and, consequently, $\rho=1.65m_y$ also is not a value constant for the entire range of the numbers of teeth used.

However, considering that with widespread values of $\phi=2$ a change in the number of teeth of the rigid component from $z_ж=100$ to $z_ж=720$ will lead to a change in the value of the modulus only from 0.953 to 0.995, and the corresponding value of the radius of the

profile from 1.57m to 1.545m, for practical calculations we take ρ=1.55m.

Figure 41 depicts the initial outline of a rack which can serve for the formation of teeth of the disk rams used in cutting the internal teeth of the rigid component, and also the formation of the hobbing cutter for the cutting of the teeth of the flexible component by the method of the reproduction of the engagement of harmonic drive (see chapter VII). In cutting the teeth of flexible components by cutters with this outline, to assure the radial clearance it is necessary to increase the diameter of the projections of rigid wheel calculated according to formula (69) by 0.10m.

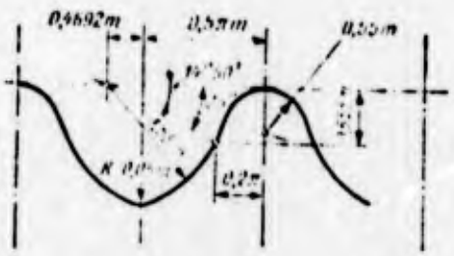

Figure 41. Initial outline of the tool for a cutting teeth.

The geometric calculation of flexible and rigid wheels with circular profiles of teeth is reduced to Table 8.

Table 8. Formulas and an example of the geometric calculation of the elements of the engagement of the flexible and rigid components of the drive ($z_{гиб}$=100, $z_{ж}$=98, m=1 mm).

Parameter	Determined parameter	Calculation formula	Example of the calculaton
Coefficient of the wall thickness of flexible component	θ	Taken from the graph fig. 51	$\theta = 1$
Deformation coefficient of the flexible component	k_Δ	$k_\Delta = 0{,}8197$	
Coefficient of radial clearance	c	$c = 0{,}2$	
Auxiliary coefficient	k_u	$k_u = \frac{z_ж + \theta}{2} + 1.8394$	$k_u = \frac{98 + 1}{2} + 1.8394 = 51{,}339$
Conditional modulus	m_y	$m_y = \frac{mz_ж}{2\sqrt{k_u^2 + 1{,}3946 k_u + 2{,}7225}}$	$m_y = \frac{1 \cdot 100}{2\sqrt{51{,}339^2 + 1{,}3946 \cdot 51{,}339 + 2{,}7225}} = 0{,}9615$ мм
Radius of circular profile	ρ	$\rho = 1{,}55m$	$\rho = 1{,}55 \cdot 1 = 1{,}55$ мм

Parameter	Determined parameter	Calculation formula	Example of the calculation
Pitch circle diameter of the rigid component	$d_{\partial ж}$	$d_{\partial ж} = mz_{ж}$	$d_{\partial ж} = 1 \cdot 100 = 100$ мм
Radius of circumference of the projections of the rigid component	$R_{ея}$	$R_{ея} = m_y \left(\frac{z_г + \theta}{2} + k_\Delta + c \right)$	$R_{ея} = 0{,}9615 \left(\frac{98 + 1}{2} + 0{,}8197 + 0{,}2 \right) = 48{,}61$ мм
Diameter of the neutral circumference of the non-deformed flexible component	$d_{гн}$	$d_{гн} = m_y z_г$	$d_{гн} = 0{,}9615 \cdot 98 = 94{,}26$ мм
Radius of the evolute of the equivelocity curve of the flexible component	r_0	$r_0 = \frac{m_y k_\Delta}{0{,}214602}$	$r_0 = \frac{0{,}9615 \cdot 0{,}8197}{0{,}214602} = 3{,}675$ мм
Radius of circumference of the projections of the flexible component	$R_{гг}$	$R_{гг} = R_{ея} + 0{,}10423 r_0$	$R_{гг} = 48{,}61 + 0{,}10423 \cdot 3{,}675 = 48{,}99$ мм

CHAPTER IV

EFFICIENCY

9. GENERAL

The correct estimate of the efficiency of harmonic gear drives in many instances should predetermine the rational use of the latter.

At present an insufficient quantity of experimental data on the evaluation of the efficiency of harmonic drives is accumulated, in consequence of which the recommendations given below for the determination of the value of the theoretical efficiency should be considered as tentative. At the same time an extremely full consideration of the different factors which affect the value of the efficiency gives the correct picture of the distribution of losses in a mechanism, which is extremely important for the designers of harmonic mechanisms.

We should consider the design in which the flexible component has the form of container flexibly joined with a shaft, and the wave generator - of a cam type with intermediate rolling contacts (balls or rollers) and a flexible external ring laid in the flexible component as most common for a harmonic drive. Lubrication of the drive is accomplished by spattering through the rotation of the wave generator.

For the indicated design the following power losses should be estimated: to friction in tooth engagement, to rolling friction in the wave generator during the action of the forces of elastic deformation of the flexible component and the backing ring of the generator, to rolling friction in the wave generator during the action of forces in engagement, to friction in the roller bearings, to friction between the backing ring and the flexible component, to the mixing of oil, and to hysteresis in the flexible component and the backing ring.

Let us explain the possibility and expediency of the theoretical estimate of the magnitude of the enumerated losses.

The power losses to friction in tooth engagement can be determined if the scheme and kinematics of the mechanism, the form of the profiles of the teeth, and the material of parts are known. However, one ought to focus attention on the fact that the friction coefficient is not a stable value for the designated materials by virtue of which the accuracy of the calculation of losses will be relative.

The determination of losses to friction in the wave generator during the action of the forces of elastic deformation of the flexible component and ring is connected with considerable difficulties. If the initial deformation of the flexible component and rings are obtained by the application of several forces, as occurs for example for the shape of a neutral line in the form of a Résal curve then, strictly speaking, with the full retention of the form of deformation the flexible component and the backing ring should affect the generator only at the points of application of the force. However, the presence of the elastic deformations of the parts, clearances in the coupling of the flexible component and the generator, and also forces of friction in the coupling of the flexible component and the backing

ring leads to some change in the form of deformation and scheme of the power effect of the components on the generator. Naturally, the forced deformation of the flexible component and ring with which the form of the elastic lines will differ from the Résal curve will cause a completely different scheme of the power effect of the components.

Thus, the nature of the distribution and magnitude of the forces applied on the part of the deformed components to the wave generator depend on many factors and cannot always be taken into account. Furthermore, the accomplished calculations (see page 89) and experimental check show that the proportion of the losses in the wave generator from the forces of elastic deformation in the total balance of losses is small, in connection with which a simplified scheme of the solution of the posed problem is proposed below.

The losses to friction in the wave generator under the action of the forces which appear in engagement with the known law of distribution of the working load between the teeth theoretically can be determined. In this case the reliability of the computations will depend in essence on the correctness of the designation of the value of the coefficient of rolling friction.

Usually the connectors of the reducers load the cantilever shafts with some forces whose vectors rotate and whose value depends on the torque applied to the shafts. These forces, just as the radial forces which appear as a result of the nonuniformity of load distribution between the zones of engagement, load the shaft bearings. The value of these forces and the losses connected with their action obviously depend on the power transferred by the mechanism.

For two or more harmonic drives and uniform pitch of the waves the losses in the antifriction bearings which support the

shafts are virtually low and, for standard designs, can be accepted on the order of 1-2% of the transmitted power.

Power losses to friction will be also insignificant because of the elastic slip between the flexible component and the backing ring, and also hysteresis losses in these components. The need of assuring a long service life of the flexible component and ring forces us to emerge at a low level of bending stresses considerably less than the elastic limit of the material, by virtue of which the hysteresis loss need not be considered in practice.

The power consumption during spraying and the mixing of oil in harmonic drives thus far cannot be taken into account with sufficient accuracy; for the quantitative estimate of this flow rate the conduct of a series of very fine experiments is required. Preliminarily, it can be noted that the jamming and the extrusion of oil from clearances in the gearing require a certain consumption of power which will depend on the scheme and loading of the gearing, and also on the viscosity of the lubrication used.

A rough estimate of losses in spraying and the mixing of oil was performed in the reducer shown in figure 60.

The determination of the efficiency of the reducer was accomplished initially with the oil level passing through the middle of the balls of the wave generator. Draining the oil (measurements were made in the period of the subsequent short-term work of the reducer) led to raising the efficiency by approximately 2%. The raising of the oil level to the middle of the height of the teeth of idle wheels caused a reduction the efficiency of the reducer by 5-6%.

Thus, for determining the approximate value of the efficiency of the harmonic drive it is necessary to find first of all the

losses in engagement, in the wave generator from the action of the forces of elastic deformation of the components, and in the generator from forces in engagement.

10. LOSSES TO FRICTION IN ENGAGEMENT AND THE GENERATOR OF A HARMONIC DRIVE

Figure 19a depicts the kinematic scheme of the mechanism of a harmonic drive of the Г-Ж-Н type. The condition of the steady motion of its components will be

$$M_н + M_г + M_ж = 0, \qquad (83)$$

where $M_Г$ is the torque applied to the flexible component; $M_Ж$ - the torque applied to the central rigid wheel; $M_Н$ - the torque applied to the shaft of the generator of the waves of the drive.

In this case, we assume that the value of the moments remains constant both in the absolute motion of the components and in relative motion.

The efficiency of the harmonic mechanism with the leading component Н and power flux from the component Н to the component Ж (subsequently designated Н→Ж) equal

$$\eta_в = \frac{N_{с.п}}{N_{с.д}},$$

where $N_{с,п}$ is the power of the forces of useful resistance; $N_{с,Д}$ - the power of the driving forces

$$N_{с.п} = N_ж = -M_ж \omega_ж,$$
$$N_{с.д} = M_н \omega_н. \qquad (84)$$

The sign of power for the leading component is designated positive since the coincidence of the direction of rotation and torque occurs. With different directions of rotation and torque

applied to the driven shaft, the sign of power is taken as negative. Then arbitrarily considering the sign of power

$$\eta_0 = -\frac{M_{ж}\omega_{ж}}{M_{н}\omega_{н}} = -\frac{M_{ж}}{M_{н}i^{н}_{ж.ж}}. \qquad (85)$$

According to formula (8) the gear ratio

$$i^{н}_{ж.ж} = \frac{1}{1-i^{н}_{ж.с}}$$

and then

$$\eta_0 = -\frac{M_{ж}}{M_{н}}(1-i^{н}_{ж.с}),$$

whence

$$M_{н} = -\frac{M_{ж}}{\eta_0}(1-i^{н}_{ж.с}). \qquad (86)$$

With power flux from component Ж to component Н (subsequently designated Ж→Н) the efficiency will equal

$$\eta_0 = -\frac{M_{н}\omega_{н}}{M_{ж}\omega_{ж}} = -\frac{M_{н}i^{н}_{ж.ж}}{M_{ж}} = -\frac{M_{н}}{M_{ж}(1-i^{н}_{ж.с})};$$

$$M_{н} = -M_{ж}\eta_0(1-i^{н}_{ж.с}). \qquad (87)$$

Let us write expressions (86) and (87) in the general form

$$M_{н} = -M_{ж}\eta_0^{k}(1-i^{н}_{ж.с}), \qquad (88)$$

where k=-1 with the power flux Н→Ж; k=+1 with the power flux Ж→Н.

Let us find the efficiency of the mechanism η^{H} with a fixed component (Н), for which we impart to the entire system rotation with speed $-\omega_{H}$.

Let component Г be the driving component and Ж - the driven (→Ж), then

$$\eta^{н} = \frac{N_{с.н}}{N_{с.з}},$$

where

$$N_{c.n} = N_{ж}^{н} = -M_{ж}(\omega_{ж} - \omega_{н}),$$
$$N_{c.д} = M_{с}(\omega_{с} - \omega_{н}) \qquad (89)$$

and after substitution we obtain

$$\eta^{н} = -\frac{M_{ж}(\omega_{ж} - \omega_{н})}{M_{с}(\omega_{с} - \omega_{н})} = -\frac{M_{ж}}{M_{с}} i_{жс}^{н},$$

whence

$$M_{с} = -\frac{M_{ж}}{\eta^{н}} i_{жс}^{н}. \qquad (90)$$

If the driving component is component Ж (Ж→), then

$$\eta^{н} = -\frac{M_{с}(\omega_{с} - \omega_{н})}{M_{ж}(\omega_{ж} - \omega_{н})} = -\frac{M_{с}}{M_{ж} i_{жс}^{н}};$$

$$M_{д} = -M_{ж}\eta^{н} i_{жс}^{н}. \qquad (91)$$

We write expressions (90) and (91) in general form in the following manner:

$$M_{с} = -M_{ж}(\eta^{н})^{m} i_{жс}^{н}, \qquad (92)$$

where m=-1 with power flux (→Ж); m=+1 with power flux (Ж→).

After the substitution of (88) and (92) in (83) we obtain

$$1 - \eta_{0}^{k}(1 - i_{жс}^{н}) - (\eta^{н})^{m} i_{жс}^{н} = 0. \qquad (93)$$

In order to explain the effect of the value $i_{ЖГ}^{Н}$ on the value of the efficiency of the harmonic drive, let us examine the relation of expressions (89) and (84)

$$\Omega_{ж} = \frac{N_{ж}^{н}}{N_{ж}} = \frac{-M_{ж}(\omega_{ж} - \omega_{н})}{-M_{ж}\omega_{ж}} = 1 - \frac{\omega_{н}}{\omega_{ж}} = 1 - i_{нж}^{г}$$

or

$$\Omega_{ж} = \frac{i_{жс}^{н}}{i_{жс}^{н} - 1}. \qquad (94)$$

If the component Ж is the driven or driving simultaneously in absolute and relative motion, then there should be $\sigma>0$. This condition obviously can occur with $i^{H}_{ЖГ}>1$ which, for the harmonic drive considered according to the scheme depicted in figure 19a, is impossible since always $z_{Ж}>z_{Г}$.[1] Consequently, only $\Omega_{Ж}<0$ can be, i.e., component Ж driven in absolute motion becomes driving in relative motion.

Analogously by accepting

$$\Omega_{e}=\frac{N^{n}_{e}}{N_{e}}=\frac{i^{n}_{exc}}{i^{n}_{exc}-1}$$

and taking into account that only inequality $i^{H}_{ГЖ}>1$ can occur, we clarify the condition under which $\Omega_{Г}>1$ occurs. This will be if the component Г is driving (or driver) both in absolute and in relative motion of the components.

$\Omega_{Ж}<0$ will occur with $i^{H}_{ЖГ}<1$ which, in turn, can be: 1) with $k=-1$ and $m=+1$ or 2) with $k=+1$ and $m=-1$.

Let us examine both cases.

I. In absolute motion driving is the H component and driven Ж; then $k=-1$; $m=+1$; $0<i^{H}_{ЖГ}<1$ and from (93) we have

$$\eta_{e}^{-1}(1-i^{n}_{exc})+\eta^{n}i^{n}_{exc}=1$$

or taking into account the fact that $\eta^{H}=1-\psi^{H}$

$$\eta^{e}_{exc}=\eta_{e}=\frac{1-i^{n}_{exc}}{1-\eta^{n}i^{n}_{exc}}\cdot\frac{1}{1-\psi^{n}(1-i^{e}_{exc})}. \qquad (95)$$

II. In absolute motion driving is the Ж component, then $k=+1$; $m=-1$; $0<i^{H}_{ЖГ}<1$ and from (93)

---

[1] An exception is the so-called heteropitch drive developed by V. K. Rubtsov.

$$\eta_{\text{в}}(1-i^{H}_{\text{вг}})+(\eta^{H})^{-1}i^{H}_{\text{вг}}=1$$

or

$$\eta_{\text{в}}=\eta_{\text{в}}\frac{1-i^{H}_{\text{вг}}}{\eta^{H}}\;\frac{1-\psi^{H}i^{H}_{\text{вг}}}{1-i^{H}_{\text{вг}}}\;\frac{1}{\psi^{H}}.$$

The analysis of expression (96) shows that with $\eta^{H}<i^{H}_{\text{вг}}$, $\eta_{\text{в}}=0$ is obtained, i.e., the self-braking of the mechanism occurs. For a harmonic drive made according to the scheme presented in figure 19a, with a fixed rigid component the efficiency of the engagement will be determined respectively from the formulas:

with power flux H→Г

$$\eta^{H}_{\text{вг}}=\eta_{\text{в}}\frac{1-i^{H}_{\text{вг}}}{1-i^{H}_{\text{вг}}\eta}\;\frac{1-\psi^{H}}{1+|i^{H}_{\text{вг}}|\psi^{H}}, \qquad (97)$$

with the power flux Г→H

$$\eta^{H}_{\text{вг}}=\eta_{\text{в}}\frac{1-i^{H}_{\text{вг}}\eta^{H}}{1-i^{H}_{\text{вг}}}=1-\psi^{H}(1+|i^{H}_{\text{вг}}|). \qquad (98)$$

Thus, the efficiency of the engagement of a harmonic drive depends only on the gear ratio and the efficiency of the mechanism in relative motion η^{H} (with a stationary wave generator).

In connection with the fact that in a harmonic drive virtually each of the components can be driven and driving, let us examine the determination of efficiency in relative motion for two cases where the driving is the rigid component and driven the flexible component and when the driving component is, on the contrary, the flexible and the driven rigid. Arbitrarily let us assume that each pair of teeth in engagement is loaded equally; then it is possible to be restricted to the examination of the engagement of one pair of teeth, considering that the entire load is transferred through it.

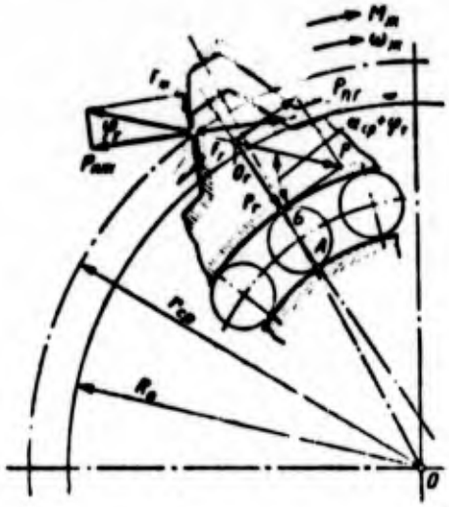

Figure 42. Determination of forces in the tooth engagement of a harmonic drive (driving - rigid component).

Figure 42 shows the forces which act in engagement and on the rolling contacts of the wave generator with the rigid driving component and flexible driven component. The action of torque $M_ж$ in this case causes the appearance of normal reaction $P_{пж}$ and of force of friction $F_ж$. Respectively equal in magnitude, forces $P_{пг}$ and $F_г$ act on a tooth of the flexible component. We transferred the resultant P of forces $P_{пг}$ and $F_г$ along the line of direction of its action to point $0_г$ lying on the axis of symmetry of a tooth of the flexible component, and resolved it in the direction of this axis and perpendicular to it. Force $P_г$ has an effect on the rolling contact of the generator, causing the appearance of a moment of resistance to the rolling over of the rolling contact during the motion of the components.

The condition of the equilibrium of forces which act on the tooth of the rigid component with involute shapes takes the form

$$M_ж = P_{nж}R_0 - F_ж R_0 \operatorname{tg} \alpha_{cp}. \tag{99}$$

At the same time

$$F_ж = P_{nж}f, \tag{100}$$

where f is the coefficient of friction.

Taking into account (99) from (100) we will have

$$F_ж = \frac{M_ж f}{R_0(1 - f \operatorname{tg} \alpha_{cp})}. \tag{101}$$

For determining friction horsepower it is necessary to find the average sliding speed of the teeth in the process of engagement. The value of this velocity can be found on the basis of the following considerations.

With the rotation of the rigid component by approximately an angle of $\pi/4$ the tooth crest of the flexible component, slipping over the tooth profile of the rigid component, covers a path equal to the deformation of the flexible component divided by the cosine of the average shaped angle. Taking into account the propositions given on page 53, this path will equal $\frac{k_\Delta m_y}{\cos \alpha_{cp}}$; then the expression for the average sliding speed acquires the form

$$v_{cp} = \frac{k_\Delta m_y \omega_{ж} 30}{\pi \cos \alpha_{cp} 0{,}5} = \frac{1{,}27324 k_\Delta \omega_{ж} m_y}{\cos \alpha_{cp}}, \qquad (102)$$

where for the geometric parameters of the components according to table 5 or 6

$$\cos \alpha_{cp} = \frac{\cos \alpha_0}{1 + \frac{2z_{ж} - 1}{z_{ж}}}. \qquad (103)$$

Then the friction horsepower will equal

$$N_{зац} = F_{ж} v_{cp} = \frac{4 M_{ж} \omega_{ж} k_\Delta m_y f}{\pi R_0 (1 - f \operatorname{tg} \alpha_{cp}) \cos \alpha_{cp}}.$$

The power of torque $M_{ж}$ is determined from the formula

$$N_{ж} = M_{ж} \omega_{ж}.$$

Loss factor $\psi_{зац}$ to friction in engagement will be determined from the expression

$$\psi_{зац} = \frac{N_{зац}}{N_{ж}} = \frac{1{,}273 k_\Delta m_y f}{R_0 (1 - f \operatorname{tg} \alpha_{cp}) \cos \alpha_{cp}}. \qquad (104)$$

Let us determine the power expended on overcoming the resistance to the rolling over of the rolling contact of the

wave generator, considering that the entire load is absorbed by one rolling contact.

Let us examine the expenditures of power in points A and B of the contact of a rolling contact with the flexible component (backing ring) and the cam of the generator

$$N_A = P_r \mu \omega_{T.K}; \quad N_B = P_r \mu (\omega_{T.K} - \omega_r^K),$$

where μ is the coefficient of rolling friction; $\omega_{T,K}$ - the angular velocity of the rolling contact in motion relative to component H; ω_r^K - the angular velocity of the flexible component relative to component H.

In turn the velocity $\omega_{T,K}$ is determined from the expression

$$\omega_{T.K} = \omega_r^K \frac{r_{BH}}{d_{T.K}}, \qquad (105)$$

where $r_{BH}=d_{BH}/2$ is the radius of the internal surface of the flexible component or backing ring in the nondeformed state along which the rolling contacts roll.

Taking into account (105), accepting that the coefficients of rolling friction in points A and B are equal, we find the total power

$$N_{\text{общ}} = N_A + N_B = P_r \mu \omega_r^K \left(\frac{2r_{BH}}{d_{T.K}} - 1 \right). \qquad (106)$$

On the basis of figure 42

$$P_r = P \sin (\alpha'_{cp} + \varphi),$$

where α'_{cp} is the profile angle in the center point of the working section of the tooth of the flexible component.

In practice it is possible to accept $\alpha'_{cp}=\alpha_{cp}$ and then

$$P_r = \frac{M_{\text{ж}}}{R_0} (\sin \alpha_{cp} + f \cos \alpha_{cp})$$

or

$$P_r = \frac{M_{ж}}{R_0} \sin \alpha_{cp} (1 + f \operatorname{ctg} \alpha_{cp}). \qquad (107)$$

Power expended on the rolling over of rolling contacts, taking into account (107), will be determined from the expression

$$N_{кач} = \frac{M_{ж} \omega_{ж}^{н} i_{ex}^{н} \mu}{R_0} \left(\frac{d_{ен}}{d_{т.к}} - 1 \right) (1 + f \operatorname{ctg} \alpha_{cp}) \sin \alpha_{cp}$$

and the loss factor connected with the rolling over of rolling contacts will equal

$$\psi_{кач} = \frac{N_{кач}}{N_{ж}} = \frac{i_{ex}^{н} \mu}{R_0} \left(\frac{d_{ен}}{d_{т.к}} - 1 \right) (1 + f \operatorname{ctg} \alpha_{cp}) \sin \alpha_{cp}. \qquad (108)$$

The efficiency in relative motion with a rigid driving component in this case will be connected with loss factors $\psi_{зац}$ and $\psi_{кач}$ in the following manner:

$$\eta_{ж.с}^{н} = 1 - \psi_{ж.с}^{н} = 1 - (\psi_{зац} + \psi_{кач}).$$

Here, as subsequently, the upper efficiency index designates the component with regard to which the motion of the remaining components is examined and the lower index means the direction of translation of motion; in this case, the first letter of the index pertains to the driving, and the second to the driven components.

On the basis of expressions (104), (108) and (7), taking into account the fact that for a two-wave drive $i_{нс}^{ж} = -\frac{z_с}{2}$, after a series of transformations we obtain

$$\psi^{н} = \psi_{ж.с}^{н} = \frac{k_{\psi}}{R_0}, \qquad (109)$$

where

$$k_{\psi} = \frac{1{,}27 k_{\lambda} m f}{\cos \alpha_{cp} - f \sin \alpha_{cp}} + \mu \left(\frac{d_{ен}}{d_{т.к}} - 1 \right) \left(1 + \frac{2}{z_с} \right) (\sin \alpha_{cp} + f \cos \alpha_{cp}). \qquad (110)$$

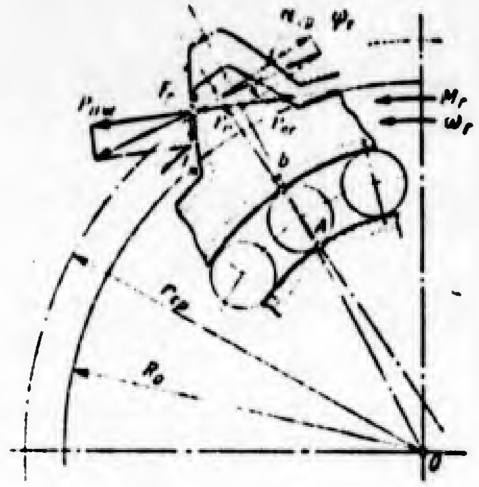

Figure 43. Determination of forces in the tooth engagement of a harmonic drive (driving - the flexible component).

A diagram of the forces which act in the tooth engagement of the flexible and rigid components and also on the rolling contacts of the wave generator if the driving component is the flexible component and the driven component is rigid is presented in figure 43. Taking into account the aforementioned assumptions, it is also possible to find the efficiency of the drive in relative motion for this case.

There is the following relation between the torque applied to the components:

$$M_{ж} = \eta^{h}_{гж} M_{г} i^{h}_{гж}. \qquad (111)$$

Then, examining the equilibrium of the forces applied to the tooth of the rigid component, we find the force of friction in engagement

$$F_{ж} = F_{г} = \frac{M_{г} i^{h}_{гж} \eta^{h}_{гж} f}{R_0 (1 + f\,\mathrm{tg}\,\alpha_{ср})}.$$

The power of force $F_{г}$ with the sliding speed determined from expression (102) is found from the formula

$$N_{зац} = \frac{1{,}27 k_{\Delta} m \omega_{г} M_{г} i^{h}_{гж} \eta^{h}_{гж} f}{\cos \alpha_{ср} R_0 (1 + f\,\mathrm{tg}\,\alpha_{ср})}$$

or after the transformation

$$N_{зац} = \frac{1{,}27 k_{\Delta} m \omega_{ж} M_{ж} \eta^{h}_{гж} f}{\cos \alpha_{ср} R_0 (1 + f\,\mathrm{tg}\,\alpha_{ср})}. \qquad (112)$$

The loss factor for friction in engagement will equal

$$\psi_{зац} = \frac{N_{зац}}{N_{г}} = \frac{1{,}27 k_{\Delta} m \eta^{h}_{гж} f}{R_0 (1 + f\,\mathrm{tg}\,\alpha_{ср}) \cos \alpha_{ср}}. \qquad (113)$$

For determining the power expended on the rolling over of the rolling contacts of the wave generator, we use expression (106) in which force P_r is found on the basis of figure 43 and is equal to

$$P_r = \frac{M_w \sin(\alpha_{cp} - \psi)}{R_0 \cos\psi}. \qquad (114)$$

Taking into account (111) expression (114) acquires the form

$$P_r = \frac{M_c \eta''_{wc} i''_{cw}}{R_0} (1 - f \operatorname{ctg} \alpha_{cp}) \sin \alpha_{cp}$$

and the value of the power expended on the rolling over of the rolling contacts is found through the formula

$$N_{кач} = \frac{M_c \omega_c \mu \eta''_{wc} i''_{cw}}{R_0} \left(\frac{d_{ш}}{d_{г.к}} - 1 \right) (1 - f \operatorname{ctg} \alpha_{cp}) \sin \alpha_{cp}. \qquad (115)$$

The corresponding loss factor $\psi_{кач}$ will equal

$$\psi_{кач} = \frac{N_{кач}}{N_c} = \frac{\mu \eta''_{wc} i''_{cw}}{R_0} \left(\frac{d_{ш}}{d_{г.к}} - 1 \right) (1 - f \operatorname{ctg} \alpha_{cp}) \sin \alpha_{cp}. \qquad (116)$$

The transmission efficiency in relative motion with a flexible driving component is determined from the expression

$$\eta''_{wc} = 1 - \psi''_{wc} = 1 - (\psi_{зац} + \psi_{кач}).$$

Taking into account (110), (113) and (116)

$$\psi'' = \psi''_{wc} = \frac{k_\psi}{R_0 + k_\psi}. \qquad (117)$$

The question concerning actual values of the coefficients of sliding friction in the engagement of teeth f and of rolling friction in the wave generator μ which enter k_ψ requires the organization of special investigation.

At the same time, the working conditions of teeth in the harmonic drives in the presence of lubrication are very close to

the working conditions of teeth of regular drives with internal gearing. This circumstance makes it possible to utilize the available experimental data on the determination of the coefficients of friction f for regular drives in the calculations. On the basis of published data [17] it is possible to accept for harmonic drives with consideration of the special lubrication conditions f=0.05-0.07. The value of the coefficient of rolling friction, just as for common antifriction bearings, should be designated μ=0.006-0.008 (for balls).

Let us compute values of the efficiency of a two-wave drive with different directions of translation of motion for the transmission ratios determined by the numbers teeth of the flexible component $z_г$=156 and $z_г$=520. In this case let us accept f=0.06; μ=0.007 mm; $d_{дг}$=156 mm; $d_{вн}/d_{т.к}$=19. For the geometry of the approximate engagement recommended above the value k_Δ is found from the graph given in figure 35; $\alpha_{ср}$=26° (with $\alpha_д$=20°).

Let us compute the value of coefficient k_ψ according to formula (110): for $z_г$=156

$$k_\psi = \frac{1{,}27 \cdot 0{,}81 \cdot 0{,}06}{0{,}9 - 0{,}06 \cdot 0{,}436} + 0{,}007\left(1 + \frac{2}{156}\right) \times$$
$$\times (19 - 1)(0{,}436 + 0{,}06 \cdot 0{,}9) = 0{,}1350 \text{ мм};$$

for $z_г$=520

$$k_\psi = \frac{1{,}27 \cdot 0{,}81 \cdot 0{,}3 \cdot 0{,}06}{0{,}9 - 0{,}06 \cdot 0{,}436} + 0{,}007\left(1 + \frac{2}{520}\right) \times$$
$$\times (19 - 1)(0{,}436 + 0{,}06 \cdot 0{,}9) = 0{,}0831 \text{ мм}.$$

The radius of the basic circumference of the rigid component will equal

$$R_0 = \frac{d_{0ж}}{2} \cos 20° = \frac{158}{2} \cdot 0{,}94 = 74{,}26 \text{ мм}.$$

Then on the basis of formulas (109) and (117) we find: for $z_г$=156

$$\psi''_{wz} = \frac{k_\psi}{R_o} = \frac{0{,}135}{74{,}26} = 0{,}001818;$$

$$\psi''_{zw} = \frac{k_\psi}{R_o + k_\psi} = \frac{0{,}135}{74{,}26 + 0{,}135} = 0{,}001815;$$

for $z_r = 520$

$$\psi''_{wz} = \frac{k_\psi}{R_o} = \frac{0{,}0831}{74{,}26} = 0{,}001119;$$

$$\psi''_{zw} = \frac{k_\psi}{R_o + k_\psi} = \frac{0{,}0831}{74{,}26 + 0{,}0831} = 0{,}001118.$$

Utilizing formulas (95), (96), (97) and (98), we find: for $z_r = 156$

$$\eta'_{wz} = 0{,}875; \quad \eta''_{wz} = 0{,}874;$$
$$\eta'_{zw} = 0{,}8581; \quad \eta''_{zw} = 0{,}857;$$

for $z_r = 560$

$$\eta'_{wz} = 0{,}775; \quad \eta''_{wz} = 0{,}774;$$
$$\eta'_{zw} = 0{,}709; \quad \eta''_{zw} = 0{,}709.$$

As is evident, the value of the efficiency drops with an increase in the gear ratio; with this, the efficiency of the reducer proves to be higher than the efficiency of the accelerator.

One ought to focus attention on the fact that the computation of the loss factor in relative motion must be performed at least with five significant decimal places since otherwise substantial errors will occur during the computation of efficiency in absolute motion.

Let us also examine the determination of power losses for rolling friction in a wave generator under the action of the forces of elastic deformation of the flexible component and the backing ring.

With the initial deformation of the components under the action of two oppositely directed forces, the effect of the deformed components on the wave generator theoretically occurs at two points. If this effect is absorbed during the rotation

of the generator by the rolling contacts which consecutively enter the zone of action of the forces, then moments of resistance to rolling over appear whose power characterizes the losses.

Forces with which the deformed components affect the generator are numerically equal to the forces which cause deformation. The value of these forces can be determined from the following expressions:

for the flexible component

$$Q_1 = c_1 \cdot 13{,}443 \frac{EJ_r k_\Delta m_y}{r^3_{rH}};$$

for the backing ring

$$Q_2 = 13{,}443 \frac{EJ_k k_\Delta m_y}{r^3_{rH.k}},$$

where J_r is the moment of inertia of the wall of the component in an axial cross section; J_k - the moment of inertia of the backing ring in the axial cross section; c_1 - the coefficient which depends on the design of the flexible component; $r_{rH.k}$ - the radius of the neutral line of the backing ring.

For a flexible component in the form of a tube with $l=1.5d_{r.H}$ $c_1=0.65$, for a flexible component in the form of a container with the same length $c_1=0.9$. Recommended values of c_1 also consider an increase in the rigidity of the ring gears in comparison with smooth rings [21].

The total force of deformation can be taken as equal (with $m \approx m_y$) to

$$Q = Q_1 + Q_2 = 13{,}443 Ek_\Delta m \left(c_1 \frac{J_r}{r^3_{rH}} + \frac{J_k}{r^3_{rH.k}} \right).$$

We determine the power expended on the rolling over of rolling contacts in absolute motion. Therefore by analogy with formula (106) for two zones it is possible to write the expression

$$N'_{кач} = 2Q\mu\omega_н\left(\frac{d_{нар}}{d_{т.к}} + 1\right),$$

where $d_{нар}$ is the diameter of the external surface of the track of the wave generator which is considered as in a nondeformed state.

The loss factor will be determined in this case according to the relation

$$\psi'_{кач} = \frac{N'_{кач}}{N_н} = \frac{2Q}{M_н}\mu\left(\frac{d_{нар}}{d_{т.к}} + 1\right).$$

For power drives the value of the loss factor is usually low, does not exceed $\psi'_{кач}=0.002$, and need not be considered. However, in kinematic drives, especially with the use of flexible components with wall thickness more than recommended by the calculation (see Chapter V) and with $d_{нар}/d_{т.к}>25$, the need to consider these losses can arise.

Thus, for determining the theoretical efficiency of the projected drive it is sufficient to consider losses to friction in engagement and in overcoming the resistance to the rolling over of the rolling contacts of the wave generator which are under the influence of the forces which arise with the application of the working load.

Table 9 gives the formulas utilized for the calculations. Selection of the required formulas is accomplished depending on the direction of translation of the motion.

Table 9. Formulas for determining the efficiency of harmonic drive with approximate engagement.

Work of drive	Efficiency in absolute motion with fixed component		Loss factor in relative motion
	Flexible	Rigid	
In accelerator mode	$\eta^{e}_{жн} = \frac{1-\psi^{н} i^{e}_{нж}}{1-\psi^{н}}$	$\eta^{ж}_{ен} = 1-\psi^{н} \times (1+\lvert i^{ж}_{не}\rvert)$	$\psi_{н} = \frac{k_{\psi}}{R_0 + k_{\psi}}$
In the reducer mode	$\eta^{e}_{нж} = \frac{1}{1-\psi^{н}(1-i^{e}_{нж})}$	$\eta^{ж}_{не} = \frac{1-\psi^{н}}{1+\lvert i^{ж}_{не}\rvert \psi^{н}}$	$\psi_{н} = \frac{k_{\psi}}{R_0}$
$k_{\psi} = \frac{1{,}27 k_{\Delta} m f}{\cos\alpha_{cp} - f\sin\alpha_{cp}} + \mu\left(1+\frac{2}{z_2}\right)\left(\frac{d_{он}}{d_{гк}}-1\right) \times (\sin\alpha_{cp} + f\cos\alpha_{cp})$			

One ought to focus attention on the fact that with large transmission ratios utilized in harmonic drives and the use of the latter as accelerators, extremely large dynamic moments arise with the starting of a mechanism. The value of these moments depends on the given moment of inertia of the mobile components referred to a slow shaft, and with massive generator cams turns out to be very large. This circumstance leads to the fact that the accelerator in many instances cannot be put into action although its efficiency with steady motion is extremely high generally speaking. In connection with the indicated, the designing of accelerators with harmonic drives should provide for their design with starting moments.

CHAPTER V

STRENGTH DESIGN OF BASIC PARTS

11. STRESSES WHICH ARISE IN THE FLEXIBLE COMPONENT

The load ability of a harmonic drive in essence is limited by the strength of the flexible component. In widespread designs the flexible component is a thin-walled cylindrical container dead-end sealed into a shaft or thin-walled tube which has free end faces.

The very operating principle of a harmonic drive entails the creation of a moving wave of deformation of the flexible component; therefore, the latter, in spite of the external simplicity of design, is a complex part which operates under very severe conditions.

Figure 44. Picture of a isochrome in a transparent model of a flexible component.

Stresses arise in the flexible component back during the assembly of the drive. Figure 44 shows the stressed state

in a deformed model of a thin-walled toothed rim (z_r=88, m=2 mm) manufactured from optically active transparent material. The dark bands (isochromes) are lines at points of which a difference in the main stresses is equal to just one whole number. In connection with the fact that on the surface of the part one of the main stresses is equal to zero, from the order of the isochromes one can judge the maximum stress at the point of the isochrome lying on the surface. Zone I is arranged along the greatest diameter of the deformed ring and zone II is arranged along the smallest. As is evident, the neutral line of the ring (in the figure points of the lines are visible as the short dashes designated by the numeral 0) acquires a zigzag form. The order of the isochrome is designated on the figure by the corresponding numerals. In zone I, the greatest stresses in the spaces of the teeth (elongated side) are determined by isochromes of the 6-th order. In zone II (compressed side) - by isochromes of the 5th order. Zone III corresponds to $\phi \approx 45°$.

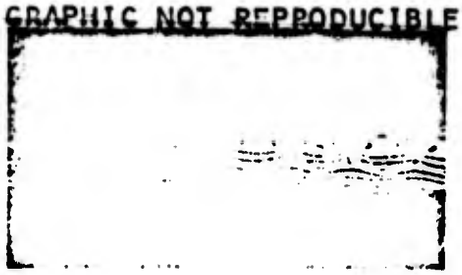

Figure 45. Comparison of stresses in the smooth and serrated sections of the model of a rack.

Figure 45 shows a picture of isochromes in a serrated rack ($z=\infty$) from the same material that has smooth and serrated sections. The height of the teeth of the rack is 1.25m, relation $\bar{\delta}=\delta/m=2.5$. The rack is loaded with a bending moment. As is evident, the presence of teeth raises the rigidity of the rack and causes the appearance of local stresses. The greatest order of the isochromes on the surface of the smooth section is the 3rd, while of the serrated it is the 4th.

It is interesting to focus attention on the fact that on the elongated side the isochromes arranged on the tooth converge

in a beam at the root of the tooth. This proposition confirms the correctness of the basic prerequisite for the geometric calculation of the teeth about the invariability of the form of the profiles of the teeth on the working section with the deformation of the flexible component.

Rotation of the wave generator before the application of the working load causes the synchronized displacement of the zone of deformation and the corresponding periodic change in the stresses at each point of the flexible component. The stressed state of the flexible component before the application of the working load depends on its design. With free ends and the arrangement of the wave generator at one of them the greatest normal stresses will occur in a direction perpendicular to the generatrix on the greatest diameter of the deformed cylinder from the direction of the wave generator.

For the flexible component made in the form of a container dead-end sealed into a shaft, the greatest normal stresses will occur in the direction of the generatrix which also passes through the greatest diameter of the deformed cylinder, but from the direction of the sealing of the latter. The value of these stresses depends on the length of the container and, with $L \leq d_r \cdot 1.5$ (d_r - the diameter of the container), exceeds the stresses along the perpendicular to the generatrix with another end deformed by the generator. At the same time, considering that on the section of the flexible component in the zone of the arrangement of the wave generator there are teeth and that the deformation of the wall of the container causes the appearance of considerable local stresses in the spaces between the teeth, the actual stresses on the section of the arrangement of teeth turn out to be greatest all the same.

The application of the working load significantly changes the picture of the deformations of the flexible component and the value of the initial stresses which arise. First of all one

ought to indicate the appearance of bending stresses variable in value in the teeth and of local bending stresses of the rim. The greatest values of these stresses depend on the form and height of the teeth, and also the design of the wave generator. Local bending stresses of the teeth are superimposed on the local bending stresses of the wall of the component; in this, their distribution along the bottom of the indentations becomes asymmetric. In the zone of tension from that side of the tooth on which the load acts, the local stresses are added and from the opposite side they are subtracted. Furthermore, because of the moment in the root of the tooth created by the applied load, a decrease in the stresses occurs on the internal surface of the flexible component. Under the effect of the torque in the flexible component torsional stresses arise which are distributed along its length differently.

From the direction of the transmission of rotation of the flexible component to the shaft, the torsional stresses are distributed over the perimeter of the container more uniformly than from the side of the toothed ring; in this, the zone of action of the maximum stresses displaces about the circumference at the speed of rotation of the wave generator.

The frequency of change in the stresses in one revolution of the generator depends on the number of waves of deformation of the flexible component. Thus, all the stresses operating in the flexible component are variables and its working capacity is determined by the fatigue of material.

The indicated circumstances require consideration of the features of the action of stresses in the strength design of the flexible component. The extremely small relative thickness of the wall of the flexible component of a harmonic drive makes it possible to consider the flexible component as a shell and to determine the deformations and nominal stresses at any point of the component by methods developed in the theory of shells [27].

At the same time, these methods are very cumbersome, barely suitable for the engineering calculations of harmonic drives and, in essence, are necessary for the disclosure of the qualitative aspect of the work of the flexible components.

The engineering method for the calculation for durability of the flexible components of harmonic drives is examined below.

As has already been indicated, most dangerous regarding the possibility of the emergence of fatigue failures are the sections of the flexible component in the area of cross section A-A (figure 46). With the arrangement of these sections in the zone of the greatest deformation the greatest normal stresses (from bending) will act in them which change in an asymmetric cycle and are close to the greatest tangential stresses which change according to a pulsating cycle. Here stresses close to maximum local stresses will occur which arise from the bending of the teeth and wall of the component and also local torsional stresses connected with a change in the cross section of the wall of the flexible component.

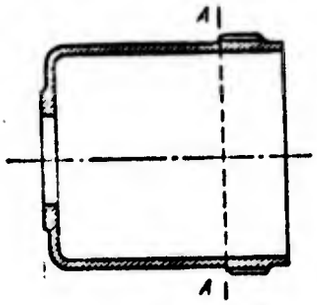

Figure 46. Position of the design cross section of a flexible component.

The wall thickness of the flexible component substantially affects the relationship between the indicated stresses in the zone being studied. An increase in the wall thickness leads to an increase in the normal stresses in the rim and teeth, and to a decrease in the tangential stresses. A decrease in the wall thickness leads to a decrease in the normal stresses in the rim and teeth and to an increase in the tangential stresses. A decrease in wall thickness is also limited by the stability of the component. Furthermore, with a decrease in the wall thickness the local normal stresses increase in the rim because of the local pliancy in the loading of the teeth.

If we proceed from the requirement for assuring the identical permissible level of the nominal stresses in the wall of the flexible component with its deformation, then with an increase in the number of teeth on the flexible component and, consequently, with decrease in the relative deformation of the component, it is possible to increase the thickness of its wall.

12. DESIGN CALCULATION OF A HARMONIC DRIVE WITH APPROXIMATE ENGAGEMENT

Above, chapter III examined the question concerning the nature of the contact of the teeth of the flexible and rigid components with approximate engagement with the use of involute profiles of teeth. By the special selection of the parameters of the teeth and deformation of the flexible component the engagement is realized with which the surface contact of the teeth virtually occurs. It is senseless to examine the contact as corresponding to a higher kinematic pair in this case and to determine the contact stresses since the width of contact area turns out to be that commensurable with the height of the teeth, by which one of the conditions is disturbed with which the use of the available solutions of the contact problem is possible.

The picture of the contact of the teeth is generally sufficiently complex. In the process of the initial operating period of the drive a certain breaking-in of the side surfaces occurs, which changes the initial contact. The operation of the drive with a liquid lubricant complicates even more the process of the joint operation of the teeth. The lubrication of the side surfaces of the teeth in harmonic drives is accomplished very energetically. The engagement itself is seemingly a pump which drives off the lubrication along the length of the perimeter of the components; in this case, in the zone of engagement the oil which is located in the indentations of the teeth is wedged

and washes the effective surfaces at a high speed, creating conditions for the semiliquid friction mode.

In connection with the fact that the kinematic pairs formed by the teeth for the nature of the relative motion of their geometric elements are close to the lowest pairs, the condition of assuring the required carrying capacity of the side surfaces of the teeth can be written in the following manner:

$$p \leqslant [p],$$

where p is the greatest specific pressure; [p] - the allowable specific pressure.

During a full cycle of engagement of a pair of teeth the contact area of their effective surfaces is continuously changed from zero to F_{max}; in this case, the magnitude of the force transmitted by the teeth is also changed. The mean specific pressure p_{cp} can be determined from the following expression:

$$p_{cp} = \frac{P_{cp}}{F_{cp}}, \qquad (118)$$

where P_{cp} is the mean value of normal force in the contact of the pair of teeth; F_{cp} - the mean value of the contact area.

In turn value P_{cp} is found from the formula

$$P_{cp} = \frac{2M_{\text{пр}}}{d_{cp} 2k_z \cos \alpha_{cp}}, \qquad (119)$$

where k_z is a coefficient which considers the number of teeth which simultaneously participate in the transmission of the load.

The mean contact area can be determined by the formula

$$F_{cp} = \frac{0{,}5h_1 B}{\cos \alpha_{cp}}. \qquad (120)$$

Taking into account that for the adopted system of geometric calculation the depth of approach $h_э \approx m$, on the basis of (118, 119) and (120), we will have

$$p_{ср} = \frac{4M_ж}{d_{ср} z k_з m B}. \qquad (121)$$

In connection with the presence of the nonuniformity of pressure distribution along teeth and between the teeth, it is possible to write

$$p = p_{ср} k_{нр}, \qquad (122)$$

where $k_{нр}$ is the variation factor of pressure distribution over the width of the toothed ring which also considers the nonuniformity of pressure distribution between teeth.

The increase in the load due to the dynamic phenomena with large multiple pairing of engagement can be disregarded. The condition of the working capacity of the side surfaces of the teeth taking into account (121) and (122) with $z = z_ж$ is written

$$p = \frac{4M_ж k_{нр}}{d_{ср} z_ж k_з m B} \leqslant [p]. \qquad (123)$$

If we accept $d_{ср} \approx d_{дж}$ (which is possible, since this assumption increases the safety factor of the part) and also introduce designation $q_ж = B/d_{дж} \approx q_г$, then expression (123) will take the following form:

$$d_{дж} = \sqrt[3]{\frac{4M_ж k_{нр}}{k_з q_г [p]}}. \qquad (124)$$

The complexity of the scheme of engagement (with large multiple pairing), its change under load because of the deformation of the teeth and wall of the flexible component, the effect on the engagement scheme of the number of teeth, and design of the flexible component do not make it possible to give a strict theoretical solution of the problem of the nonuniformity of load

distribution between the teeth and along the teeth which is considered by coefficient $k_{нр}$. At the same time, in the procedure for the structural design of the flexible components this coefficient should receive a quantitative evaluation. Below is given the approximate solution of the problem in the computation of values of $k_{нр}$ based on a number of conditional propositions and data of the experiment.

We will assume that the flexible component in a Г-Ж-Н drive according to figure 19a, from the direction of the end which transmits rotation to a shaft, also has such connections with the shaft which permit the wave generators to retain the parallelism of its linear generatrices of the axes of rotation with the deformation of the component. In this case, the nature of the tooth engagement in any cross section perpendicular to the axis of rotation will remain constant. Figure 47a shows an idealized diagram of the contact of the teeth of the flexible and rigid components for the surface of the deformation of a flexible component developed to a plane.

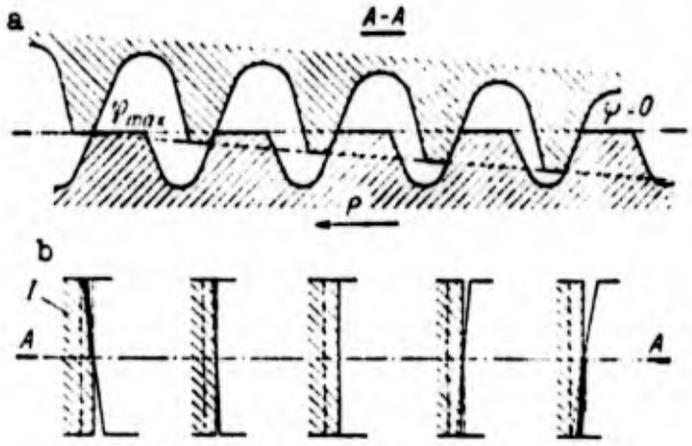

Figure 47. Diagram of the contact of the teeth in a drive of the Г-Ж-Н.

It is completely obvious that with the action of force P the change in area and height of the contact of the teeth along the zone of engagement will lead to the nonuniformity of load distribution between the teeth.

Let us replace the load distributed over the surface of each tooth participating in the transmission of forces with a concentrated normal force applied on the middle of the height of the

area of contact. The sum of the moments of all these forces P_i applied to the teeth of the rigid component relative to the axis of rotation of the latter, not allowing for forces of friction, can be equalled to the torque $M_ж$ applied to the rigid component. For a two-wave drive

$$M_ж = 2R_0 \sum_{i=1}^{i=\frac{z_ж k_2}{2}} P_i.$$

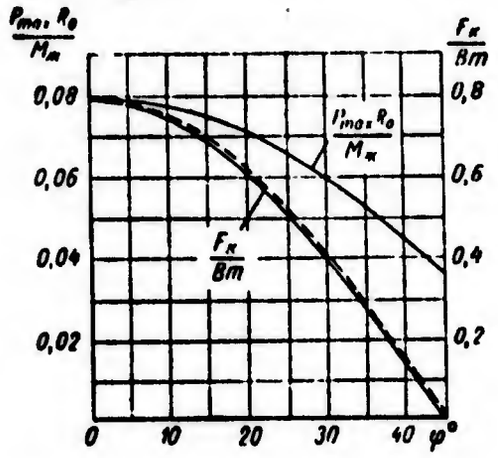

Figure 48. Graph of load distribution between teeth on an arc of 45° and graph of change in the contact area of the teeth.

As particular experiments carried out on the models of engagement showed, the minimum value of force of P_i acting on the teeth in zone φ_{max} (figure 47) can be half the force P_i in zone $\varphi=0$.

Figure 48 depicts a typical graph of the loading of the teeth by force P_i on an arc of engagement $\varphi=45°$. It is also necessary to consider that the recommended engagement scheme (see chapter III) with an involute equivelocity curve envisions the initial contact of the teeth in a zone of 45°. This can lead to the fact that the approximate law of distribution of a load between teeth presented in figure 48 will be changed and force $P_{(45°)}$ will increase substantially.

Let us now move on to an examination of the specific pressures which arise on the effective surfaces of the teeth. The specific pressure on the surface of the teeth is determined by the relation $p_i=P_i/F_i$, where F_i is the contact area of the i-th pair of teeth. As is evident from figure 48 and the diagram given in figure 47a, the contact area upon transition from $\varphi=0$ to φ_{max} changes from F_{max} to 0 and, therefore, the specific pressure should change from

the value P_0/F_{max} to infinity $\left(\frac{P_{(\varphi=0)}}{0}=\infty\right)$. It is completely natural that this position virtually cannot exist. In the first operating period of the drive the wear of the profiles in the upper part of the teeth will occur where the value of specific pressure turns out to be very large and the greatest sliding speed occurs, as a result of which the load which acts on the teeth will be redistributed. On figure 48 the dashed line shows the possible form of the curve of the change in load on the teeth in a broken-in drive. With this law governing load change, the specific pressure on the effective surfaces of all teeth participating in the engagement becomes approximately identical. In the realized drives with the recommended geometry of engagement, in the first operating period a bright strip appears on the upper edges of the teeth of the flexible and rigid components which testifies to the presence of wear and pressing-down of the surfaces.

Let us clarify what will occur in the engagement of the above examined broken-in drive if we change the nature of the connection of the flexible component with the shaft after giving the form of a circle to the central line of the component in the cross section lying on the section of transition to the shaft. With this form of deformation of the flexible component the inclination of the cylinder generatrix with regard to its axis will appear. Figure 49 shows how the generatrices change position with such deformation of the component.

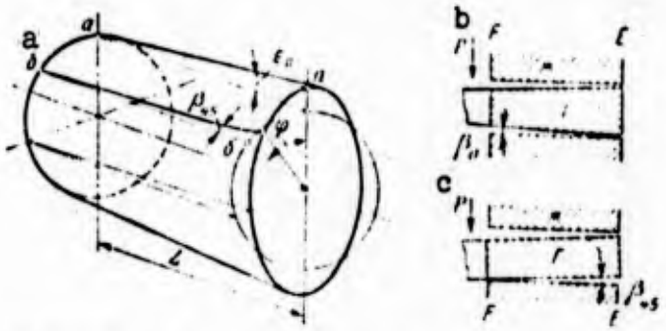

Figure 49. Determination of the angles of the generatrices of a deformed flexible component.

In zone $\varphi=0$ the change in the position of the generatrix is determined by angle ε_0 . The value of this angle depends on the ratio of radial deformation $k_\Delta m_y$ to the length of the component L

$$\operatorname{tg} \varepsilon \approx \frac{k_\Delta m_y}{l}. \qquad (125)$$

In this case the angle between the generatrices of the surfaces of the teeth of the rigid and flexible component (figure 49b) will equal

$$\operatorname{tg} \beta_0 = \operatorname{tg} \varepsilon \sin \alpha_{cp} \approx \frac{k_\Delta m_y}{l} \sin \alpha_{cp}. \qquad (126)$$

In the zone $\varphi=45°$ the change in the position of the generatrix is characterized by the angle β_{45} (figure 49c). Determination of this angle with the shape of deformations accepted in chapter III is accomplished on the basis of the condition of the retention of arc length ab of the neutral line with the deformation of the flexible component. For $\varphi=45°$ this condition takes the following form:

$$\frac{\pi}{4} r_{cm} = \frac{1}{2} r_0 (\psi_0 + \lambda)^2 - \frac{1}{2} r_0 \psi_0^2.$$

Taking into account (33-34) and (53), after transformations we obtain

$$\lambda = -\psi_0 + \sqrt{\psi_0^2 + 0{,}3370947 \frac{z_c}{k_\Delta}}. \qquad (127)$$

Utilizing equation (37), we find

$$\operatorname{tg} \gamma = \frac{(\psi_0 + \lambda) \sin \lambda + \cos \lambda - 1}{(\psi_0 + \lambda) \cos \lambda - \sin \lambda + 1}.$$

In connection with the smallness of the angle $\zeta=\gamma-\lambda$, it is possible to consider that $\zeta=\operatorname{tg}\zeta$, and then

$$\operatorname{tg} \beta_{45} = \frac{\zeta r_{cm}}{L}.$$

For the accepted range of gear ratios angles β_0 and β_{45} prove to be approximately equal. Taking this circumstance into account, we will accomplish the determination of angles β_0 and β_{45} according to the simpler relation (126) subsequently accepting $\beta_{45} \approx \beta_0$.

As is evident from a comparison of figure 49b and of figure 49c, with the passage of the arc of engagement $\varphi=45°$ by a pair of teeth concentration of the contact changes from the end of teeth E to the end of F. The changes which occurred in the contact of the teeth are also shown on the simplified diagram in figure 47b. At the first moment of a change in the form of deformation of the flexible component the teeth of the rigid component occupy a flexible position relative to the teeth shown by the dashed line 1, and the entire load will be transferred by the first and last teeth in each zone of engagement. Under the action of this load the teeth will begin to be transformed until the subsequent pairs of teeth enter into work, and the forces of elastic deformation of all the teeth will not balance the external load. With the deformation of the teeth, their contact will occur not on the edge, but over the surface, but in this case the specific pressure along the length of the contact surface will be distributed unevenly. This nonuniformity can be estimated by theoretical coefficient $\theta_{нр}$, which in this case will be equal to

$$\theta_{нр} = \frac{q_{max}}{q_{ср}}, \qquad (128)$$

where q_{max} is the maximum load per unit of length of the tooth; $q_{ср}$ - the average load per unit of length of the tooth.

The value q_{max} is found from the formula

$$q_{max} = Cl\beta,$$

where C is the specific rigidity of the teeth; l - the length of the area of contact.

Accordingly

$$q_{cp} = \frac{P_n}{B},$$

where P_n is the normal force in the contact of the pair of teeth; B - the length of the tooth (width of the toothed ring).

The value of the coefficient of specific rigidity C depends on many factors. Data on the value of coefficient C for harmonic drives as yet does not exist and it is possible to accept values of C=60,000-100,000 kgf/cm^2 obtained for the thin-walled toothed rims of common involute gear drives extremely approximately.

On the basis of known considerations [17], disregarding the low relative width of the toothed ring the deformations of the twisting of the flexible component and considering that according to figure 47b the length of the contact spot will be $l \leq B$, the variation factor of load distribution along the length of the tooth will be determined according to the formula

$$\theta_{HP} = B \left| \frac{2C\beta}{P_n} \right|, \qquad (129)$$

in which, on the basis of the conclusions drawn above,

$$P_n = p_{cp} F_l.$$

If we assume that the height of the area of contact of the teeth is constant along the length, then coefficient θ_{HP} will also equal

$$\theta_{HP} = \frac{p_{max}}{p_{cp}}. \qquad (130)$$

Let us examine an example of the determination of the value of coefficient θ_{HP} for a drive with the following data: $i^{III}_{HГ}$=132; m_y=0.6 mm; α_{cp}=26°; p_{cp}=700 kgf/cm^2; k_Δ=0.81; L=$d_{Г.Н}$; C=80,000 kgf/cm^2; B=25 mm; φ=0

$$\beta = \frac{k_\lambda n_u}{L} \sin \alpha_{cp} = \frac{0,81 \cdot 0,6}{160} \sin 26^\circ = 0,00134.$$

$$F_{\varphi=0} = h_3 B = 0,6 \cdot 25 = 15 \text{ мм}^2 = 0,15 \text{ см}^2.$$

$$P_n = p_{cp} F_{\varphi=0} = 700 \cdot 0,15 = 106 \text{ кГ}.$$

$$\theta_{нр} = B \sqrt{\frac{2C\beta}{P_n}} = 2,5 \sqrt{\frac{2 \cdot 80\,000 \cdot 0,00134}{106}} = 3,52.$$

In the zone of $\varphi=45°$ coefficient $\theta_{нр}$ will be even larger, but this will already be the index of the low loading of the contact. With the operation of the drive the picture of contact gradually changes. In zone $\varphi=45°$ intensive break-in of the teeth occurs because of the wear of their upper edges; the break-in of the teeth in zone $\varphi=0$ proceeds less intensively and consists not only of the wear, but also of the plastic deformation of the surface layers of metal. It is natural that an increase in the hardness of the flexible and rigid components worsens the condition of the breaking-in of the teeth.

As a result of the break-in of the teeth the nonuniformity of pressure distribution over their length is decreased considerably. This circumstance makes irrational the use of the values of the theoretical variation factor of pressure distribution $\theta_{нр}$ in calculations since in this case the dimensions of the transmission are unjustifiably exaggerated.

At the same time the fact of the presence of large nonuniformity in the new drive is very dangerous since it can turn out that the time necessary for the break-in of the teeth, in which the nonuniformity of pressure will be eliminated, will prove to be more than the time during which the fatigue fracture of the teeth or wall of the flexible component will begin in places of large overloads.

The way out of the apparent contradiction between the striving to decrease the dimensions of the drive through the use of lower

values of $\theta_{нр}$ and the striving to eliminate breakage of parts of the drive in the period of the break-in of the teeth, which is assured by the use of the theoretical coefficient of $\theta_{нр}$ during the calculation, can be found if we consider the break-in of the drive as a necessary element of the production process of its manufacture and assembly. In this case, in the calculation of a drive the effective variation factor of pressure distribution along the length of the teeth $k_{нр}<\theta_{нр}$ should be utilized and the necessary break-in should be conducted in such a way as to eliminate the possibility of the emergence of inadmissibly large stresses in the parts in the process of its conduct.

The criterion of achievement of the break-in can be the requirement for obtaining the necessary length of the contact spot l on the effective surfaces of the teeth. The testing should be performed with the use of a paint with the minimum load on the driven component of the drive (the teeth of the rigid component are smeared with paint). If after the check of the length of the contact spot on the teeth of the flexible component $l \sim B$ and in the middle part the spot does not have gaps, this bears out the fact that the teeth were broken in and acquired a barrel-shaped form.

The requirement for the loading of the drive during cnecking with the minimum torque ($M_{пров} \approx 0.05 M_{ном}$) ensues from an examination of figure 47b. The contact of the unloaded teeth with the propagation of the contact spot on their entire length and the absence of a gap in the middle part can occur only in the case where it occurs on sections designated by a heavy line which characterizes the form of the broken-in teeth. Until break-in attains the indicated stage, during checking (without load) the breakage of the contact spot in the middle part will be detected. The break-in of the transmission should be conducted with stepped loading and the greatest torque on the driven component

$$M_{прир} \leq \frac{k_{нр}}{\theta_{нр}} M_{ном}.$$

It is necessary to show that if the safety factor for normal stresses during the checking of the flexible component for durability (see page 143) will be $n_\sigma \geq 2$, then the break-in can also be conducted with nominal torque $M_{ном}$. In this case, in the determination of the safety factor n_σ the bending stresses are calculated from the formula

$$\sigma_{из} = \frac{\theta_{нр}}{k_{нр}} \sigma_{из(k_{нр})},$$

where $\sigma_{из(k_{нр})}$ is the bending stresses of the teeth found with the load coefficient $k_{нр}$.

In the calculations of drives of the Г-Ж-Н type and $m_y/L \leq 0.006$ we recommend using a value of the effective variation factor of pressure distribution $k_{нр}=2$.

The reasonings carried out above concerned in essence precisely drives of the Г-Ж-Н type for which the nonuniformity of pressure distribution along the length of the teeth is their organic shortcoming.

In drives of the Г-Ж-Н type the nonuniformity of pressure distribution along the length of the teeth can arise only due to the twisting of the component and misalignments connected with the presence of gaps in the coupling of the parts and the errors in the manufacture of the drive; therefore it should be approximately accepted that $k_{нр}=1.5$.

In drives of the Г-Ж-Н type, for a decrease in the value $\theta_{нр}$ some design and technological measures can be adopted. As design measures, we can recommend in the first place the use of alloyed chrome-nickel steel for the flexible components with hardness $HB \leq 350$ and endurance limit $\sigma_{-1} \geq 4000$ kgf/cm^2. As technological measures, it is possible to recommend the shaving of the teeth of the flexible component with the formation of their barrel-shaped form.

The elimination of the initial edge contact can be realized with the cutting of the teeth of the flexible component with the reproduction of the process of the engagement of the harmonic drive (see chapter VII).

Finally, the cutting of conical teeth on the flexible component can be realized through the creation of an angle between the directions of motion of the feed of the hobbing cutter and the axis of the flexible component being cut. This is achieved most simply by the inclination of the axis of the part through a shift of the holding support (with the spherical center of the mandrel of the flexible component) and by introduction, between the platen and the mandrel, of the part of a synchronous guide clutch. The slope of the axis in this case should not be more than $0.6\frac{k_\Delta m_y}{L}$, since a decrease of $\theta_{нр}$ in zone $\varphi=0$ can cause an inadmissibly large value of $\theta_{нр}$ in zone $\varphi=45°$.

The breaking in of the teeth also pertains to technological measures.

The value of coefficient k_z which enters formula (124) is determined by the selected engagement scheme. For a developed system of approximate engagement $k_z=0.22-0.25$.

The value of the permissible specific pressure [p] in the formula should be determined by experiment. For steel gears we recommend taking [p]=600-650 kgf/cm^2. We obtained this value by processing data and characteristics of the realized and serially produced power harmonic drives published abroad and in our country in which the contact of the teeth over the surfaces is provided for. In particular, according to formula (124) with recommended values of [p] and $k_{нр}$ the dimensions of all basic general purpose reducers made by the firm "United Shoe Machinery Corporation" (USA) and having $q_r=0.15$ are determined completely

accurately. The level of specific pressures permissible in harmonic drives uncommonly high for kinematic pairs is apparently possible because of the aforementioned special conditions of the lubrication of the surfaces of the teeth.

Regardless of the type of engagement used, the task of the design calculation of a harmonic drive includes the determination of the wall thickness of the flexible component. As noted above, the bending stresses in the wall of the flexible component arise with the assembly of the drive. The presence of teeth on the deformed part causes the appearance of stress concentration, as a result of which normal stresses in the wall of the component prove to be extremely great and depend on its thickness. For purposes of simplification, instead of a shell we will examine the deformation of a flexible ring in which its neutral line on arc $\pi/2$ acquires the form of an involute of a circle. As a result of the deformation the radius of curvature of the neutral line of the ring changes. In the place of the greatest positive deformation, the radius of curvature of the neutral line instead of $r_{гн}=0.5m_y z_г$ becomes

$$r_{min} = r_{гн} + k_\Delta m_y - r_0.$$

This change in the radius causes the tension of the material on the external and compression on the internal surfaces of the ring.

Let us designate by l_0 the length of the elementary arc of a neutral line in the cross section of the flexible component before its deformation (figure 50). Then the arc length of the external circumference l_e of the same central angle is connected with l_0 by the relation

$$l_0 = \frac{r_{гн}}{r_{гн} + \frac{\delta}{2}} l_e. \qquad (131)$$

If we designate by r_{min} the minimum radius of curvature of the neutral line after the deformation of the flexible component, then the relationship

$$l_0 = \frac{r_{cp}}{r_{min} + \frac{\delta}{2}} - l'_e \qquad (132)$$

will occur where l'_e is the arc length of the external circumference of the deformed component.

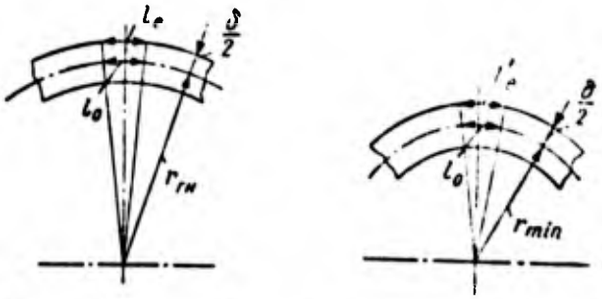

Figure 50. For determination of stresses in a deformed flexible ring.

Then the elongation of the material on the external surface will be

$$\Delta l = l'_e - l_e = \sigma \frac{l_e}{E}. \qquad (133)$$

Equating (131) and (132), we find that

$$l'_e = l_e \frac{1 + \frac{\delta}{2r_{min}}}{1 + \frac{\delta}{2r_{cp}}}.$$

Substituting the value l'_e in (133), after transformation we find

$$\sigma = \frac{\delta E \left(\frac{r_{cp}}{r_{min}} - 1 \right)}{2r_{cp} + \delta}. \qquad (134)$$

If one considers that the second term in the denominator for real drives is considerably less the first, then it is possible to accept

$$\sigma = \delta E \frac{\frac{r_{cp}}{r_{min}} - 1}{2r_{cp}}.$$

After the conversion of this expression it is possible to write the condition of strength of the part in the following form:

$$\sigma = \frac{\Delta E}{m_y z_2 \left(0{,}1366 \frac{z_2}{k_\Delta} - 1\right)} \leqslant [\sigma], \qquad (135)$$

whence the necessary thickness of the ring δ is determined

$$\delta \geqslant \frac{[\sigma]}{E} \left(0{,}1366 \frac{z_2}{k_\Delta} - 1\right) z_2 m_y. \qquad (136)$$

For the preliminary design calculation of the flexible component when value m_y is unknown, it is necessary to know the value of the coefficient of the thickness of the component $\vartheta = \delta/m_y$ (in view of the small difference in m and m_y it is also possible to accept $\vartheta = \delta/m$).

From (136) it follows that

$$\vartheta = \frac{[\sigma]}{E} \left(0{,}1366 \frac{z_2}{k_\Delta} - 1\right) z_2. \qquad (137)$$

For an equivelocity curve of arbitrary form the coefficient is calculated from the formula

$$\vartheta = \frac{[\sigma] z_2}{E \left(\frac{r_{cm}}{r_{min}} - 1\right)}. \qquad (138)$$

Taking into account that the stresses in a loaded flexible toothed component differ significantly from the stresses in a deformed smooth ring, in formula (137) one ought to utilize the extremely understated values of permissible stress. Thus, for steels with HB$\leq$350 that have endurance limit $\sigma_{-1} \geq 4000$ kgf/cm^2, it is possible to recommend values $[\sigma]$=500-750 kgf/cm^2. These recommendations correspond well to the uniform strength of the walls of the flexible component for bending and torsion. The condition of the strength of the walls of the flexible component with consideration of only torsional stresses takes the form

$$\tau = \frac{2M_c}{d_{zH}^2 \pi \delta} \leq [\tau]. \qquad (139)$$

If we accept as dangerous stresses in the work of the component for bending and for torsion the corresponding yield points σ_T and τ_T and proceed from the known relation $\tau_T = 0.58\sigma_T$, then with the identical safety factors for normal and tangential stresses taking into account expressions (135), (139), it is possible to write the equality

$$\frac{2M_c}{d_{zH}^2 \pi \delta} = \frac{0{,}58E\delta}{m_y z_c \left(0{,}1366 \frac{z_c}{k_A} - 1\right)}. \qquad (140)$$

In (140) $m_y z_\Gamma = d_{\Gamma H}$. Solving (140) relative to δ, we will have

$$\delta = \sqrt{\frac{M_c \left(0{,}1366 \frac{z_c}{k_A} - 1\right)}{0{,}91 E d_{\Gamma H}}}. \qquad (141)$$

The relation $M_\Gamma / d_{\Gamma H}$ in (141) can be also replaced by the relation $M_ж / d_ж$; then we obtain

$$\delta = \sqrt{\frac{M_ж \left(0{,}1366 \frac{z_c}{k_A} - 1\right)}{0{,}91 E d_ж}}.$$

The pitch circle diameter of the rigid component is connected with value $M_ж$ by relation (124), with consideration of which we will obtain the following formula for determining the wall thickness of the flexible component:

$$\delta = d_{\partial ж} \sqrt{\frac{k_z q_c [p] \left(0{,}1366 \frac{z_c}{k_A} - 1\right)}{3{,}64 E k_{np}}}. \qquad (142)$$

The coefficient of the wall thickness in this case will be equal to

$$\theta = \frac{\delta}{m} = z_ж \sqrt{\frac{k_z q_c [p] \left(0{,}1366 \frac{z_c}{k_A} - 1\right)}{3{,}64 E k_{np}}}. \qquad (143)$$

Figure 51 presents a graph for determining coefficient $, constructed within the limits of $250<z_r<600$ according to formula (143) with [p]=650 kgf/cm^2, $k_{нр}=2$ and $E=2.1\cdot10^6$ kgf/cm^2. As will be shown below, the use of flexible components with wall thickness $\delta<m$ is inadmissible, in connection with which the minimum value $=1 is accepted on the graph. Formula (143) written in general form and suitable for determining $ with any form of equivelocity curve takes the form

$$\$ = \sqrt{\frac{0{,}35k_{нр}[p]}{E\ln\left(\frac{r_{min}}{r_{min}-1}\right)}} \qquad (144)$$

where r_{min} is the minimum radius of curvature of the equivelocity line of the deformed component.

We investigate on which stress level the uniform strength in bending and torsion of the walls of the flexible component with thickness δ will occur. For this purpose let us compute according to formula (135) the value σ for the corresponding values of δ. A graph of a change in the bending stress in the wall of a deformed flexible component with a change in the number of teeth from $z_r=100$ to $z_r=600$ is given in figure 52. It is natural that on the section from $z_r=100$ to $z_r=250$ the condition of uniform strength is disrupted.

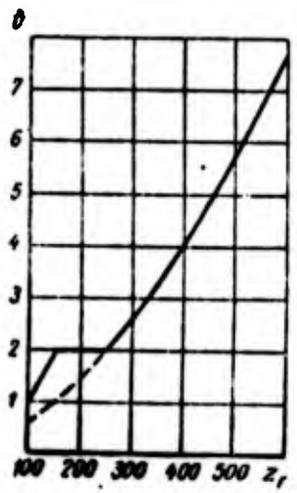

Figure 51.

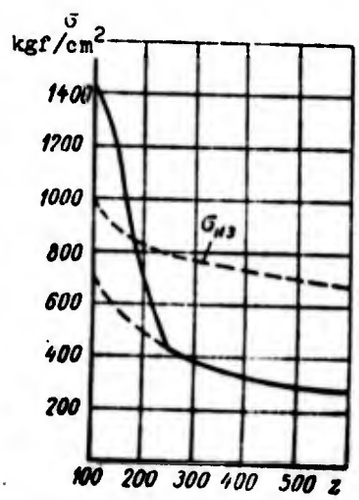

Figure 52.

Figure 51. Graph for determining coefficient $.

Figure 52. Change in the stresses in the root of teeth of the flexible component depending on the number of teeth.

As is evident, the greatest nominal bending stresses in the wall of the flexible component with $z_r > 150$ turn out to be extremely low. However, on the section of the arrangement of the teeth a completely different picture will occur. First, the presence of teeth on the component causes a concentration of stresses which is well evident from figure 44. An increase in the bending stresses in the tooth spaces with regard to the nominal stresses on the dedendum which are determined from expression (135) can be estimated by the theoretical concentration factor α_σ. The value of this coefficient depends on the relationship between the height of the teeth, the radius of transition curves in the spaces, the thickness of the teeth, and the wall thickness of the flexible component. The dimensions of the teeth and radii of the transition curves depend in essence on the modulus; therefore, the concentration factor will depend on the relationship of modulus and the wall thickness of the component. Figure 53 gives a graph of the dependence of the concentration factor α_σ on the parameter s (taking into account ruggedizing effect of teeth) with the geometric parameters of the teeth and the initial outline taken in the proposed system of calculation according to the GOST [ГОСТ - All-Union State Standard] 3058-54. For the initial outline according to the GOST 9587-61 values of α_σ from the graph should be increased 1.2 times. We constructed the graph on the basis of the study of transparent models of toothed rings and racks. The dashed line in figure 53 shows the relation without the ruggedizing effect of teeth.

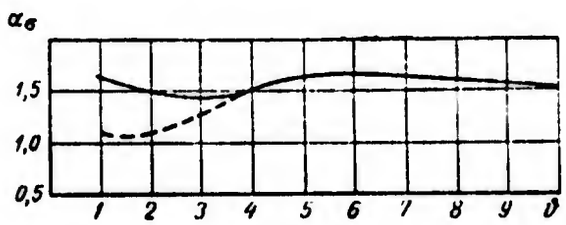

Figure 53. Graph for determining theoretical concentration factor α_σ.

In the second place, the application of torque to the flexible component causes the appearance of bending stresses in the root of the teeth. These stresses along one side of the teeth are made up with the normal

stresses which appear in the same zone as a result of the deformation of the wall of the flexible component; along the other side of teeth the stresses are subtracted.

Let us determine the value of the greatest local bending stresses of the teeth. According to the known relation for involute teeth

$$\sigma_{из} = \frac{P_{ок}}{mBY}, \qquad (145)$$

where $P_{ОК}$ is the maximum value of the peripheral force on the dividing circumference transmitted by one pair of teeth; Y - the form factor of the tooth.

In this case, on the basis of the considerations given on page 97 it is possible to accept

$$P_{ок} = ph_3 B \cos \alpha_{ср}, \qquad (146)$$

where p is the specific pressure in a broken-in drive determined according to formula (123).

The value p according to formula (123) already considers the nonuniformity of load distribution along the length of the teeth. In spite of the fact that the nonuniformity of the stress distribution of the bending in this case can be less than the nonuniformity of the load, we will accept that nonuniformity during the computation for bending and for specific pressure are identical.

Expression (146) already considers the greatest nonuniformity of load distribution between the teeth, which will increase with the breaking-in of the teeth and equalizing the amount of specific pressure in the contact.

The value of the form factor of the teeth Y in this case for involute teeth of the flexible component can be approximately

accepted according to known recommendations [16]; with this we equate $Y=Y_\varepsilon$, where Y_ε is the form factor of the teeth for the case of application of a load along the line of single pair engagement.

If we select recommended values of Y_ε for the contact point distant by approximately the value m from the tooth crest (a height of regular teeth of 2.25m [sic] is envisaged), and in this case we consider the displacement factor of the initial outline, then for $\xi=0.022z_e$ (see chapter III) as a result of the processing of the corresponding graphs from [16] the following formula can be obtained:

$$Y = 0{,}376 \lg z_e - 0{,}0835, \qquad (147)$$

which provides a sufficiently correct result for the recommended range of numbers of teeth of the flexible component.

After substitution of the values of $P_{ок}$ from (146) in (145), taking into account that $h_з \approx m$ and cos 26°=0.9, we will have

$$\sigma_{из} = \frac{0{,}9p}{Y}. \qquad (148)$$

On the graph given in figure 52, the dashed line shows the dependence of $\sigma_{из}$ on the number of teeth $z_г$ obtained on the basis of formulas (147) and (148) with $p=[p]=650$ kgf/cm^2.

The greatest bending stresses correspond to the minimum number of teeth $z_{г\ min}$. It should be noted that the indicated relation will occur with the sufficiently large wall thickness of the component. For fine walls the joint examination of the deformation of the teeth themselves and the wall on the section between the teeth is required; in this case another result will occur.

In the general case it is possible to recommend using a wall thickness of the component $\delta \geq m$. Then the nature of a change

in the stresses with an increase in the number of teeth of the component and a corresponding increase in the relative wall thickness should remain without essential change.

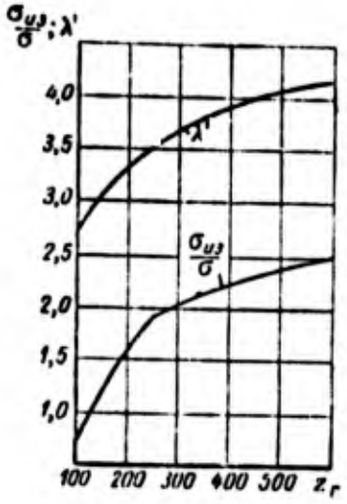

Figure 54. Graph for determining concentration λ'.

As is evident, a specific relationship occurs between the stresses which appear in the wall of the flexible component with its deformation by the wave generator and the local greatest bending stresses of the teeth superimposed on them. Figure 54 depicts a graph which shows the value of relation $\sigma_{из}/\sigma$ as a function of the number of teeth $z_г$. The use of relation $\sigma_{из}/\sigma$ at the present stage of development of the method for the calculation of harmonic drives permits not determining separately and then totaling the nominal normal stresses in the wall of the flexible component obtained with different deformations but determining only greatest nominal stress which arises with the deformation of the component by the wave generator and multiplying it by some coefficient λ' which considers the concentration and the action of the bending stresses of the teeth, i.e.

$$\lambda' = \alpha_\sigma + \frac{\sigma_{из}}{\sigma}. \qquad (149)$$

Figure 54 also depicts a graph of the function $\lambda' = f(z_г)$. The graphs depicted on figures 51, 53, 54, can be used with all forms of deformations of the flexible components examined in chapter III.

13. DESIGN CALCULATION OF A HARMONIC DRIVE WITH PRECISE ENGAGEMENT WITH CIRCULAR PROFILES OF THE TEETH

The precise engagement theoretically envisages the existence of linear contact of the teeth. For the developed geometry (page 69) with circular profiles of the teeth of the rigid component the value of the contact stresses with certain assumptions can be determined by the Hertz formula

$$\sigma_к = 0{,}418 \sqrt{p_в \frac{E_{пр}}{\rho_{пр}}} \leq [\sigma]_н, \qquad (150)$$

where $p_в$ is specific load; $E_{пр}$ - the reduced* elastic modulus; $\rho_{пр}$ - the reduced* radius of curvature of the teeth; $[\sigma]_н$ - the permissible value of contact stresses.

The value of quantity $p_в$ taking into account the nonuniformity of load distribution between the teeth and along the length of the teeth is found from the expression

$$p_в = p_{ср.в} k_{нр.z} k_{нр.в}, \qquad (151)$$

in this case

$$p_{ср.в} = \frac{M_н}{BR_ц \cos\alpha_{ср} z k_z}. \qquad (152)$$

In these formulas: $k_{нр.z}$ is the coefficient which considers the nonuniformity of the load distribution between the teeth participating in the work; $M_н$ - the torque applied to the rigid component; $R_ц$ - the radius of the circle of the centers of the circular profiles of the teeth; $\alpha_{ср}$ - the average value of pressure angle in engagement.

In connection with the fact that almost on the entire height the profiles of the teeth of the flexible component have very low

---

*[Translator's Note. May also be "given".]

curvature (see figure 31) it is possible to consider with sufficient accuracy that (see page 88) the reduced radius of curvature $\rho_{пг}=\rho=1.55m$. For the geometry of engagement taken above $\alpha_{ср}=25$ and $\cos\alpha_{ср}=0.906$. After substitution and transformation formula (150) takes the form

$$\sigma_к = 0{,}418\sqrt{\frac{M_ж k_{нр.к} k_{нр.z} E_{пр}}{BR_и z_ж k_z 1{,}55m\cos 25^\circ}} \leqslant [\sigma_к].$$

Squaring it, we obtain

$$\sigma_к^2 = 0{,}1741\,\frac{M_ж k_{нр.к} k_{нр.z} E_{пр}}{BR_и z_ж k_z 1{,}55m\cos 25^\circ} \leqslant [\sigma_к]^2. \qquad (153)$$

Multiplying expression (153) by 0.918, after a series of transformations we have

$$\frac{0{,}918\sigma_к^2}{E_{пр}} = 0{,}114\,\frac{M_ж k_{нр.к} k_{нр.z}}{BR_и z_ж m k_z} \leqslant \frac{0{,}918[\sigma_к]^2}{E_{пр}}. \qquad (154)$$

According to the method of the strength calculation of the gear drives of Professor V. N. Kudryavtsev [16], value $0.918\frac{\sigma_к^2}{E_{пр}}$ is called the coefficient of contact stresses. The reduction of the calculated formulas for harmonic drives to form (154) makes it possible to utilize permissible values $[C]_к$ for the calculation since the nature relative to the motion of the components and the very type of the kinematic pair in the engagement of teeth of common gear and harmonic drives with this version of engagement are similar.

In formula (154) $R_и = \frac{d_{0ж}}{2} = \frac{z_ж m}{2}$, in connection with which the condition of contact strength of the teeth takes the form

$$\frac{0{,}114\cdot 2M_ж k_{нр.к} k_{нр.z}}{Bd_{0ж}^2 k_z} \leqslant [C]_к,$$

whence

$$d_{0ж} \geqslant \sqrt[3]{\frac{0{,}228M_ж k_{нр.к} k_{нр.z}}{Bk_z[C]_к}}.$$

Accepting for this geometry of the teeth $k_z = 1.33$ we will have

$$d_{0m} \geqslant \sqrt[3]{\frac{0{,}7M_m k_{нр.к} k_{нр.з}}{B[C]_к}}. \qquad (155)$$

Let us examine the determination of the values which enter the formula. The permissible value of the coefficient of contact stresses will equal $[C]_к = [C]_{к.в} k_{реж}$, where $[C]_{к.в} = \frac{0{,}918[\sigma]_{к.в}}{E_{пр}}$ is the coefficient of contact stresses which corresponds to the limit of prolonged contact durability. Below are given values of $[C]_{к.в}$, determined depending on the least hardness of the material of one of the components [16].

НВ	270	280	290	300	310	320	330	340	350
$[C]_{к.в}$ in kgf/cm^2	19.4	20.3	21.2	22.1	22.9	23.8	24.6	25.4	26.1

The coefficient of mode $k_{реж}$ is found through the formula

$$k_{реж} = 1{,}45\sqrt[9]{\frac{10^7}{N_ц}},$$

utilized with the hardness of the flexible component HB$\leq$350 and the number of cycles of change in stress $N_ц < 3 \cdot 10^6$, or according to the graph presented in figure 55 [16] with $N_ц > 3 \cdot 10^6$. The number of cycles of a change in the stresses of the flexible component of a two-wave drive is determined from the formula

$$N_ц = 120nT, \qquad (156)$$

where n is the rotational speed of the generator in r.p.m.; T - the period of service of the drive in hours.

It should be noted that in actuality

$$N_{\Sigma} = 2 \cdot 60 (n_1 + n_2) T$$
$$= 120 (i + 1) n_2 T;$$

$$N_{\Sigma 2} = N_{\Sigma} \frac{z_2}{z_1}.$$

However $|i| = 1/50$ and $1{,}02 \geq \frac{z_2}{z_1} \geq 1$, in connection with which for practical calculations formula (156) is completely suitable.

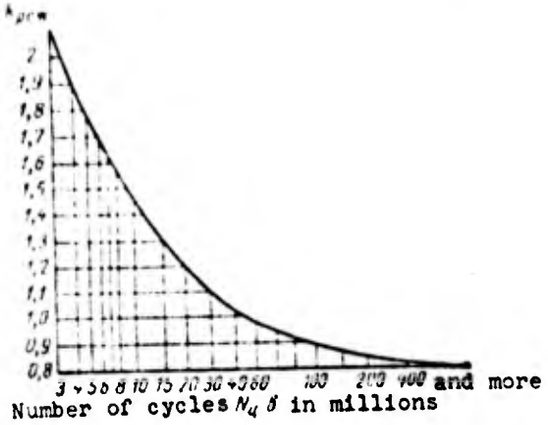

Figure 55. Graph for determination of $k_{рем}$.

In accordance with the conclusions given in paragraph 12, we consider it possible, for the practical calculations of drives of the Г-Ж-Н type with the hardness of the flexible components HB≤350, to use the value $k_{нр.к}=2$, trying with this to maintain relation $m_y/L=0.006$.

By the coefficient of nonuniformity of load distribution between the teeth of each zone of engagement we will mean the relation

$$k_{нр.з} = \frac{P_{max}}{P_{ср}}, \qquad (157)$$

where P_{max} is the greatest load per pair of teeth; $P_{ср}$ - the average value of the load.

On the basis of approximate calculations for the recommended range of numbers of teeth of the drive, the ratio of the maximum load to the minimum comprises approximately 3.8. Force P_{max} occurs generally with the coincidence of the centers of curvature of the profiles of the teeth, by virtue of which the contact stresses, in spite of the action of the greatest load, turn out to be

minimum. The greatest contact stresses for the range of the rational numbers of teeth will be with φ=10-12°. Corresponding to this angle is

$$k_{нр.z} = \frac{P_{\varphi=10^\circ}}{P_{z,p}} \approx 1{,}3 \div 1{,}4.$$

Subsequently we recommend utilizing precisely these values in the calculations.

Thus, we have the data which make it possible to use formula (155) for the design calculation of a harmonic drive with precise engagement.

Let us examine an example of the calculation. Determine the dimensions of a two-wave drive with $z_{ж}$=100; $z_{г}$=98; $M_{ж}$=15.5 kgf·m; $k_{нр.к}$=2; $k_{нр.z}$=1.3; B=1.5 cm; HB280-320; $HB_{ж}>HB_{г}$; T=5000 hs; n=1440 r.p.m.

We take $[C_{к.в}]$=20.3 kg/cm^2.

The number of loading cycles of the teeth will be $N_{ц}=60\cdot1440\cdot2\times5000=840\cdot10^6$. In this case, according to figure 55, $k_{реж}$=1 and then

$$[C_к] = [C_{к.в}]\,k_{реж} = 20{,}3\cdot1 = 20{,}3 \text{ kgf/cm}^2.$$

$$d_{ож} = \sqrt[3]{\frac{0{,}7M_ж k_{нр.к} k_{нр.z}}{B[C_к]}} = \sqrt[3]{\frac{0{,}7\cdot1550\cdot2\cdot1{,}3}{1{,}5\cdot20{,}3}} = 9{,}6 \text{ cm}.$$

It is necessary to note that the design calculation of a harmonic drive by the examined procedure, in spite of the fact that it reflects the physics of the phenomena proceeding sufficiently correctly, is approximate all the same and needs refinement according to the results of experimental studies.

14. CALCULATION OF FLEXIBLE COMPONENTS FOR DURABILITY

Above it was indicated that the efficiency of the flexible component is determined by its fatigue strength. Actually, all the stresses effective in the flexible component are variables and change according to a specific law, which should also be taken into account during calculations. It is expedient to perform the calculations on durability in the form of check calculations; in this case, the purpose of the calculation should be the determination of the safety factor in the part. Obviously the cross section lying on the boundary of the smooth and toothed sections of the flexible component should be selected as the calculated cross section. In this cross section one ought to expect the greatest concentration of torsional stresses.

By utilizing a known procedure for determining the safety factor for normal n_σ and tangential n_τ stresses, in the plane stressed state we use the following formulas:

$$n_\sigma = \frac{\sigma_{-1}}{\sigma_a \lambda_\sigma + \sigma_m \psi_\sigma}, \tag{158}$$

$$n_\tau = \frac{\tau_{-1}}{\tau_a \lambda_\tau + \tau_m \psi_\tau}, \tag{159}$$

where σ_a; τ_a are the nominal values of the amplitude of the effective stresses; σ_m; τ_m - the nominal values of the average stresses of the cycle; λ_σ; λ_τ - the coefficients which consider the difference of the endurance limits of a real part from endurance limit of the sample; ψ_σ; ψ_τ the coefficients for reduction of an operating cycle to a symmetrical one.

The value of the amplitude and average stresses is determined from the relations

$$\sigma_a = \frac{\sigma_{max} - \sigma_{min}}{2}; \quad \tau_a = \frac{\tau_{max} - \tau_{min}}{2};$$

$$\sigma_m = \frac{\sigma_{max} + \sigma_{min}}{2}; \quad \tau_m = \frac{\tau_{max} + \tau_{min}}{2}.$$

For normal stresses taking into account their concentration on the basis of (135) and (149)

$$\sigma_{max} = \frac{6M_z\alpha'_\sigma}{z_c m_a\left(0.1366\frac{z_c}{k_x}\quad 1\right)},$$

$$\sigma_{min} = \frac{6M_z\alpha'_\sigma}{z_c m_a\left(0.1366\frac{z_c}{k_x} - 1\right)},$$

where α'_σ is the concentration factor for the space between the teeth situated at the smallest diameter of the deformed flexible component; $\alpha'_\sigma \approx \alpha_\sigma$.

Here, instead of the nominal stresses we utilize the maximum local stresses. Subsequently, during the determination of n_σ this will be taken into account. For computation of σ_m the use of the maximum local stresses is completely admissible.

For tangential stresses (with r=0).

$$\tau_{max} = \frac{2M_z}{\pi d_{cn}^2\delta};\quad \tau_{min} = 0.$$

The value of coefficients ψ_σ and ψ_τ depends on the kind of materials and their heat treatment.

Usually, for alloyed steel with hardness $HB \leq 350$ $\psi_\sigma = 0.1$; $\psi_\tau = 0.05$.

Coefficients λ_σ and λ_τ, in turn, are equal to

$$\lambda_\sigma = \frac{k_\sigma}{\varepsilon_\sigma\beta_\sigma};\quad \lambda_\tau = \frac{k_\tau}{\varepsilon_\tau\beta_\tau},$$

where k_σ and k_τ are the effective concentration factors; ε_σ and ε_τ - the scale coefficients which consider the difference in the dimensions of a part from the dimensions of the sample; β_σ and β_τ - the coefficients which consider the effect, on the endurance limits of the part, of finish and the method of surface hardening of the part.

With a change in the diameter of the flexible component from 20 to 300 mm it is possible to accept ε_σ=0.83-0.56 and ε_τ=0.89-0.63 [38]. For the surface finish of the flexible component ∇7, ∇8 it is also possible to accept β_σ=0.9; β_τ=0.9 [38].

As a result of the conclusions drawn above, on the basis of experiments and from literature sources we know the values of the theoretical stress concentration factors with the different examined types of deformation of the teeth and wall of the flexible component. Thus, the theoretical concentration factor with the calculation of teeth for bending according to the local stresses $\alpha_{\sigma(из)} \leq 2.2$ [17].

The stress concentration factor with the deformation of the flexible component by the wave generator is determined from the graph given in figure 53. The theoretical torsional stress concentration factor because of a change of the form of the cross section of the wall of the flexible component in the place of the transition from a smooth section to a toothed one, taking into account the nonuniformity of the torsional stress distribution because of the transmission of peripheral forces on several sections of the perimeter of the flexible component (in a two-wave drive - on two sections of arc $\pi/4$ each), can be accepted equal to α_τ=1.95 and depends little on the number of teeth and size of the components.

As is known, values of the effective concentration factors are lower than the theoretical one; in this case the connection between them is established through the sensitivity index $q_\sigma(q_\tau)$. Thus, for normal stresses

$$q_\sigma = \frac{k_\sigma - 1}{\alpha_\sigma - 1}.$$

Value q_σ depends on the hardness of the material. Figure 56 depicts a graph for determining q_σ in the range of the hardnesses of material recommended for flexible components [22]. As is evident, it is possible to consider $k_\sigma \approx \alpha_\sigma$ and $k_\tau \approx \alpha_\tau$.

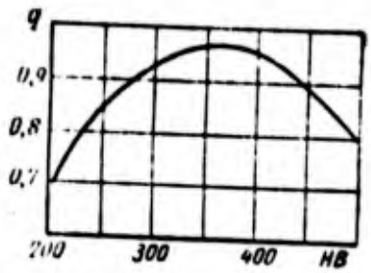

Figure 56. Graph for determining sensitivity index q.

On the basis of the given propositions we convert formulas (158) and (159) after performing the corresponding substitutions in them

$$n_\sigma = \frac{\sigma_{-1}}{\frac{\sigma_a}{\varepsilon_\sigma \beta_\sigma} + \sigma_m \psi_\sigma}, \tag{160}$$

$$n_\tau = \frac{\tau_{-1}}{0{,}5\tau_{max}\left(\frac{\alpha_\tau}{\varepsilon_\tau \beta_\tau} + \psi_\tau\right)}. \tag{161}$$

The overall safety factor is found through the formula

$$n = \frac{n_\sigma n_\tau}{\sqrt{n_\sigma^2 + \nu n_\tau^2}}, \tag{162}$$

where ν is the coefficient which considers the effect of axial normal stresses σ_{oc}:

$$\nu = 1 - \frac{\sigma_{oc}}{\sigma_{-1}} + \frac{\sigma_{oc}^2}{\sigma_{-1}^2}.$$

For this case we take $\nu \approx 0.7$.

In connection with the fact that the flexible component is the most important part of the drive, it is possible to recommend the minimum safety factor $n \geq 1.5$. If during the calculation value $n < 1.5$ is obtained, it is necessary to investigate the reasons for this and to take the necessary measures to assure $n > 1.5$ through a change in the various dimensions of the part.

Example of calculation. Determine the dimensions of a two-wave drive with approximate engagement and check for strength a

flexible component manufactured from steel KH2N4A with the following initial data: $M_г$=120 kgf·m; i=132. The flexible component is driven. Hardness of the material of the flexible component HB300.

We assign $L=d_ж$; $q_г$=0.15; [p]=600 kgf/cm^2; the approximate engagement is cut by a tool with $\alpha_д$=20°. According to formula (124), we determine the pitch circle diameter of the rigid component

$$d_{дж} \geq \sqrt[3]{\frac{4M_{гр}k_{нр}}{k_z q_г [p]}} = \sqrt[3]{\frac{4 \cdot 120 \cdot 2}{0{,}25 \cdot 0{,}15 \cdot 600}} = 16{,}2 \text{ см}.$$

The gear ratio i=132 is assured with $z_г$=264 and $z_ж$=266. For $z_г$=264 from the graph figure 35 we find $k_Δ$=0.82 and, according to formula (142), we determine the wall thickness of the flexible component

$$\delta = d_{дж} \sqrt{\frac{k_z q_г [p] \left(0{,}1366 \frac{z_г}{k_Δ} - 1\right)}{3{,}64 E k_{нр}}} =$$

$$= 16{,}2 \sqrt{\frac{0{,}25 \cdot 0{,}15 \cdot 600 \left(0{,}1366 \frac{264}{0{,}82} - 1\right)}{3{,}64 \cdot 2{,}1 \cdot 10^6 \cdot 2}} = 0{,}129 \text{ см}.$$

We find the engagement modulus

$$m = \frac{d_{дж}}{z_ж} = \frac{162}{266} = 0{,}61 \text{ мм}.$$

We take the nearest standard modulus m=0.6 mm and finally obtain the pitch circle diameter of the rigid component $d_{дж}$=0.6·268=159.6 mm. The coefficient of the wall thickness of the flexible component

$$\theta = \frac{\delta}{m} = \frac{1{,}29}{0{,}6} = 2{,}15.$$

On the section of the disposition of the teeth we take the wall thickness: δ_{max}=3m=1.8 mm, the coefficient of thickness: θ_{max}=3. For $z_г$ we find $\xi_г$=0.022·$z_г$=0.022·264=5.71 and we determine the arbitrary modulus

$$m_y = \frac{m}{z_c}\left[z_c - 2(f_0 + c_0) + 2\xi_w - \theta_{max}\right] =$$

$$= \frac{0,6}{264}\left[264 - 2 \cdot 1,35 + 2 \cdot 5,71 - 3\right] = 0,614 \text{ мм}.$$

We also find

$$r_{cm} = \frac{m_y z_c}{2} = \frac{0,614 \cdot 264}{2} = 81,05 \text{ мм}.$$

We determine the greatest nominal bending stress of the wall of the component on the section of the disposition of the teeth

$$\sigma_z = -\frac{\delta E}{m_y z_c \left(0,1366 \frac{z_c}{k_\Delta} - 1\right)} =$$

$$= \frac{0,18 \cdot 2,1 \cdot 10^6}{0,0614 \cdot 264 \left(0,1366 \frac{264}{0,82} - 1\right)} = 494 \text{ kgf/cm}^2.$$

From the graph given in figure 54, we find value $\lambda' = 3.55$. With: $\$ = 3 > 2.15$ value λ' is obtained somewhat exaggerated. Coefficient $\alpha'_\sigma \approx \alpha_\sigma = 1.45$. We find σ_{max} and σ_{min}.

$$\sigma_{max} = \sigma_z \lambda' = 494 \cdot 3,55 = 1750 \text{ kgf/cm}^2;$$

$$\sigma_{min} = -\frac{\delta E \alpha'_\sigma}{z_c m_y \left(0,1366 \frac{z_c}{k_\Delta} - 1\right)} =$$

$$= -\frac{0,18 \cdot 2,1 \cdot 10^6 \cdot 1,45}{264 \cdot 0,0614 \left(0,1366 \frac{264}{0,82} - 1\right)} = -790 \text{ kgf/cm}^2.$$

The amount of torsional stress in the wall of the flexible component on the boundary of the toothed section is determined from formula (139)

$$\tau_{max} = \frac{2M_c}{\pi d_{cm}^2 \delta} = \frac{2 \cdot 12000}{3,14 \cdot 16,21^2 \cdot 0,18} = 160 \text{ kgf/cm}^2.$$

The amplitude and the average stress of the cycle in this case will be

$$\sigma_a = \frac{1}{2}(\sigma_{max} - \sigma_{min}) = \frac{1}{2}(1750 + 790) = 1270 \text{ kgf/cm}^2;$$

$$\sigma_m = \frac{1}{2}(\sigma_{max} + \sigma_{min}) = \frac{1}{2}(1750 - 790) = 480 \text{ kgf/cm}^2;$$

$$\tau_a = \tau_m = \frac{1}{2}\tau_{max} = \frac{160}{2} = 80 \text{ kgf/cm}^2.$$

Safety factors for normal and tangential stresses are determined from formulas (160) and (161) (σ_{-1} and τ_{-1} - see table 11).

$$n_\sigma = \frac{\sigma_{-1}}{\frac{\sigma_a}{\varepsilon_\sigma \beta_\sigma} + \sigma_m \psi_\sigma} = \frac{5000}{\frac{1270}{0,6 \cdot 0,9} + 480 \cdot 0,1} = 2,09;$$

$$n_\tau = \frac{\tau_{-1}}{0,5\tau_{max}\left(\frac{\alpha_\tau}{\varepsilon_\tau \beta_\tau} + \psi_\tau\right)} =$$

$$= \frac{2500}{0,5 \cdot 160\left(\frac{1,95}{0,68 \cdot 0,9} + 0,05\right)} = 9,6.$$

The overall safety factor (162) will equal

$$n = \frac{n_\sigma n_\tau}{\sqrt{n_\sigma^2 + 0,7 n_\tau^2}} = \frac{2,09 \cdot 9,6}{\sqrt{2,09^2 + 0,7 \cdot 9,6^2}} = 2,42.$$

15. STRUCTURAL DESIGN OF A WAVE GENERATOR WITH INTERMEDIATE ROLLING CONTACTS

The design of a wave generator with intermediate rolling contacts is similar to the design of a radial antifriction bearing. We should distinguish two types of generators: 1) with a stressed internal ring; 2) with an unstressed internal ring.

A generator with a stressed internal ring consists of the following parts: a cam which has a profile equidistant to the equivelocity curve of the flexible component; an internal cylindrical ring with one or several races for the motion of the rolling contacts pressed on the cam of the generator; intermediate rolling contacts (balls or rollers); a separator (one-piece or composite), and external cylindrical ring smooth or with races for rolling contacts. With the assembly of the generator and the putting of the internal ring on the cam, bending stresses appear in the ring in consequence of which the thickness of the ring should be selected from the condition of assuring its static bending strength.

A distinctive feature of a generator with an unstressed internal ring is the fact that instead of a cam the generator has

a cylindrical disc on which the internal ring of the generator is pressed which has an internal cylindrical surface and external surface (along the races for rolling contacts) equidistant to the equivelocity curve of the flexible component. With this design, bending stresses do not appear in the internal ring after the assembly of the generator.

The external ring of the generator is located under the most severe conditions and with any design is stressed and, besides variable contact stresses, variable bending stresses arise in it.

Below are given recommendations regarding the structural design of the basic parts of wave generator.

An external ring with a smooth internal surface which works in a pair with balls is designed according to flexural and contact stresses. The bending computation is performed in the form of a check. For this the thickness of ring $\delta_к$ within the limits of $2\delta<\delta_к<2.5\delta$ is assigned. The strength condition of the ring is written in the following form:

$$\sigma = \frac{\delta_к E\left(\frac{r_{ск.к}}{r_{min\,к}} - 1\right)}{2r_{ск.к}} \leqslant [\sigma], \qquad (163)$$

where

$$r_{ск.к} = \frac{d_{ск} - (\delta + \delta_к)}{2},$$

$$r_{min\,к} = r_{ск.к} - 3{,}66k_\Delta m_y.$$

The value of the permissible stress is accepted equal to

$$[\sigma] = \frac{\sigma_{-1}}{n}.$$

The safety factor is taken as n=3.5. The ring is manufactured from ball-bearing steel. For steel ShKh-15 (GOST [ГОСТ - All-Union State Standard] 801-60) σ_{-1}=6900 kgf/cm^2.

Determination of the contact stresses $\sigma_к$ at the point of contact of the ring and the most loaded ball is performed by formula [2]

$$\sigma_к = \frac{n_p}{\pi}\sqrt[3]{\frac{3}{2}\left(\frac{\sum k}{\phi_1}\right)^2 P_{max}}, \qquad (164)$$

where n_p is a coefficient which depends on the reduced curvature of the bodies in contact; Σk - the reduced curvature; ϕ_1 - the constant of elasticity of the bodies in contact.

The value Σk is determined from the formula

$$\sum k = \frac{2}{\rho_ш} + \frac{1}{\rho_{к1}} + \frac{1}{\rho_{к2}}.$$

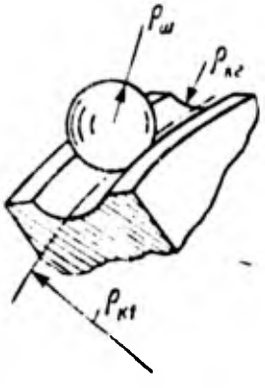

Figure 57. For the determination of radii of curvature in the contact of a ball and race of a generator ring.

For an internal ring with a groove (figure 57)

$$\rho_{к1} > 0 \text{ and } \rho_{к2} < 0;$$

for an external ring with a groove

$$\rho_{к1} < 0 \text{ and } \rho_{к2} < 0;$$

for an external ring without a groove

$$\rho_{к1} < 0 \text{ and } \rho_{к2} = \infty.$$

For chrome steel with $E=2.1\cdot10^6$ kgf/cm^2; $\mu=0.3$

$$\phi = 0{,}858\cdot10^{-6} \text{ cm}^2/\text{kg}.$$

The value of coefficient n_p is found from table 10 depending on the value of the parameter

$$\frac{\frac{1}{\rho_{к1}} - \frac{1}{\rho_{к2}}}{\sum k}.$$

The amount of force P_{max} is determined approximately from the relation

$$P_{max} = \frac{M_ж}{R_0}(\sin\alpha_{cp} + f\cos\alpha_{cp}) - \frac{2T_ш}{z_ж k_z z_ш},$$

where $T_ш$ is the pitch of the rolling contacts.

Table 10. Values of coefficient of n_p.

$\frac{\frac{1}{\rho_{к1}}+\frac{1}{\rho_{к2}}}{\sum k}$	n_p	$\frac{\frac{1}{\rho_{к1}}+\frac{1}{\rho_{к2}}}{\sum k}$	n_p	$\frac{\frac{1}{\rho_{к1}}+\frac{1}{\rho_{к2}}}{\sum k}$	n_p	$\frac{\frac{1}{\rho_{к1}}+\frac{1}{\rho_{к2}}}{\sum k}$	n_p
0,0000	1,0000	0,7579	0,8306	0,8270	0,7800	0,8922	0,7123
0,0466	0,9990	0,7620	0,8278	0,8340	0,7764	0,8958	0,7062
0,1075	0,9970	0,7661	0,8264	0,8350	0,7734	0,8994	0,7027
0,1974	0,9921	0,7702	0,8230	0,8389	0,7692	0,9030	0,6983
0,2545	0,9852	0,7743	0,8197	0,8428	0,7657	0,9065	0,6925
0,3204	0,9756	0,7784	0,8177	0,8468	0,7622	0,9100	0,6873
0,3951	0,9633	0,7825	0,8144	0,8507	0,7587	0,9131	0,6821
0,4795	0,9434	0,7866	0,8117	0,8545	0,7574	0,9269	0,6600
0,5342	0,9276	0,7907	0,8084	0,8584	0,7508	0,9428	0,6297
0,5819	0,9158	0,7948	0,8065	0,8623	0,7474	0,9458	0,6227
0,6113	0,9025	0,7988	0,8026	0,8661	0,7429	0,9488	0,6161
0,6521	0,8865	0,8029	0,8000	0,8699	0,7386	0,9517	0,6089
0,6716	0,8772	0,8069	0,7962	0,8737	0,7342	0,9574	0,5915
0,6920	0,8673	0,8110	0,7947	0,8774	0,7299	0,9705	0,5531
0,7126	0,8561	0,8150	0,7899	0,8811	0,7257	0,9818	0,5038
0,7332	0,8460	0,8190	0,7871	0,8849	0,7205	0,9909	0,4409
0,7538	0,8333	0,8230	0,7831	0,8885	0,7168	0,9979	0,3503

The condition of strength will take the form

$$\sigma_{к\,max} \leq [\sigma]_к.$$

The permissible value of contact stress for a ring and balls made of steel ShKh-15 and ShKh-15SG $[\sigma]_н$=35,000 kgf/cm^2. It should be considered that the places of action of the greatest contact and flexural stresses coincide. By virtue of this, the contact compression of metal is accompanied by compression as a result of bending and local contact stresses seemingly create the effect of the concentration of bending stresses. This explains the designation of a high safety factor in the calculation of the ring for bending.

The external ring with the ball race is designed only for bending according to formula (163). In this case, the thickness of the ring $\delta_н$ is measured over the thickest cross section

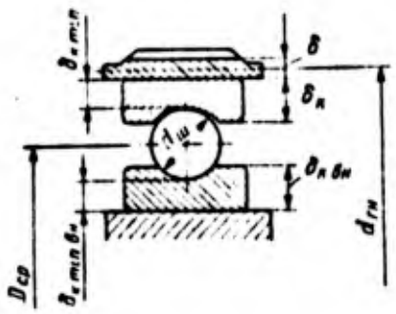

Figure 58. Designation of the dimensions of the parts of a wave generator.

(figure 58). The radius of the groove in the axial cross section of the ring is taken according to recommendations for antifriction bearings ($\rho_{к1}=0.515d_{ш}$). The wall thickness under the ball should be $\delta_{к\ min}\approx 0.75\delta_{к}$. With the use of an external ring with a groove, the contact stresses are determined in the contact of the balls and internal ring from formula (164).

When using generators with a stressed internal ring the check calculation of the ring for bending stresses is performed. The greatest wall thickness of the ring is accepted as $\delta_{к.в}=(2-3)\delta$; in this case, the stresses are determined from the formula

$$\sigma=\frac{\delta_{к.в}E\left(\frac{r_{сн.к.в}}{r_{min\ к.в}}-1\right)}{2r_{сн.к.в}}\leqslant[\sigma]_{вн}, \qquad (165)$$

in which

$$r_{сн.к.в}=\frac{1}{2}[d_{ш}-(\delta+2\delta_{к\ min}+2d_{ш}+2\delta_{к\ min\ вн}-\delta_{к.в})],$$

$$r_{min\ к.в}=r_{сн.к.в}-3{,}66k_{\Delta}m_{\mu}.$$

In these formulas designation $\delta_{к\ min}$; $\delta_{к\ min\ вн}$; $\delta_{к.в}$ are according to figure 58. It is possible to accept $\delta_{к\ min\ вн}=2\delta_{к\ min}$. Permissible stress $[\delta]_{вн}=\sigma_{в}/2.5$. If the unstressed internal ring is made by the method of treatment in the deformed state (see chapters VI, VII), then the admissibility of the wall thickness of the billet is checked from the condition of bending strength according to the formula

$$\sigma=\frac{\delta_{зад}E}{2r_{сн.к}}\left(\frac{r_{сн.к}}{r_{min\ к}}-1\right)\leqslant[\sigma], \qquad (166)$$

in which

$$r_{\text{ск.к}} = \frac{d_e + d_i}{4},$$

$$r_{\min к} = r_{\text{ск.к}} - 3{,}66 k_{\Delta} m_y,$$

where d_e is the external diameter of billet; d_i - the internal diameter of the billet.

CHAPTER VI

DESIGNING DRIVES

16. REDUCERS WITH A Г-Ш-Н DRIVE

Chapter I examined the different designs of harmonic reducers with a mechanism having one flexible and one rigid components and one wave generator. Chapter II examined in detail the kinematic possibilities of these mechanisms and their structure. Taking into account that in the family of harmonic gear mechanisms Г-Ш-Н mechanisms are basic, it is advantageous first of all to examine the questions of the design of the latter in detail.

The design of a reducer with a Г-Ш-Н mechanism in essence depends on which of the components (flexible or rigid) is driven. If the flexible component is driven, then it is required to carry out the transmission of torque from the deformed flexible component to the output shaft and to connect the rigid component with the housing, and vice versa. The selection of the driven component thus requires completely different design solutions in the creation of the mechanism.

Figure 3 presented the cross section of a general purpose series reducer of the United Shoe Machinery Corporation with a driven flexible component. The design of the reducer was thoroughly developed and is very efficient. The advantages of the design include: the use of a flexible component manufactured from a

tubular billet; the fastening of the generator cam to the driving shaft with the aid of a rubber washer, which creates the necessary conditions for uniform load distribution between the zones of engagement[1]; the use of a welded perforated bottom of the flexible component, thanks to which the circulation of air and oil within the housing is facilitated; the successful design solution of the housing itself with an interchangeable cover for the realization of different methods of fastening the reducer; successful use of one of the housing lids for the placement of the fins blown off by air.

In the case of employing a similar reducer for the short-term working drive of coaxial devices the use of rolling contact bearings of a driven shaft with a smaller external diameter is possible, because of which best use of the volume within the flexible component and a reduction in the length of reducer are attained. The design of a unit for the support of the driven shaft with the use of the volume within the flexible component developed by the author is presented in figure 59, where 6 are the bearings of the driven shaft; 5 - the housing lid with an internal branch connection; 2 - the half-coupling of the flexible component; 1 - the flexible component. In this design the flexible component is connected with the driven shaft with the aid of a toothed clutch. Since in work the flexible component has a tendency to be displaced in an axial direction, in a half-coupling 2 wire rings 3 and 4 are laid which prevent the flexible component from axial displacement.

In striving to decrease the volume of the reducer the thermal mode of its operation should be investigated. Small overall dimensions of wave reducers with comparatively high losses limit a further decrease in their dimensions.

---

[1]Because of the possibility of the radial shifts of the generator within the limits of the clearance between the aperture of the hubs and the shaft.

The design of the reducer presented in figure 3, with its fastening on feet and the carrying of the bearing assembly outside the volume of the basic housing is not by chance.

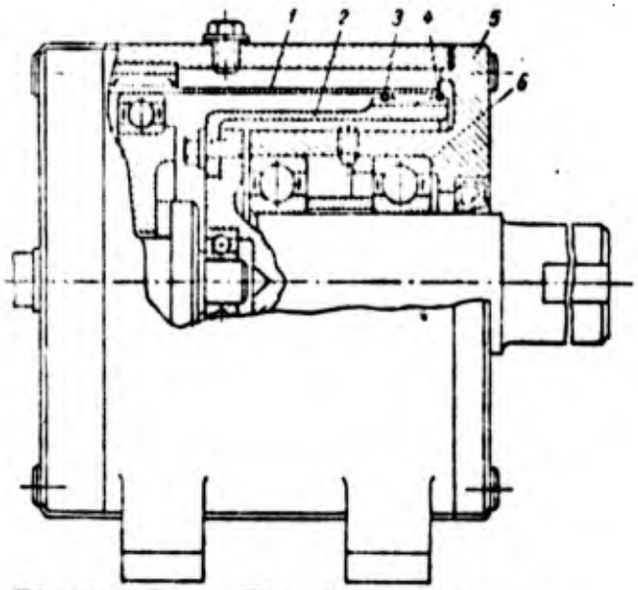

Figure 59. The design of a reducer with a harmonic drive of the Г-Ж-Н type and the use of the volume for the placement of the support assembly of the driven shaft.

The designers attempted to increase the surface blown off by air. The quantity of heat Q given off by the reducer is determined from the formula

$$Q = 860N_1(1-\eta) \text{ kcal/h} \qquad (167)$$

where N_1 is the power on the driving shaft of the reducer in kW; η - the efficiency of the reducer.

The quantity of heat Q_1 removed from the reducer into surrounding air equals

$$Q_1 = (k_{t1}S_1 + k_{t2}S_2)(t - t_{воз}), \qquad (168)$$

where S_1 is the surface area of the reducer from which natural heat removal is realized; S_2 - part of the surface area which undergoes blowout; k_{t1} - the coefficient of heat transfer from area S_1; k_{t2} - the coefficient of heat transfer from area S_2; t - maximum temperature of the reducer; $t_{воз}$ - the temperature of surrounding air.

With natural heat removal k_{t1}=10-18 kcal/m^2·deg·h[2]; with blowout $k_{t2} \approx 14\sqrt{v}$ (where v is the peripheral velocity of the impeller in m/s).

[2]The recommended value k_{t1} requires further refinement from the results of a large number of experiments.

The maximum temperature of the reducer depends on the type of oil used. In the general case, one ought to consider t=80-85°C. If we proceed from the published data on the efficiency of reducers of the "United Shoe Machinery Corporation", then with η≈0.75-0.85 they operate in a normal thermal mode because of their peculiar layout and the combined system of heat removal.

For harmonic drives the use of a liquid lubricant is recommended. The addition of anti-scoring additives (of type 23-K) is possible. The level of lubricant should not be higher than the middle of the balls of the generator. The assembled wave generator (without the flexible component) should be thoroughly balanced.

Figure 60 shows a reducer with a Г-Ж-Н mechanism whose driven component is the rigid component. The kinematic scheme of the reducer was examined in chapter II and was presented in figure 22b. Besides the Г-Ж-Н mechanism the reducer contains a simple gear mechanism which is a high-speed stage. The total gear ratio of the reducer i=432; the harmonic mechanism has $i_{вол}$=115.

A high-speed direct-current motor 1 with a power of 2 kW with a built-in brake clutch which has speed of rotation n=6500 r.p.m. is connected through a toothed clutch with the driving gear 5 of the reducer installed on two bearings 4 in the housing of the reducer 2. Through three idler gears 9 the gear 5 transfers rotation to a toothed ring 7 pressed in and fastened by pins in the unstressed internal ring of the generator 8. The generator ring is fixed and rotates on a bearing 17. The ring has two specially profiled ball races 6 which ensure the appropriate form of deformation of the flexible component. The external smooth ring 15 of the generator is pressed in the flexible component 18 and has a shoulder for support in the latter.

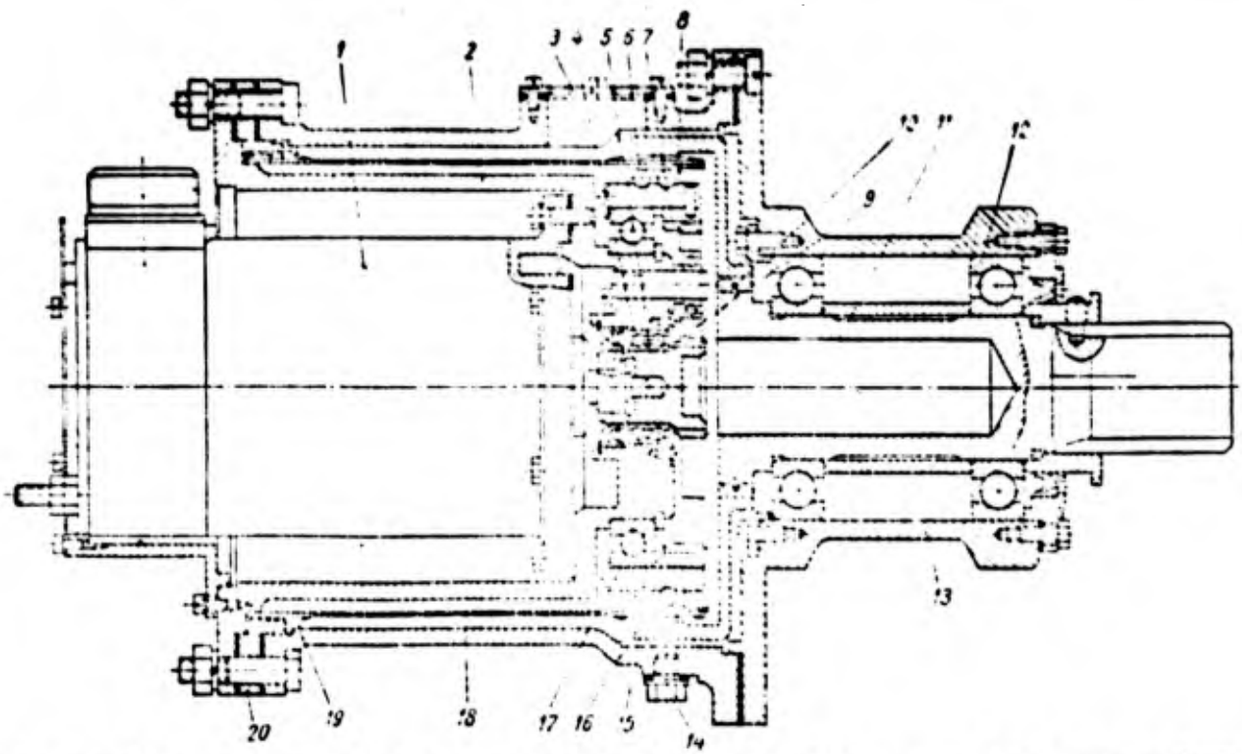

Figure 60. Reducer with combined drive and the use of the volume within the flexible component for the placement of the rotor.

The flexible component 18, which is a tubular part with two identical toothed threads, is inserted in the half-coupling by the left end and is restrained from axial displacement by a split ring 19 placed between the housing and flange of the half-coupling. The rigid component 16 is connected with the driven shaft 11 with the aid of a toothed clutch and is restrained from axial displacement by a spring ring 10. The driven shaft is installed on two bearings 12 in the housing lid 13. The fastening of the reducer in the device for which it is intended is realized by clamps slipped over the cover. Above the reducer is an inspection window with cover 3. Below is a plug 14 for an oil drain and a plug for determination of the oil level. The reducer is intended for periodic short-term operation with torque on the output shaft of 90 kg-m. Because of the arrangement of the motor with the brake within the reducer and the use of a compound scheme, the overall dimensions and the weight of the obtained unit prove to be 2.3 times less than of the unit with the same output parameters which consists of an engine with brake with $n_{дв}$=2500 r.p.m. and planetary reducer 3K.

The combination of a simple geared Г-Ж-Н mechanism with the use of the volume within the flexible component for the placement of the motor can be widely used in the drives of different machines. In the case of intending a drive for prolonged continuous operation the electric motor can be equipped with a fan which blows air through the motor into the cavity between the motor and the reducer, which can create an additional cooling surface of the reducer. It should be noted that with the recommended relationships between the diameter, length, and the power of electric motors the radial dimensions of the reducer and weight prove to be greater than are determined by the strength of the flexible component, but, on the other hand, the acceptance of this scheme makes the heaviest parts of the reducer lightly loaded, which guarnatees their high reliability.

In the examined reducer the equalizing of the load distribution between the zones of engagement is accomplished due to the movable connection of the rigid component with the driven shaft; the flexible component of the reducer is extremely effective technologically and can be made from a tubular billet. For this reducer the conduct of research of the thermal operational mode is also required and, in case of need, the adoption of the necessary design measures.

In the planning of drives of the Г-Ж-Н type with a driven rigid component special attention should be given to assuring the rigidity of this component. The radial deformation of the toothed rim of the rigid component under the action of the forces of engagement should not exceed 0.05m, since with large deformation the scheme of engagement is disrupted, the progressive wear of the teeth begins, and even their slipping can begin.

The amount of radial deformation of the rims of steel rigid wheels u is calculated approximately from the formula

$$u = 21 \cdot 10^{-6} \frac{M_{ж}}{m z_{ж} B} \beta_u^2 \qquad (169)$$

where $\beta_u = r/h$ is the ratio of radius r of the average circumference according to thickness h of the wall of the rim on the section of the arrangement of the teeth to wall thickness h; m - modulus of engagement in cm; $M_{ж}$ - maximum torque on the rigid component in kgf·cm; B - the width of the rim in cm.

17. REDUCERS WITH A Г-2Ж-Н DRIVE

The kinematic possibilities of Г-2Ж-Н mechanisms were examined in chapter II. As follows from formula (11), the gear ratio of the mechanism can have both a positive and negative sign, thanks to which the required direction of rotation of the driven shaft in the invariable direction of rotation of the driving shaft is obtained.

If, according to the scheme in figure 20, the number of teeth of the toothed rings of the drive will be connected by the following relationships: $z_1 = z_2 + 2$; $z_4 = z_3 + 2$; $z_2 = z_3 + 2$, then the gear ratio has a positive sign, and the synthesis of the mechanism can be performed with the use of the formula

$$z_2 \quad 2 | i, \qquad (170)$$

obtained from expression (11).

If the obtained number z_2 turns out to be a fraction, the nearest whole number z_2 is accepted and the actual gear ratio is determined

$$i_{факт} = \frac{z_2^2}{4}. \qquad (171)$$

Figure 6 presents the design of an instrument reducer with a Г-2Ж-Н mechanism for a gear ratio i^1_{H4}=10,818.

A wave generator connected with the driving shaft 17 is made composite with intermediate rolling contacts (balls), without a separator and with an unstressed internal ring. The boss of the generator is made lightened (it is also desirable to use a light alloy for it). The internal ring 1 has two identical ball races 2 which ensure the required form of deformation of the flexible component. After the seating of the internal ring on the hub the ends of the hubs are expanded. The external rings 7 with grooves are inserted in the flexible component 3 with the assurance of the fit A/C. To fix the axial position of the flexible component 3, rings 7 have shoulders which abut against the ends of the flexible component.

The fixed rigid component is made together with the housing 16. The mobile rigid component 6 with driven shaft is installed in the housing lid 10 on two radial ball bearings 9. The driving shaft of the reducer with the wave generator is also installed on two radial ball bearings 8 and 15, one of which is installed in the housing, and the other is installed in the mobile rigid component. The fixing of the axial position of the wave generator is realized by rings 12 and 14. Elimination of axial clearances is realized by selection of the thickness of the packing 11.

The reducer is lubricated by liquid oil which is poured through a plug 5. The oil level is checked by plug 13. Engagement in the reducer is approximate. All rims have the identical modulus m=0.2 mm. Engagement of rings z_2 and z_1 is accomplished according to the recommendation in chapter III, for which with the number of teeth of the flexible component z_2=2-6 the displacement factor $\xi_2=0.022z_2=0.022\times206=4.532$ and the number of teeth of the second ring of the flexible component z_3=208. For the possibility of the arrangement of this number of teeth on the same

flexible component the displacement factor of the initial outline is taken one larger, i.e., $\xi_3=\xi_2+1=5.532$, in connection with which the engagement z_1 and z_2 falls out of the examined system. At the same time, the transmission of rotation at this stage is realized without the interference of the teeth and with a precise gear ratio, although with less multiple pairing of the engagement.

The presented design can be recommended as standard in the planning of reducers with a Г-2Ж-Н mechanism.

The dimensions of the rings for drive z_4-z_3 are determined from the same formulas as z_2-z_1, but with the use of a displacement factor ξ_3.

It is necessary to examine some questions of the structural design of drives of the Г-2Ж-Н type connected with design features of the latter. First, one ought to consider the absence of the organic misalignment of the teeth characteristic of drives of the Г-Ж-Н type. A consequence of this is a considerable decrease in the nonuniformity of load distribution along the length of the tooth. Instructions on selection of the value of the effective variation factor of load distribution are given on page 141. In the second place, in connection with the fact that the engagement of the teeth of the rings of the flexible component and rigid z_3 and z_4 in the recommended scheme does not correspond to the accepted method for geometric calculation, the number of simultaneously working pairs of teeth is decreased approximately by 50% and in determining $d_{д4}$ (for part 6, figure 6), taking into account that $d_{д4}\approx d_{д2}$, one ought to accept $k_z=0.15$.

In chapter III discussion centered on the peculiar advisability of the use of the scheme of engagement with the zone of complete contact of teeth for drives of the Г-2Ж-Н type and data were given for the calculation of engagement. Let us examine some features of the use of this engagement for Г-2Ж-Н drives. A diagram of the drive is presented in figure 20. After the synthesis of the drive,

the geometric calculation of the engagement of rings z_1 and z_2 is performed in the manner shown on page 78; in this case $\xi_2=\xi_г=0.22z_2$ and $\xi_1=\xi_ж=\xi_2-(1-m_y/m)$. For rings z_3 and z_4, the displacement factors of the initial outline are determined from the expressions:

$$\xi_3 \quad \xi_2 + 1; \quad \xi_4 \quad \xi_1 + 1.$$

Then the diameters of the projections of rings z_3 and z_4 will equal:

$$d_{e3} = d_{e1} \text{ and } d_{e4} \quad d_{e3}.$$

In the planning of Г-2Ж-Н drives it is necessary to insure the rigidity of the rim of the component 4 (figure 20). The testing of rigidity is performed according to formula (169) taking into account the considerations expressed on page 161.

18. MATERIALS AND CONSTRUCTION OF FLEXIBLE COMPONENTS

Chapter V examined the features of operation of flexible components and their stressed state. It was explained that in a correctly designed drive the level of stresses, even taking into account their concentration, can be considerably lower than the endurance limit of the material. At the same time, requirements should be made on the materials of flexible components and their design with respect to the assurance of prolonged service life of the parts.

The use of alloyed chrome-nickel steel with strength limit $\sigma_в \geq 9000$ kgf/cm^2 and endurance limit $\sigma_{-1} \geq 4500$ kgf/cm^2 is expedient as materials for the manufacture of the flexible components of power drives.

The heat treatment should entail hardening with high tempering (improvement) and the obtaining of a fine-grained structure. The use of steels with this form of heat treatment is caused by the

requirement to insure the breaking-in of the teeth, which is especially important for drives of the Г-Ж-Н type.

The flexible components of Г-2Ж-Н drives can have higher hardness (up to HRC 62). However, the use of a high hardness is not always advantageous since the dimensions of the drive in this case will be limited by the overall dimensions of the parts of the wave generator, and the strength capabilities of the flexible component will not be completely used. Furthermore, hardening to a high hardness is fraught with the appearance of quenching cracks and internal stresses, which is extremely dangerous.

Table 11 gives the marks of steels recommended for the manufacture of flexible components and also mechanical characteristics and data on the modes for the heat treatment of these steels.

Flexible components with a welded-in bottom and the bottom itself, for example, can be made of steel 12Kh2N4A which possesses a good weldability (see table 11). In the planning of flexible components one ought to envision the use of standard seamless tubes as a billet.

The flexible components of kinematic drives can be made from nonmetallic materials. Table 12 gives data on the nonmetallic materials tested and recommended for flexible components by engineer Ye. G. Matyushin. For these materials $[p] \leq 50 kgf/cm^2$.

Figure 61 shows the design of a flexible component with a welded bottom for a drive of the Г-Ж-Н type. The section of the arrangement of the teeth has a thicker wall than the smooth portion of the part. For purposes of a decrease in the stress concentration a smooth transition from the surface of the projections of the teeth to the external surface of the smooth tube is realized. From the direction of the deformed end there is a smooth band relieved of the torsional stresses and bending stresses of the teeth.

Table 11. Approximate modes of heat treatment and the mechanical properties of the alloyed structural steels recommended for the manufacture of flexible components.

Mark of Steel	GOST	Temperature of heating for quenching in °C	Cooling Medium	Temperature of the tempering in °C	Mechanical properties				
					Hardness HB	$\sigma_в$	σ_T	σ_{-1}	τ_{-1}
						kgf/mm^2			
40KhN	4543-61	800-840	Oil	500	280	100	80	46	27
40KhNMA		830-850		610	≥302	110	95	60	34
37KhNZA		810-840		525-573	321-387	110	100	55	32
36KhN1MFA		850-860		590	≥331	115	100	-	-
30KhGSA		890-910		540	337-390	110	85	48	28
30KhMA		860-890		460	>320	110	90	42	24
20KhNZA		820-840		500	>292	95	85	43	24
12Kh2N4A		780-855		180-200	≥	110	85	50	25
ShKh-15	801-60	835-855		150-200	HRC64-61			6900	

This band eliminates the possibility of emergence of cracks on the end whose development usually leads to the destruction of the flexible component. From the direction of the bottom the wall thickness of the tube can be increased if according to the calculations it proves to be $\delta<1$ mm. The diameter of the internal surface of the flexible component on the section of the installation of the external ring of the wave generator is made according to class II precision in the basic hole system; on the remaining length manufacture according to class III precision is allowed. The finish of all surfaces of the flexible component should not be below ∇7 (according to GOST 2789-59). The sharp edges on the butt ends of the tube should be rounded off.

Taking into account that we are dealing

Table 12. Basic physico-mechanical characteristics of plastics recommended for the manufacture of flexible components.

Marks	Specific gravity in g/cm^3	Coefficient of linear expansion $\times 10^{-5}$	Tensile strength $\sigma_в$	Compression strength $\sigma_{сж}$	Cross-breaking strength $\sigma_{из}$	Fatigue limit on the basis of σ_{-1} 10^6 cycles	Elastic modulus in tension E	Poisson ratio	Brinell hardness HB	Frictional drag coefficient over a clean polished steel plate without lubricant
			kgf/cm^2							
Caprolon V MRGU 6-0.5-988-66	1.16	9.8	1000-1100	1200-1250	1200-1500	300	20,600-23,100	0.44	20-25	0.08-0.12
Caprolon SN (experimental production)	1.55	-	3500-4500	2500-3500	4000-5000	-	25,000-30,000	0.42	25-30	-
Polyformaldehyde STU 36-13-8-64	1.4	8.1	650-700	1300	900-1100	350	29,000-35,000	0.35	20-25	0.09-0.13
Epoxy-novolak composition 6 EI-60	1.21	7	550-650	1600-1700		180-190	38,000-47,000	0.35	HV 23-24	0.12

[Translator's Note: MRGU - МРГУ - Probably Inter-republic State Standard; STU - СТУ - Special technical specification.]

actually with non-involute engagement, the precision norms in GOST 1643-56 or in GOST 9178-59 do not completely characterize the accuracy of the toothed rings of a harmonic drive. The questions of the study of the precision of harmonic drives have not yet found a complete solution. It is possible to utilize at present the aforementioned GOSTs and the corresponding indices of precision by applying the following complexes for the duct of the parts:

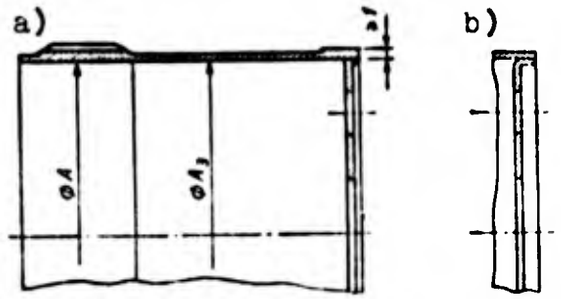

Figure 61. Design of a welded flexible component.

for kinematic precision - kinematic error ΔF_{Σ} or the accumulated error of circular pitch Δt_{Σ} (with a known kinematic precision of the machine tool this index need not be checked);

for the contact of teeth - the error in the direction of tooth ΔB_0 (it makes sense to check only for a Г-2Ж-Н drive).

It is necessary to keep in mind that in kinematic two-wave Г-Ж-Н drives with non-floating flexible or rigid components and the presence of a side clearance the kinematic error of the drive proves to be approximately half the sum of the accumulated errors of the toothed rings.

Checking the thickness of the teeth is performed, as a rule, by the measurement of the length of the total normal or according to rollers. Tolerance is selected according to the type of coupling C (with zero guaranteed clearance) for the degree of corresponding kinematic precision.

The check of all dimensions of the flexible component is realized in the process of machining since in a finally prepared

part these dimensions cannot be tested. The bottom of the flexible component is welded with a finally processed cup in the device. The bottom itself has a thickness equal to the wall thickness of the cup, and at the internal aperture is doubly thickened. In the bottom there should be three or four apertures for the circulation of the lubricant and fastening the bottom in the welding device. If the welding is performed by the contact method, then the bottom has a cylindrical band welded to the cup (figure 61). The bottom, in turn, is welded by two welds to the driven shaft of the reducer (also in the device). After trimming the welds, stress relief in a salt bath, and cleaning, the surfaces of the tube and bottom are coated with anticorrosive coatings or are parkerized.

The welds are checked for strength using the formula

$$\tau_{cp} = \frac{2M_c}{\pi d_{cp}^2 0{,}7h} \leqslant [\tau]^* \gamma, \qquad (172)$$

where d_{cp} is the average diameter of the weld; h - the throat; γ - concentration factor.

For an alternating load $\gamma=3/5$, for a pulsating load $\gamma=3/4$.

The value of the permissible stress is accepted with automatic welding $[\tau]^*=1100$ kgf/cm^2, with manual welding $[\tau]^*=900$ kgf/cm^2. For the connection of the bottom of the flexible component with the shaft with two welds only the weld located on the large diameter is checked; in this case, in formula (172) instead of M the value

$$M_c' = \frac{M_c}{1 + \frac{d_i}{d_e}},$$

is substituted where d_i is the average diameter of the internal weld; d_e - the average diameter of the external weld.

The flexible components of solid construction do not have advantages over welded, since their manufacture is complicated and is fraught with the large consumption of metal and the high cost of machining.

The pressing of components from the recommended materials is no less complicated. The pressed components should have a thickening of the wall for a flange and for a toothed ring and, just as precision components, are welded to the shaft. Nevertheless, during the manufacture of single drives the use of solid components made of a forged billet with the observance of special technology can turn out to be advisable. A version of the construction of a solid flexible component is shown in figure 62.

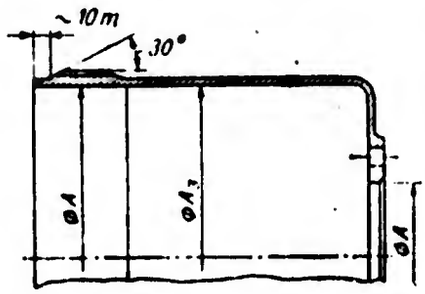

Figure 62. Design of a flexible component with a flange.

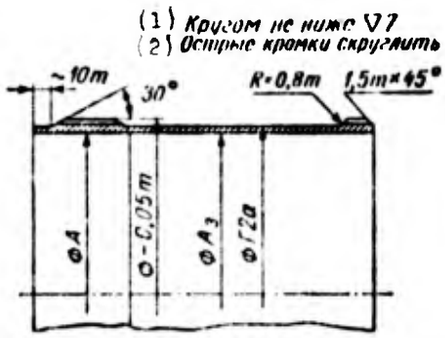

Figure 63. Design of a tubular flexible component.
Key: (1) With a disk not below ∇7; (2) Round off sharp edges.

Figure 63 depicts the construction of the flexible component of a drive of the Г-Ж-Н type with a driven rigid component. The flexible component has two toothed rings with identical parameters of the teeth. The toothed ring which is part of the coupling which connects the component with the housing is made half the width of the basic ring. Furthermore, a smooth transition from the surface of the projections of the teeth of this ring to the surface of the smooth portion is made in the form of rounding with a radius equal to 0.8m instead of a taper. This form of transition is necessary for the creation of a supporting surface in contact with the thrust ring which fixes the axial position of the

component in assembly (see figure 60). All remaining construction elements of the flexible component are the same as in the one examined above.

The design of tubular flexible components is very simple and technologically effective.

Figure 64 presents a flexible component of the Г-2Ж-Н drive. The component is completely symmetrical although the toothed rings have a different number of teeth. The width of the groove between the rings is determined by the radius of the hob [11] and is calculated from the formula

$$a \geq \sqrt{R_{\phi p}^2 - (R_{\phi p} - h_з)^2},$$

where $R_{\phi p}$ is the external radius of the hob; $h_з$ - the height of the tooth.

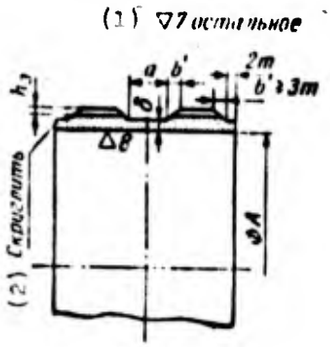

Figure 64. Construction of the flexible component of a Г-2Ж-Н drive.
Key: (1) remainder; (2) Round off.

The length of the end bevel b' at the height of the tooth should be $b \geq 3m$, and the width of the cylindrical bands not less than 2m.

The internal cylindrical surface is machined along the entire length with a tolerance for diameter according to 2nd class in the basic hole system.

19. DESIGN OF WAVE GENERATORS

We describe only the construction of wave generators of forced deformation with intermediate rolling contacts, since only they are capable of insuring and supporting the recommended scheme of tooth engagement with various types of load.

Section 15 has already given the classification of generators and some recommendations regarding the design necessary for an examination of the methods of their calculation.

As rolling contacts for drives of the Г-Ж-Н type one should use balls and for drives of the Г-2Ж-Н type the use of rollers is permissible. Regardless of whether the internal ring is stressed or unstressed, the generator can be made with a separator or without it.

For separatorless generators with a clearance between the rolling contacts of 0.02-0.03 mm the number of bodies n is determined from the formula

$$n = \frac{180}{\arcsin \frac{d_ш + (0.02 \div 0.03)}{D_{ср}}},$$

where $d_ш$ is the diameter of the ball (roller) in mm; $D_{ср}$ - the diameter of the arrangement of the center of the balls (rollers) with a nondeformed external ring in mm.

In turn, on the basis of figure 65

$$D_{ср} = 2r_{ж} - (\delta + 2\delta_{min}) - d_ш. \qquad (173)$$

After determining n the number of rolling contacts $n_{факт}$ next lowest to n is taken. With a large clearance between the balls (rollers), during operation their collision occurs and the drive makes noise; therefore, it is recommended that $n - n_{факт} \leq 0.2$.

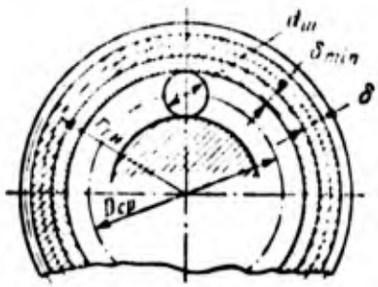

Figure 65. Determining the diameter of the circle of the centers of the balls. [$d_ш = d_{ball}$.]

Condition (174) can be satisfied through a change in diameter D_{cp} or the selection of the diameter of the balls (rollers). The necessary increase or decrease in the nominal diameter D_{cp} can be found from the formula

$$\Delta D_{cp} \approx \frac{|n - n'_{факт}|}{\pi} d_w + (0{,}06 \div 0{,}08),$$

where $n'_{факт}$ is the next smaller or larger number of rolling contacts to n.

The possibility of a change in diameter D_{cp} and a corresponding change in the wall thickness of the ring $\delta_{н\ min}$ should be checked by a strength calculation.

The use of separatorless generators is possible with smooth external rings or rings which have a groove with a low collar through which the set of balls is pressed because of the deformation of the ring.

The height of the collar (figure 66a) is determined from the formula

$$h_б = 1{,}6 \cdot 10^{-3} [r_{вн} - (\delta + \delta_{н\ min})].$$

The smooth external rings should have a shoulder 0.1-0.15 in height for a detent in the end of the flexible component (figure 66b).

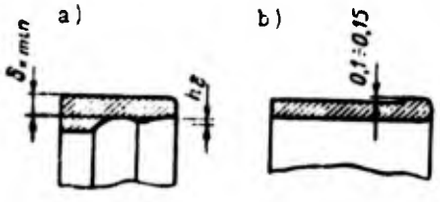

Figure 66. Construction of the external rings of a wave generator.

The use of external and internal rings with axial grooves for the consecutive laying of the balls is undesirable since the external deformed ring acquires a strong stress concentrator.

It is expedient to utilize as separators light textolite or aluminum rings. The clearance between the internal diameter of the separator and the greatest diameter of the internal ring is determined by fitting Ш$_3$. The clearance between the external diameter of the separator and the minimum diameter of the external ring should be not less than $0.2d_ш$. When using smooth external rings or rings which have a collar through which the balls are pressed, the separator is made one-piece, and when using rings with grooves - open or built-up of two halves.

A built-up separator is made of two riveted parts: a ring with open slots and a smooth ring (figure 67a). The open separator is held in the generator because of the presence of an end collar on the hub or cam of the generator (figure 67b). The slots in the separator are made with flat parallel lateral surfaces or shaped (figure 67c). In the assembled generator the clearance between the spheres and the parts of the generator over the width of the slot should be within limits of from 0.03 to 0.05 mm.

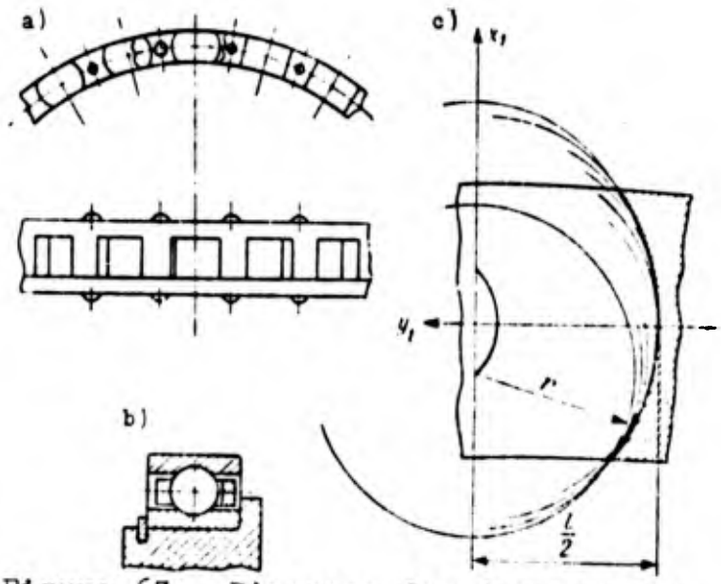

Figure 67. Diagrams for determining the length of the slots of the separator.

Cam slots make it possible to restrict the freedom of motion of rolling contacts in the slots especially with their passage through the unloaded zone and thereby to decrease the possibility of the striking of the spheres against the separator. The shape of the cam slots is determined by analytical calculation and graphical construction.

For an involute equivelocity curve the shape of the slots is found in the following manner. From equations (174) the coordinates are determined of the points of the curve, which is the locus of the centers of the family of the circles whose envelope is also the known profile.

Equations (174) are written in a coordinate system whose horizontal axis is a normal, and vertical axis - tangent to a circle with radius R_{cp} of the arrangement of the centers of the spheres of the generator in the nondeformed state of its rings.

The indicated equations take the form:

$$\left.\begin{aligned} x_1 &= r_0 [(\psi_0 + \lambda) \cos(\lambda - \varphi) - \sin(\lambda - \varphi) + \\ &\quad + \cos\varphi - \sin\varphi] - R_{cp}, \\ y_1 &= r_0 [(\psi_0 + \lambda) \sin(\lambda - \varphi) + \\ &\quad + \cos(\lambda - \varphi) - \sin\varphi - \cos\varphi], \end{aligned}\right\} \qquad (174)$$

where

$$\psi_0 = \frac{R_{cp}}{r_0} - \frac{1}{4},$$

$$\varphi = \left(\frac{2\psi_0\lambda - \lambda^2}{2R_{cp}}\right) r_0.$$

In determining the points of the curve from equations (174), parameter λ is taken in the range 15-75° every 15°. The plotting of the curve determined by equations (174) is accomplished in a scale of not less than 20:1, whereupon the family of circles with radius $r=0.54d_ш$ is plotted and the envelope is drawn. The

coordinates of the points of the envelope are plotted in the drawing of the separator.

For determining the dimensions of a slot with flat surfaces the tangent to the envelope parallel to axis OX is drawn. The distance of the tangent to the axis determines the half the width of the slot $l/2$.

If the equivelocity curve is described by several conjugate circular arcs, then the profile of the walls of the slot will consist of the same number of sections. Determining the shape of the profile for each of the sections is performed with the use of the following equations:

$$x_i = r_i \cos\left[\varphi_i\left(\frac{R_{cp}}{r_i} - 1\right)\right] + a_i \cos\varphi_i + b_i \sin\varphi_i - R_{cp},$$

$$y_i = r_i \sin\left[\varphi_i\left(\frac{R_{cp}}{r_i} - 1\right)\right] - a_i \sin\varphi_i + b_i \cos\varphi_i,$$

in which r_i is the radius of the arrangement of the centers of the balls on each of the sections; a_i; b_i - the abscissa and the ordinate of the center of the arc of radius r_i (see figure 27c).

Angle ϕ_i for every section changes respectively from $\phi_{i\ min}$ to $\phi_{i\ max}$ according to geometric calculation.

Construction of the family of curves and their envelope and the determination of the dimensions of the slot is performed just as in the case with an involute equivelocity curve.

When using separators, the distance between the centers of adjacent balls is taken as approximately $2d_ш$. Number of rolling contacts in this case is determined from assembly conditions with the aid of the formula and the next smallest whole number is taken:

$$n = \frac{1.57 D_{cp} + [d_ш - (\delta_к - \delta_{к\ min}) - (\delta_{к\ on} - \delta_{к\ min\ on})]}{d_ш},$$

in which the designations correspond to figure 58.

The cam of the wave generator is a disc mounted on the driving shaft and fixed with a key or put on with a clearance and connected with the shaft by a flexible element (in the design shown in figure 3, a rubber washer is vulcanized on the disc and shaft flange). The ends of the cam can have cylindrical necks for putting on washers which fix the internal ring of the generator. The washers are fastened by 4-6 bolts. Dimension A between washers should have a positive tolerance from the nominal width of the internal ring; tolerance for the width of ring is designated in the body. In assembly the clearance determined by fitting A_3/X_3 (figure 68) should be assured.

The external surface of the cam is shaped depending on the selected parameters of deformation of the flexible component. The equation of the profile with an involute equivelocity curve in accordance with formulas (36) will be

$$\left.\begin{aligned} x &= r_0 [(\psi_{0\kappa} + \lambda)\cos\lambda - \sin\lambda + 1]; \\ y &= r_0 [(\psi_{0\kappa} + \lambda)\sin\lambda + \cos\lambda - 1]. \end{aligned}\right\} \qquad (175)$$

where

$$\psi_{0\kappa} = \frac{1}{r_0}[r_{cH} + k_\Delta m_\mu - (0{,}5\delta + \delta_{\kappa\,\min} + d_m + \delta_{\kappa\,\min\,cH})]. \qquad (176)$$

in equations (175) and (176) λ is the polar angle; $\delta_{к\ \min\ вн}$ - the minimum thickness of the internal ring of the generator; $\delta_{к\ \min}$ - the minimum thickness of the external ring of the generator.

Generators with a stressed internal ring and grooves for balls in both rings are first assembled in an assembly (in this case for putting the assembled bearing on the cam a special device is utilized, and then the generator is inserted in the flexible component of the reducer.

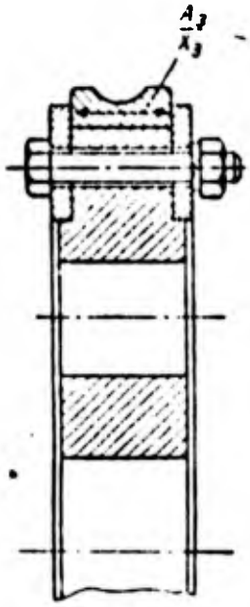

Figure 68. Diagram of the fastening of the internal stressed ring of a wave generator.

In generators with an unstressed internal ring a disc with a cylindrical external surface is used instead of the cam, and the internal ring itself has one or several grooves whose profile (in the cross section perpendicular to the axis of rotation of the generator) is made in accordance with the required form of deformation of the flexible component. The remaining parts of the wave generator and its general design remain the same as in the foregoing description.

One of the interesting design features of the generator with the unstressed ring is the possibility of the arrangement of two-three rows of balls; in this case, each groove for balls can be made according to the form of the deformation of the flexible component in the cross section passing through the centers of the balls of a given row. This is especially important for drives of the Г-Ж-Н type when by design the external ring of the wave generator is made smooth and in the contact of one row of balls with the ring high contact stresses are obtained.

For the grinding of the grooves of the internal ring on a regular cylindrical grinder a method can be utilized in which during machining the ring itself is in the deformed state. The essence of this method is clear from an examination of figure 69. The billet of the ring is machined over the internal surface in accordance with the drawing (figure 69a) with the aid of a special device deformed in the manner shown in figure 69b. In this state, the grinding of the external grooves of the ring on a cylindrical

grinder to diameter $D_{i\ нар}$ equal to $D_{i\ нар}=D_{e\ вн}-2d_{ш}$ (figure 69c, e) is performed. Simultaneously the external surface of the ring is ground to the required size. After this, the ring is removed from the device and is pressed on a cylindrical disc - the hub of the wave generator (figure 69d). In this shape, the profile of the grooves will correspond to the required shape of deformation of the flexible component.

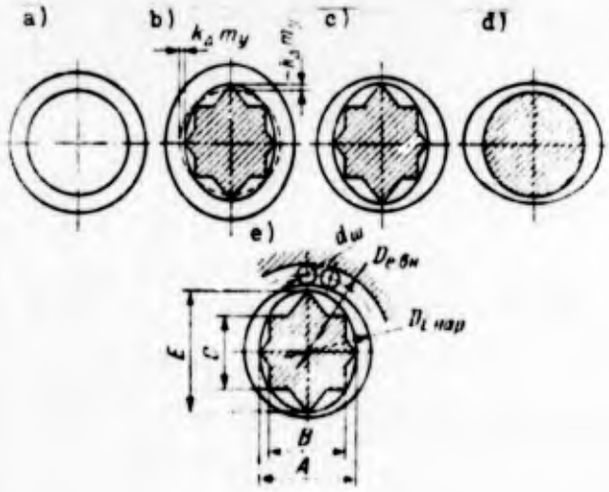

Figure 69. Diagram of the shaping of the unstressed ring of a wave generator by the method of machining in the deformed state.

The parameters of deformation of the ring necessary to obtain an involute equivelocity curve which approximates an arc of Résal's curve on the working section are determined in accordance with figure 69e with the following formulas:

$$\left.\begin{aligned} A &= D_{i\,вн} - 2k_{\Delta}m_y;\\ B &= 2r_0\left[\left(\varphi_{0к}+\frac{\pi}{4}\right)0{,}70711-0{,}29289\right];\\ C &= 2r_0\left[\left(\varphi_{0к}+\frac{\pi}{4}\right)0{,}70711+0{,}29289\right], \end{aligned}\right\} \qquad (177)$$

where $D_{i\ вн}$ is the internal diameter of the ring;

$$\varphi_{0к}=\frac{1}{r_0}(0{,}5D_{i\,вн}+k_{\Delta}m_y)-1;$$

$$E = D_{i\,вн}+2k_{\Delta}m_y.$$

Dimension E is reference. The slackening to dimension E should be performed to the contact of the ring with prisms along dimension A. In the points of contact of the ring with the prisms over dimensions B and C the bending stresses in the ring with its full deformation will virtually be absent. It should be noted that as a result of a change in the stressed state in the ring in proportion to its grinding distortions will be obtained in the form of deformation of the latter which affect its final dimensions. The investigations accomplished by us showed that when using approximate engagement distortions in the shape of a ring virtually have no effect on nature and the scheme of engagement. For precise engagement the effect of distortions is excluded by the very method of cutting the flexible component with reproduction of the process of engagement in the drive with the cutting.

In the case where several grooves are ground on the ring for a Г-Ж-Н drive, for each groove, depending on the parameters of deformation of the flexible component, a separate device should be envisioned in the corresponding cross section.

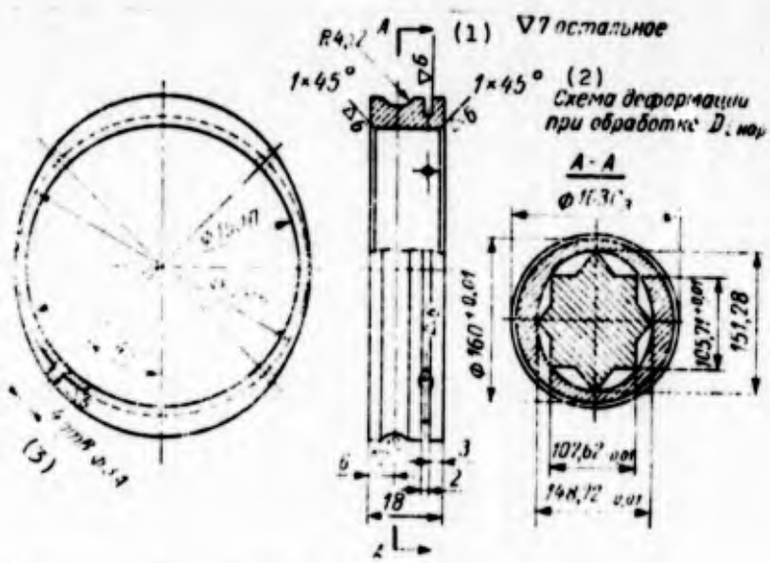

Figure 70. Design of an unstressed internal ring of a wave generator. Key: (1) remaining; (2) Diagram of deformation during machining $D_{i\ нар}$; (3) aperture.

Figure 70 presents the drawing of the ring of a generator made in the aforementioned manner. If there should be grooves in both rings of generator, then the assembly of the generator unit is performed before the removal of the internal ring from the grinder or on a special device of similar design.

CHAPTER VII

THE TECHNOLOGY OF MANUFACTURE OF THE BASIC PARTS, ASSEMBLY AND TESTING OF HARMONIC DRIVES

20. THE TECHNOLOGY OF MANUFACTURE OF FLEXIBLE COMPONENTS

The manufacture of thin-walled tubular parts by the machining method is usually connected with a number of technological difficulties and the use of specific procedures. The flexible components of harmonic drives combine the properties of precisely those parts and gear wheels which by themselves are sufficiently complex in machining. The scale of production affects the choice and sequence of operations in the manufacture of flexible components extremely substantially.

Information is encountered in the literature [29] about the use, for the forming of the flexible components, of the methods of drawing, working with pressure, and the forming of the flanges and flanging the thickened part. The internal surface of the component is flattened by special heads. The use of this technology in the series manufacture of harmonic drives is extremely effective since it makes it possible to lower considerably the consumption of metal and the cost of the manufacture of the flexible components, and also to raise endurance limits of the parts through the compaction of the metal.

During the preparation of the production of harmonic drives in large series different methods for the manufacture of flexible components can be tested and the most productive and economically expedient for the corresponding production are selected. At the same time, at the present stage of development of harmonic drives when basically experimental drives or small series of drives used in the different branches of machine-building and instrument manufacture are produced, we consider it advisable to give recommendation regarding the technology of manufacture of flexible components in small-scale and individual production.

The simplest technologically are the flexible components of Г-Ж-Н drives with a driven rigid component. As is evident from figure 63, parts of this type have a through smooth internal cylindrical surface for the machining of which methods developed in a number of production works can be applied (deep boring, honing, etc.). The external surface of the parts is also extremely simple and can be machined on lathes with the use of hydraulic duplicating devices; cylindrical and conical surfaces can be ground and polished.

The open ends and the identical parameters of two serrated threads (basic and for a toothed clutch) make it possible to perform the cutting of teeth on gear milling machines of any types from one or two settings of the parts, and also in the case of need to grind the teeth. Let us examine in more detail the sequence and the content of the various operations of the manufacture of the indicated type of metal flexible components.

The most rational form of billet should be considered to be seamless tubes from the appropriate marks of steel or tubes obtained by machining with the use of deep drilling and preliminary deep boring. Only during the manufacture of experimental drives is the use of rolled stock or piece forgings allowed.

The preliminarily machined flexible component should be a tube with the relations of wall thickness to the internal diameter 1:10 and with the leaving of an allowance for finishing of up to 3 mm on a side. The allowance for the length of a part made from a piece billet necessary for the fastening of the part in the lathe chuck should be not less than 30 mm. If a tube is machined which is utilized on a multiple number of parts, then allowance for the length of the entire tube should also consider the width of cut during the separation of the tube into separate parts.

The preliminarily machined tube undergoes heat treatment (quenching with high tempering); see the table 11. After preliminary machining a data sheet is initiated which accompanies it on all operations and is transferred on assembly.

The finishing of the flexible components is accomplished in the following order. With individual production and the production of piece billets lathe boring and the polishing of the internal surface are performed with the placement of the part in a general-purpose chuck. In series production with the manufacture of several parts from one tube the clean deep boring of the tube (on the appropriate machine tools), its honing, and cutting into the required number of parts are performed. Then both ends are undercut to size in turn with the formation of roundings-off. The turning of the parts over the external surface is accomplished on an expanding collet mandrel with a detent in one end. Turning is performed with a small depth of cut in several passes. At first the part is turned to a finish according to the diameter of the circles of the projections of the teeth, whereupon bevels are made and the smooth surface is machined to a finish. The final formation of the surfaces can also be performed with the use of hydraulic duplicating devices. The final machining of all cylindrical and conical surfaces separately can be performed by grinding. If finishing is realized by turning, then the external surfaces are polished to finish ∇8-∇9 according to GOST 2789-59.

In this form, the parts are checked for the absence of cracks with the aid of magnetic flaw detection.

The order of the first stage of the technological process of manufacture of flexible components for welding remains the same for Г-Ж-Н drives with a driven flexible component and for the Г-2Ж-Н drives.

The second stage (gear formation) is usually accomplished with gear milling machines of the corresponding dimensions. The part is based on the clamping expanding mandrel of the same design as a turning mandrel; the flexible components of the Г-2Ж-Н drives are based on a smooth mandrel with a detent with the clamping of the part by a washer in the end.

Figure 71. Mandrel for machining of a flexible component.

Figure 71 shows a flexible component and the corresponding clamping mandrel utilized both for turning and gear-cutting operations.

The flexible components of Г-2Ж-Н drives with modulus up to 1 mm whose hardness should be HRC$\geq$50, are first machined with low allowances of 0.5-0.7 mm at the diameters (tubes are cut into separate parts). In this form, the parts are made red hot on the mandrels, whereupon the honing of the internal surface to size and the grinding of the external surfaces and ends with the placement of the part on a clamping mandrel (without detent) are performed. The roundings-off on the ends are done by polishing wheels. After the machining of all surfaces the parts are checked for the absence of cracks. Teeth are cut through and are ground on machine tools which have as a tool an abrasive worm

disc (models 5832, 5833, and also machine tools of the firms "Reyskhauer [as transliterated] "Fellow", "Matrix", etc.) [11].

After the grinding of the teeth a careful inspection of the part for the absence of cracks is performed. If the flexible components should have anticorrosive coatings, then they are made after the final inspection of the parts.

A feature of the checking of flexible components is the fact that as a result of small wall thickness the testing and recording of the geometric dimensions of the parts and the dimensions of the teeth in the data sheet are performed in essence directly on the machine tool after the execution of the operation. The final check, besides the checking of the parts for the absence of cracks, provides for the aggregate check of completion of the data sheet and conformity of recorded dimensions to the drawing.

In chapter III it was said that for the cutting of the flexible components of the drives with precise engagement with the aid of hobbing cutters the method of reproduction, in the process of cutting, of the tooth engagement of the flexible and rigid components can be utilized.

Naturally, the simplest realization of the geometry of engagement would be the use of a ram with internal teeth which copies the rigid component as a cutting tool. However, this method of cutting is virtually unrealizable due to the extreme complexity of manufacture and short service life of the corresponding tool (ram).

Examined below is a method of reproduction of the engagement of the harmonic drive developed by the author with the cutting of the flexible components by hobs. This method is recommended for use with the cutting of flexible components with circular profiles of the teeth of the rigid component.

The essence of the method consists of the fact that by the rotation of the hob, the table (with the adjustment of the division swing bracket for the number of teeth of the rigid component), and the feed of the cutter along the axis of rotation of the table, an imaginary rigid component is created in space, in engagement with which the cut flexible component assembled with the wave generator is introduced.

By rotation of the generator relative to the flexible and imaginary rigid components rotating and being machined the operation of the drive is simulated and the cutting of the teeth of the flexible component with the formation of the required profiles occurs. A schematic diagram of the conduct of the process is presented in figure 72a.

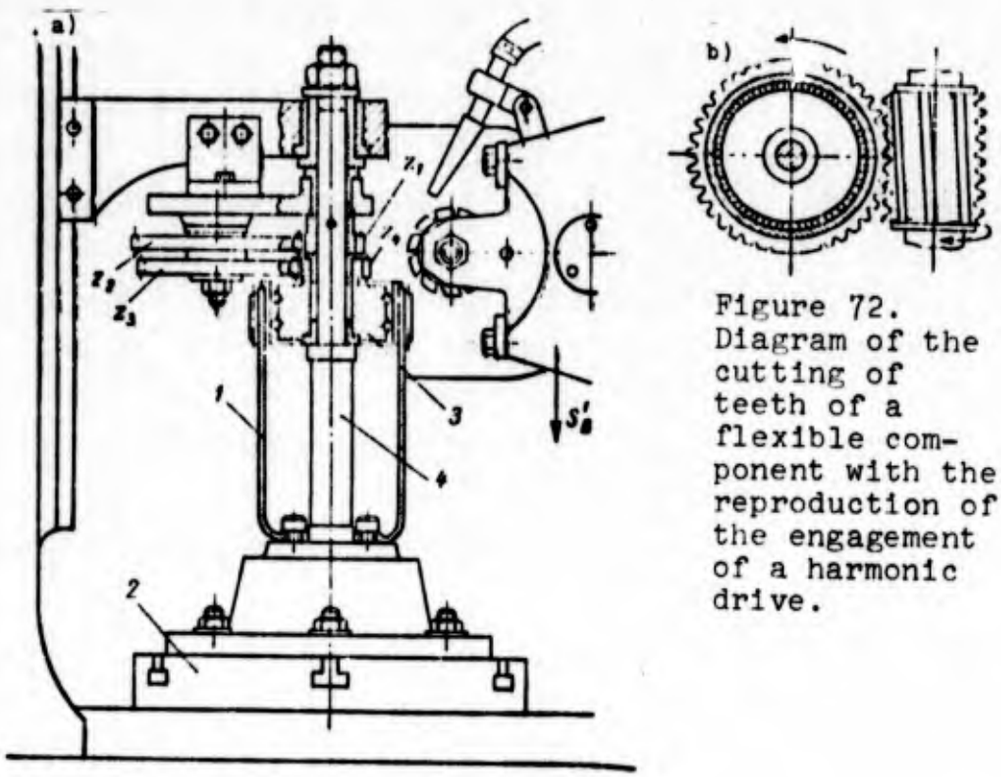

Figure 72. Diagram of the cutting of teeth of a flexible component with the reproduction of the engagement of a harmonic drive.

The shaft-mandrel 4 fastened on table 2 of the gear milling machines carries the attached gear z_1 with the aid of which, through toothed wheels z_2; z_3 and z_1 the wave generator 3 which rotates

freely on the shaft-mandrel is put into motion. The wave generator has exactly the same design and dimensions as a standard one. The flexible component 1 is also fastened on the table of the machine tool in a device and rotates together with the table.

By the selection of wheels z_1, z_2, z_3 and z_4 it is possible to insure the desired lead or lag of the wave generator relative to the rotation of the table because of which the rotation of the wave of deformation of the flexible component relative to the table occurs. Since the division swing bracket of the machine tool is adjusted for the number of teeth of the rigid component, during the first revolution of the table with the presence of the feed of the cutter the cutting of the teeth will occur on the flexible component in the manner shown in figure 72b. With the subsequent revolutions of the table in connection with the displacement of the wave of deformation, the teeth on other sections of the flexible component are cut and completely profiled. The continuity of the displacement of the wave of deformation assures the complete cutting and profiling of all teeth of the flexible component. At the same time the complete revolution of the wave generator relative to the table should cause the rotation of the flexible component relative to the rigid one through two angular pitches of the teeth (for a two-wave generator) as occurs in the drive itself. Thus, during the full revolution of the wave generator relative to the table the table should accomplish an additional rotation in the corresponding direction through two angular pitches of the teeth. This additional rotation is realized with the aid of the differential circuit of the machine tool.

One ought to focus attention on the fact that the complete machining of the teeth along the perimeter of the flexible component occurs during a half turn of the wave generator relative to the table, in connection with which the longitudinal feed of the cutter is calculated not for the revolution of the table, but for the revolution of the generator relative to the table. This feature of the process requires the use of very small feeds

(0.01-0.1 mm/rev). Such feeds are not found in all models of machine tools; therefore, in a number of cases the modernization of the swing bracket for the feeds of the machine tool can be required for installation of a set of not four, but of six and even eight interchangeable wheels.

During one revolution of the imaginary rigid wheel or, in other words, during $z_ж$ revolutions of the cutter (with a single-thread cutter) the flexible component and, consequently, also the table should accomplish $n_г$ revolutions

$$n_г = \frac{z_ж}{z_г + 2i_{ж2}}, \qquad (178)$$

where

$$i_{ж2} = \frac{z_1}{z_2} \cdot \frac{z_3}{z_4}.$$

The value of the transmission ratio $i_{нг}$ actually determines the circular feed. It is possible to take $i_{нг}$=0.95-0.98; in this case the wave generator will accomplish rotation towards the motion of the table. During a revolution of the table the generator will turn $(1-i_{нг})$ revolutions relative to the table itself. In order for the generator to turn 0.5 revolutions in relative motion, it is required to make $0.5/1-i_{нг}$ revolutions of the table. Since the longitudinal feed is calculated for 0.5 revolutions of the generator, the feed for one revolution of the table

$$S_г = 2S'_в(1 - i_{нг}).$$

where $S'_в$ is the feed for 0.5 revolutions of the wave generator.

Let us examine an example of the calculation of the adjustment of a machine tool model 5D32 for cutting teeth on the flexible component of a two-wave drive with z_1=228. We take the circular feed $i_{нг}$=0.96.

From formula (178) we find

$$n_c = \frac{z_k}{z_k + 2i_{kd}} = \frac{230}{228 + 2\cdot 0,96} = 1,0003479 \text{ r.p.m.},$$

then in 230 revolutions of a single-thread cutter the table should make 1.0003479 revolutions (with the adjustment of the division swing attachment of the machine tool to 230 teeth). The equation of the kinematic circuit in this case for the machine tool model 5D32 will take the form

$$(230\cdot 4 + \Delta n) \times \frac{1}{2} \times \frac{48}{230} \times \frac{1}{96} = 1,0003479, \qquad (179)$$

where Δn is the additional number of revolutions of the table obtained because of the circuit of the differential mechanism and computed according to the equation

$$\Delta n = 1,0003479 \times 96 \times \frac{2}{24} \times \frac{1}{i_s} \times \frac{1}{i_d} \times \frac{1}{30} \times 2. \qquad (180)$$

In expression (180) the gear ratio of the feed swing bracket i_s is determined in the following manner:

$$i_s = \frac{10}{3S_в}.$$

From the joint solution of equations (179) and (180) we obtain the formula for the computation of the gear ratio of the swing bracket of the differential

$$i_d = \frac{8\cdot 1,0003479}{15\cdot 920\cdot 0,0003479\cdot i_s}.$$

We take $S'_в$=1 mm; then we have

$$S_в = 2S'_в(1 - i_{kd}) = 2\cdot 1\,(1 - 0,96) = 0,08 \text{ mm/rev};$$

$$i_s = \frac{10}{3\cdot 0,08} = 41,66666.$$

We see that i_s can be realized on the machine tool by a set of 6 interchangeable wheels (100/20; 100/20; 100/60); therefore the modernization of the feed swing bracket can be required (the extended plate of the swing bracket is made).

We finally find the gear ratio of the swing bracket of the differential

$$i_0 = \frac{8 \cdot 1,0003479}{1.5 \cdot 920 \cdot 0,0003479 \cdot 0,08} = 20,82981.$$

According to this number, we select interchangeable gears of the swing bracket of the differential

$$\frac{z_1}{z_2} \cdot \frac{z_3}{z_4} \quad \frac{20}{98} \cdot \frac{20}{85}.$$

The required thickness of the teeth is assured through the precise setting of the distance between the axes of the part and cutter on the machine tool (with its known diameter).

The examined method can be also applied for the cutting of teeth of the flexible component with approximate engagement. In this case, the use of a hob with a standard working outline makes it possible to obtain some localization of contact, which achieves a reduction in the time of the break-in wear of the teeth (for drives of the Г-Ж-Н type). Furthermore, the height of the teeth of the flexible component can be raised with the elimination of any interference in engagement. The diameter of the projections of the teeth on the billet is determined on the strength of the standard height of the teeth equal to $(2f_0+c_0)m$. In the process of cutting some shearing of the head of the teeth will be obtained automatically and the latter will acquire the form shown by the dot-dash line in figure 36. It is expedient to perform the cutting of the teeth of the flexible components with approximate engagement with the indicated method with small series of articles and with a value of the modulus of $m>2$ mm.

A general view of the device and the process of cutting teeth by the described method are shown in figure 73.

Figure 73. Process of cutting teeth of a flexible component.

21. THE TECHNOLOGY OF THE MANUFACTURE AND ASSEMBLY OF PARTS OF A FORCED DEFORMATION GENERATOR

Depending on the type of wave generator, it is possible to distinguish the basic parts whose machining has certain specifics. For a generator with a stressed internal ring this part is the hub-cam, for a generator with an unstressed ring it is the internal ring itself. We will examine the technology of the manufacture of these parts below.

The unstressed internal ring of the generator is actually the internal bearing race and the corresponding requirements are made of it with respect to the quality of machining and heat treatment. A distinctive feature of the ring is the fact that the ball races (rollers) have a form which ensures the necessary deformation of the flexible component. In connection with this, the clean grinding of the grooves requires the use of equipment and methods usually employed for the grinding of cam profiles.

Utilized for this purpose are copying cylindrical grinders with the use of a disk master form or relieving lathes with special cams for the displacement of the support. In the absence of the corresponding equipment even during the series manufacture of drives the method of the grinding of rings in the deformed state whose substantiation is given a chapter VI can be used.

Figure 74 gives the approximate design of a mandrel for the grinding of rings in the deformed state.

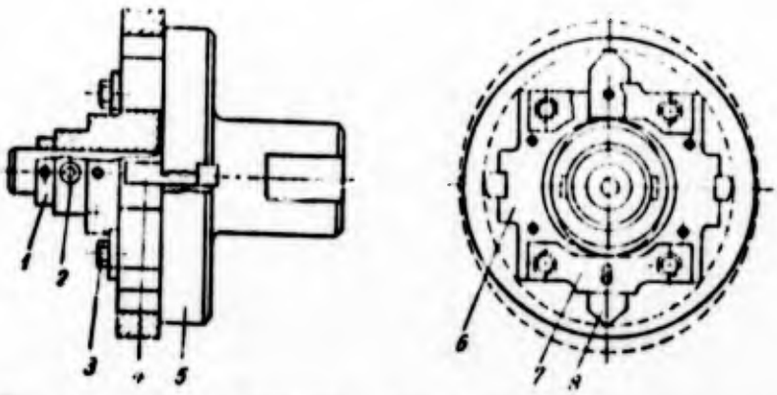

Figure 74. Mandrel for the machining of the unstressed ring of a wave generator in the deformed state.

The housing of the mandrel 5 has center apertures for placement on the centers of the grinder. Fastened to the face plate of the housing are two adjusting shoes 6 whose dimensions are made in accordance with figure 69. The shoes are also connected with each other by laths 7. In the slots formed by the shoes, two prisms 8 move which are moved apart by a cam 3 rotating on the rod of the mandrel.

In the shoes 6 there are also slots in which measuring mounting pads 4 are inserted through windows in the face plate which ensure the dimension A of the ring being ground (figure 69). A thrust ring 1 is put on the rod of the mandrel and is pegged. Two stop screws 2 are intended for the locking of the cam 3.

The ring being ground is put on the shoes 6. The mounting pads 4 are laid in the slots and by the rotation of the cam 3 by the prisms 8 the deformation of the ring is performed, until the ring presses the mounting pads 4. The cam is locked in this position by screws 2. Before installing the mandrel on the machine tool the adjoining of the ring to the end of the face plate is also checked.

The grinding of the external surface of the ring which is in the stressed state should be performed at low rates with abundant cooling since the ring can break as a result of the formation of burns and fine polishing cracks.

The check of the external diameter and diameters of the grooves is performed before the removal of the ring from the mandrel.

The hub-cam of the generator with the stressed internal ring is made of low-alloy improved steels and should have hardness HB$\leq$350. With this hardness of the billet, the external surface can be machined by any methods utilized for the machining of the cams. Simplest is the method of templet milling on a contour copying-milling machine tool with subsequent filing according to two superimposed master forms (figure 75). With the presence of possibilities, it is advantageous first to grind the machined external surface on special polishing or relieving lathes.

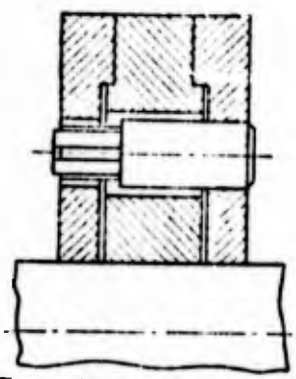

Figure 75. Superimposed master forms for the filing of the cam profile of a wave generator.

Below is examined the method of slotting the cam profile on a gear-shaping machine with a special ram. This method is productive, precise, simple, and interesting by the fact that the manufacture of the ram can be easily accomplished by the same method as the unstressed internal ring

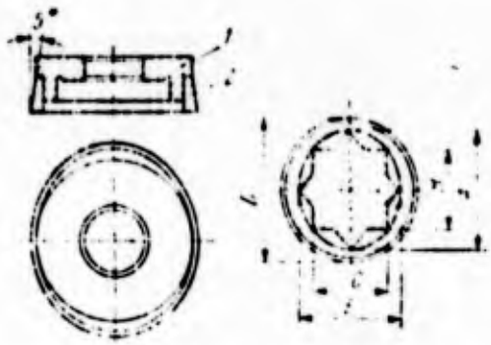

Figure 76. Ram for the slotting of the cam of a wave generator.

of the generator, i.e., by grinding in the deformed state. The design of the ram and the parameters of deformation of its rim during machining are shown in figure 76.

The ram consists of a hub 1 with an opening for the placement of the ram and cutting rim 2 of steel KhVG pressed on the hub. The cutting rim in the calculated cross section should have a profile mutually enveloping with the profile of the cam being cut. For this purpose the parameters of deformation of the cutting rim are designated during its machining according to figure 76 in accordance with the formulas

$$A_u = D_{вн.u} + 2k_\Delta m_y,$$

$$B = 2r_0\left[\left(\varphi_{0к} + \frac{\pi}{4}\right)0{,}70711 + 0{,}29289\right],$$

$$C = 2r_0\left[\left(\varphi_{0к} + \frac{\pi}{4}\right)0{,}70711 - 0{,}29289\right],$$

where

$$\varphi_{0к} = \frac{1}{r_0}(0{,}5D_{вн.u} + k_\Delta m_y) - 1;$$

$$E = D_{вн.u} - 2k_\Delta m_y.$$

Dimension E is reference.

The cutting rim is installed on the mandrel which creates the required deformation with the aforementioned parameters. In case of need and according to dimension E measuring packings which ensure the absence of play between the rim and the mandrel are laid. The rim is ground to a cone with dimension at the base $D_u = D_{i\ вн}$, where $D_{i\ вн}$ is the internal diameter of the internal ring of the wave generator.

The cone is made for the creation of a rear cutting angle of 5-6°. After grinding, the cutting rim is pressed on the hub and by means of grinding a front cutting angle of 0-1° is created.

With the slotting of the cam the machine tool is adjusted as for the cutting of wheels with $z=z_u$ and the check during cutting is conducted along the dimension of the greatest diameter of the cam. Regrinding of the ram is performed on the front face. The manufacture of the hub-cam by the ramming method (as with grinding) permits making the part with a collar for the detent of the internal ring with the presence of a groove for the removal of the tool. The axial fixing of the ring in another direction is accomplished in this case by a spring ring.

Pressing the ring on the hub-cam requires the preliminary deformation of the ring or the entire assembly which consists of two rings with balls (rollers). The deformation of the ring or the entire assembly requires the manufacture of a special device; furthermore, the cam should have a conical entry face which gives the required direction of the parts during pressing.

22. ASSEMBLY AND TEST OF HARMONIC DRIVES

A basic feature of the assembly of harmonic drives is manifested in the case of using a generator without a separator with an unstressed internal ring and external smooth ring. In this design, the pre-lubricated external ring is inserted to detent in the flexible component. The internal ring, assembled with a hub, is coated with a layer of cooled technical vaseline or grease in which the balls are laid (assembly is conducted with the vertical arrangement of the axis of rotation of the generator), whereupon the flexible component with the external ring is installed from above. Light pressure on the flexible component in an axial direction leads to the fact that the spheres deform the ring and the flexible component to the required form. If the

assembled drive will work with liquid lubricant, the grease or vaseline should be thoroughly removed by washing the reducer with the appropriate solvent. In other respects, the assembly of the harmonic drives is very simple and does not cause any difficulties.

The assembled drive should be rolled with stepped loading. Figure 77 shows a very simple device for rolling and testing harmonic drives. The unit consists of a frame 1 on which a band brake 3 and reducer 7 being tested are fastened with the motor (in the reducer shown on figure 77 the motor is located within the harmonic drive). The driven shaft of the reducer is connected with the brake drum by an intermediate shaft 6 with two toothed clutches. The device has a control panel 8 for the measurement of the parameters of current. The brake has a superimposed shoe 5 and band 2 tightened by screws 4. The shoe 5 has detents with which, during the creation of the braking moment, it exerts pressure on the rod of one of two hydraulic cylinders 9. The amount of braking moment is determined directly from the readings of manometers 10. With prolonged operation water for cooling is passed through the hollow brake drum. The block carries a pin which, during rotation, presses on the contact device of a revolution counter.

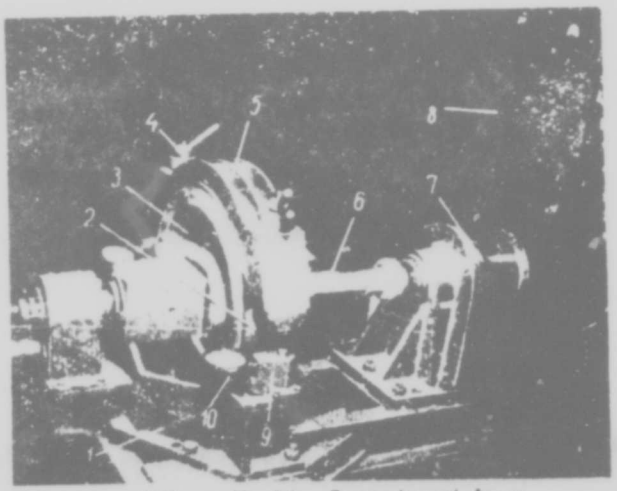

Figure 77. Unit for testing harmonic drive.

The rolling modes depend on the design of the drive and in each case should be determined experimentally taking into account the considerations given on page 100.

The first copy of the reducer should be subjected to a prolonged endurance test; in this case the number of cycles of change in stress

in the flexible component during the test period should be more than $3 \cdot 10^7$. After each million cycles it is recommended that the reducer be inspected and the condition of its parts recorded. After the first million cycles the flushing of the reducer and replacement of the lubricant should be performed.

For the experimental determination of the efficiency of the reducer the motor should be installed according to the motor-balance scheme or a special calibration chart should be available. Efficiency in this case is determined from the formula

$$\eta = \frac{M_{тор}}{M_{дв} i},$$

where $M_{тор}$ is the moment on the brake; $M_{дв}$ - the moment on the motor; i - the gear ratio of the reducer.

It is necessary to note that this method of determining efficiency can give substantial errors. If possible, the drive should be tested by the closed method. Figure 78 presents a diagram of a closed device for testing drives of the Г-Ж-Н type. The shafts of two drives connected with the flexible components are interconnected with the aid of a coupling. The shafts of the wave generators are interconnected with the use of two drives with cylindrical wheels. The motor installed according to the motor-balance scheme rotates the shaft 1 of the loop. The loading of the loop is performed through the application of torque $M_к$ to one of the drives. If we consider that the efficiency of the reducer is approximately equal to the efficiency of an accelerator,

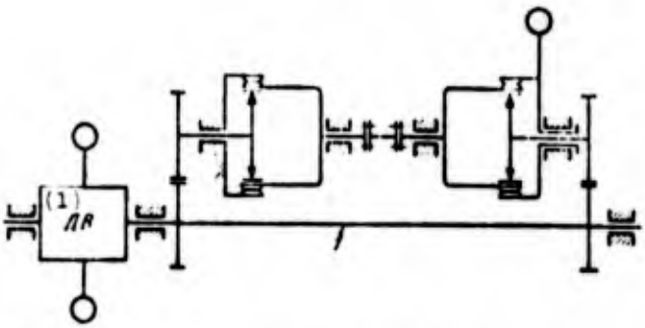

Figure 78. Diagram of a closed device for testing harmonic drives.
Key: (1) Motor.

the efficiency of each of the drives can be determined by the formula

$$\eta = 1 - \frac{M_{дв}}{2M_к} - \psi_{уст},$$

where $M_{дв}$ is the moment on the axis of the motor; $\psi_{уст}$ - loss factor in additional drives.

BIBLIOGRAPHY

1. Артоболевский И. И. Механизмы. Пособие для инженеров-конструкторов и изобретателей. М., АН СССР, 1951.

2. Байзельман Р. Д., Цыпкин Б. В., Перель Л. Я. Подшипники качения. Справочник. Изд. 5-е испр. и доп., М., изд-во «Машиностроение», 1967.

3. Баранов Г. Г. Курс теории механизмов и машин. М., изд-во «Машиностроение», 1967.

4. Гавриленко В. А. Зубчатые передачи в машиностроении. М., Машгиз, 1962.

5. Гинзбург Е. Г. Анализ конструкции волновых передач. Исследование зацепления в волновых передачах. — Некоторые вопросы геометрии, кинематики и прочности зубчатых и кулачковых механизмов. ЛВИКА им. А. Ф. Можайского, 1963.

6. Гинзбург Е. Г. Синтез зацепления волновых зубчатых передач. — Сборник докладов научно-технической конференции по волновым зубчатым передачам. ЛВИКА им. А. Ф. Можайского, 1965.

7. Гинзбург Е. Г. Структура и кинематика волновых зубчатых механизмов. Теория передач в машинах. М., изд-во «Машиностроение», 1966.

8. Гинзбург Е. Г. Профилирование зубьев волновой передачи. Надежность и качество зубчатых передач. 18—67—56, М., НИИинформтяжмаш, 1967.

9. Гинзбург Е. Г. Расчет волновых зубчатых передач. Исследование нагрузочной способности и живучести зубчатых передач машин специального назначения. ЛВИКА им. А. Ф. Можайского, 1967.

10. Гинзбург Е. Г. Волновая передача. Авт. свид. № 152761 с приоритетом от 16 декабря 1961 г. — «Бюллетень изобретений», 1962, № 2.

11. Голованов Н. Ф., Гинзбург Е. Г., Фирун Н. Б. Зубчатые и червячные передачи. Справочник. Л., изд-во «Машиностроение», 1967.

12. Глухарев Е. Г. К вопросу о распределении нагрузки по зубьям волновых зубчатых передач. Сборник докладов научно технической конференции по волновым зубчатым передачам. ЛВИКА им. А. Ф. Можайского, 1965.

13. Иванов М. Н. Приближенные методы расчета напряженного и деформированного состояния гибкого стакана волновой зубчатой передачи. — Сборник докладов научно-технической конференции по волновым зубчатым передачам. ЛВИКА им. А. Ф. Можайского, 1965.

14. Иванов М. Н. О кинематике волновой передачи. Надежность и качество зубчатых передач. 18—67—60, М., НИИинформтяжмаш, 1967.

15. Иванов М. Н., Шувалов С. А., Артанов А. К. Волновые зубчатые передачи. М., Известия вузов. — «Машиностроение», 1963, № 8.

16. Кудрявцев В. Н. Упрощенные расчеты зубчатых передач. М.—Л., изд-во «Машиностроение», 1967.

17. Кудрявцев В. Н. Планетарные передачи. Изд-во 2-е, переработ. и доп., М.—Л., изд-во «Машиностроение», 1966.

18. Куровский Ф. М. Теория плоских механизмов с гибкими звеньями. М., Машгиз, 1963.
19. Колчин Н. И. Аналитический расчет плоских и пространственных зацеплений. Машгиз, 1949.
20. Литвин Ф. Л. Теория зубчатых зацеплений. Л., Физматгиз, 1960.
21. Осипова О. М. Исследование концентрации напряжений у зубьев гибких колес волновой передачи. Известия вузов. — «Машиностроение», 1965, № 11.
22. Пантюхин К. Н. Предельные напряжения по выносливости зубьев изгибу при различных методах упрочнения зубчатых колес. — Исследование нагрузочной способности и живучести зубчатых передач машин специального назначения. ЛВИКА им. А. Ф. Можайского, 1967.
23. Рубцов В. К. О выборе профиля зуба волновой передачи. — Анализ и синтез машин автоматов. М., изд-во «Наука», 1965.
24. Рубцов В. К. Об условиях интерференции зубьев волновой передачи. — «Машиноведение», 1966, № 3.
25. Семенов М. В. Теория одно- и двухступенчатых планетарных передач. М.—Л., изд-во «Машиностроение», 1966.
26. Семин Ю. Н. Геометрия эвольвентной волновой зубчатой передачи. — «Машиноведение», 1966, № 4.
27. Тимошенко С. П., Войновский-Кригер С. Пластинки и оболочки. М., изд-во «Наука», 1966.
28. Цепков А. В., Меньшенин В. Н. Профилирование и технология изготовления долбяков для зубчатых колес Новикова. — Зубчатые передачи с зацеплением Новикова. Доклады, вынесенные на всесоюзную научно-техническую конференцию (Одесса, 1964). М., ЦНИТИАМ, 1964.
29. Центлин Н. Н. и Цукерман Э. М. Волновые передачи. — «Вопросы ракетной техники», 1965, № 8.
30. Цукерман Э. М. Выбор геометрических параметров волновой зубчатой передачи. — «Вестник машиностроения», 1961, № 11.
31. Шувалов С. А. Графоаналитический метод анализа геометрии зацепления в волновой зубчатой передаче. Известия вузов. — «Машиностроение», 1965, № 2.
32. Шувалов С. А., Скворцова Н. А., Семин Ю. Н. Повышение надежности и долговечности волновых зубчатых передач. М., ГОСИНТИ, 1966.
33. Шувалов С. А. Двухволновая зубчатая передача с четырехроликовым регулируемым генератором. Надежность и качество зубчатых передач. 18—67—26, М., ЦНИИинформтяжмаш, 1967.
34. Dudley D. W. Harmonic Drive Arrangements, Gear Handbook.
35. Harmonic Drive, Harmonic Drive Division, Unites Schoe Mashinery, Beverly.
36. Musser W. Пат. США № 2906143.
37. Musser W. Пат. США № 2930254.